$^{40}Ar/^{39}Ar$ thermochronology of the SE Central Gneiss Belt, Grenville Province, Ontario

Emily K. Gesner

Submitted in Partial Fulfilment of the Requirements
for the Degree of Bachelor of Science, Honours.
Dalhousie University, Halifax, Nova Scotia
March 1997

Distribution License

DalSpace requires agreement to this non-exclusive distribution license before your item can appear on DalSpace.

NON-EXCLUSIVE DISTRIBUTION LICENSE

You (the author(s) or copyright owner) grant to Dalhousie University the non-exclusive right to reproduce and distribute your submission worldwide in any medium.

You agree that Dalhousie University may, without changing the content, reformat the submission for the purpose of preservation.

You also agree that Dalhousie University may keep more than one copy of this submission for purposes of security, back-up and preservation.

You agree that the submission is your original work, and that you have the right to grant the rights contained in this license. You also agree that your submission does not, to the best of your knowledge, infringe upon anyone's copyright.

If the submission contains material for which you do not hold copyright, you agree that you have obtained the unrestricted permission of the copyright owner to grant Dalhousie University the rights required by this license, and that such third-party owned material is clearly identified and acknowledged within the text or content of the submission.

If the submission is based upon work that has been sponsored or supported by an agency or organization other than Dalhousie University, you assert that you have fulfilled any right of review or other obligations required by such contract or agreement.

Dalhousie University will clearly identify your name(s) as the author(s) or owner(s) of the submission, and will not make any alteration to the content of the files that you have submitted.

If you have questions regarding this license please contact the repository manager at dalspace@dal.ca.

Grant the distribution license by signing and dating below.

_____ _____

Name of signatory Date

Dalhousie University

Department of Earth Sciences
Halifax, Nova Scotia
Canada B3H 3J5
(902) 494-2358
FAX (902) 494-6889

DATE May 1, 1997

AUTHOR Emily K. Gesner

TITLE $^{40}Ar/^{39}Ar$ Thermochronology of the SE Central Gneiss Belt, Grenville Province, Ontario

Degree BSc Hons Convocation May Year 1997

Permission is herewith granted to Dalhousie University to circulate and to have copied for non-commercial purposes, at its discretion, the above title upon the request of individuals or institutions.

Abstract

As different minerals begin to retain Ar at distinct "closure temperatures", $^{40}Ar/^{39}Ar$ dating of suites of minerals can be used to reconstruct the cooling history of rocks in ancient orogenic belts. This information furthers our understanding of tectonic processes by placing constraints on the timing and relative rates of cooling, uplift and erosion.

The Grenville Province, exposed from Georgian Bay, Ontario to southern Labrador, is generally accepted to represent the deeply eroded remains of a collisional mountain belt formed during the ca 1.0-1.3 Ga Grenville Orogeny. During this event, a composite magmatic arc, represented in Ontario by the Central Metasedimentary Belt (CMB) was accreted to the pre-existing Laurentian craton. The Central Gneiss Belt (CGB) represents the reworked Laurentian craton and is separated from the CMB by the Central Metasedimentary Belt boundary thrust zone (CMBbtz) a major crustal scale thrust belt. This study was designed to complement U/Pb thermochronology work in progress. Results are presented for 6 hornblende and 4 Keldspars from the Muskoka domain, McClintock domain, Kawagama shear zone which lie in the footwall of the CMBbtz.

Five hornblende spectra yielded concordant $^{40}Ar/^{39}Ar$ age spectra, from which preferred (near-plateau) ages of 969 ± 9 Ma to 1001± Ma were interpreted. Excess argon is present in one sample. No correlation between age and structural position is evident from the present data set. More data are required to determine whether variations in hornblende ages across the study area reflect differences in cooling history or argon retentivity between the samples. Preferred ages for K-feldspar samples from the Muskoka domain (807 ± 5 Ma and 820 ± 5 Ma) are ~ 70 My younger than those from the McClintock subdomain. This may indicate that cooling rates in the McClintock domain were higher than in the Muskoka domain over the ~ 500-350°C interval. However, further modelling of the data are required. Approximate cooling rates for the Muskoka and McClintock domain were calculated based on the available data. Co-existing titanite and hornblende from one location in the Muskoka domain suggest more rapid cooling (5°C/My) followed by slower cooling (0.7°C/My). Cooling rates calculated for the McClintock domain between hornblende and K-feldspar closure are on average faster than in the Muskoka domain, however they overlap within error.

Acknowledgments

I would first like to thank my supervisor, Dr. Becky Jamieson, whose incredible enthusiasm both in the classroom and in the field has been an important stimulus of my interest in Earth Science during the past four years. Without her knowledge, advice, encouragement and financial support this project would not been started, let alone finished. I would like to thank my co-supervisor, Dr. Peter Reynolds for introducing me to $^{40}Ar/^{39}Ar$ dating. His patient explanations, insight and expertise were extremely helpful, particularly in understanding the interpretation of $^{40}Ar/^{39}Ar$ spectra. I also wish to thank Dr. Martin Gibling and Dr. Nick Culshaw for discussions and editorial advice that greatly improved this thesis.

Hilke Timmermann introduced me to the study area, and patiently answered my questions all year long. She provided samples, reference material and assisted with revisions.

Keith Taylor performed the $^{40}Ar/^{39}Ar$ analysis. I am particularly indebted to him fulfilling many last-minute requests for data. I would also like to thank Sandy Grist for assisting with density separation and Gordon Brown for preparing the thin sections.

Finally, I would like to thank my friends, my classmates, my sisters and especially my parents for providing invaluable support and encouragement.

TABLE OF CONTENTS

TABLE OF FIGURES

Chapter I - Introduction

1.1 The Grenville Province

The Grenville Province, a belt of mostly high-grade metamorphic rocks exposed from Georgian Bay, Ontario to southern Labrador, is widely accepted to represent the deeply eroded remains of an ancient collisional orogenic belt formed during the ~1.0-1.3 Grenville Orogeny. This event is generally thought to have involved the accretion of magmatic arcs to the Laurentian craton due to collision with an unknown continent to the southeast (Rivers *et al.*, 1989). Rocks now exposed at the surface in southern Ontario are generally accepted to represent crustal depths of 20-30 km (Culshaw *et al.* 1997). Studying them provides the rare opportunity to investigate the behavior of the lower orogenic crust, inaccessible to direct observation in present-day collisional orogens such as the Himalayas. However, in the absence of a stratigraphic record, detailed structural, metamorphic and geochronological studies must be conducted to understand the mechanisms and timing of tectonic events.

One of the most widely used techniques for investigating tectonic processes in ancient orogenic belts is thermochronology, radiometric dating that provides temperature information. Ages calculated using isotopic dating methods including the U/Pb and $^{40}Ar/^{39}Ar$ systems reflect the time at which a mineral became closed to the diffusion of the daughter isotope (Cliff, 1985). As different minerals have different "closure temperatures", suites of minerals from the same area can be used to construct cooling histories (Figure 1). $^{40}Ar/^{39}Ar$ ages of K-bearing minerals, including hornblende,

muscovite, biotite and K-feldspar, record cooling in the ~500°C - 200°C range which can be used to distinguish between contrasting times/rates of cooling that could reflect contrasting styles of exhumation.

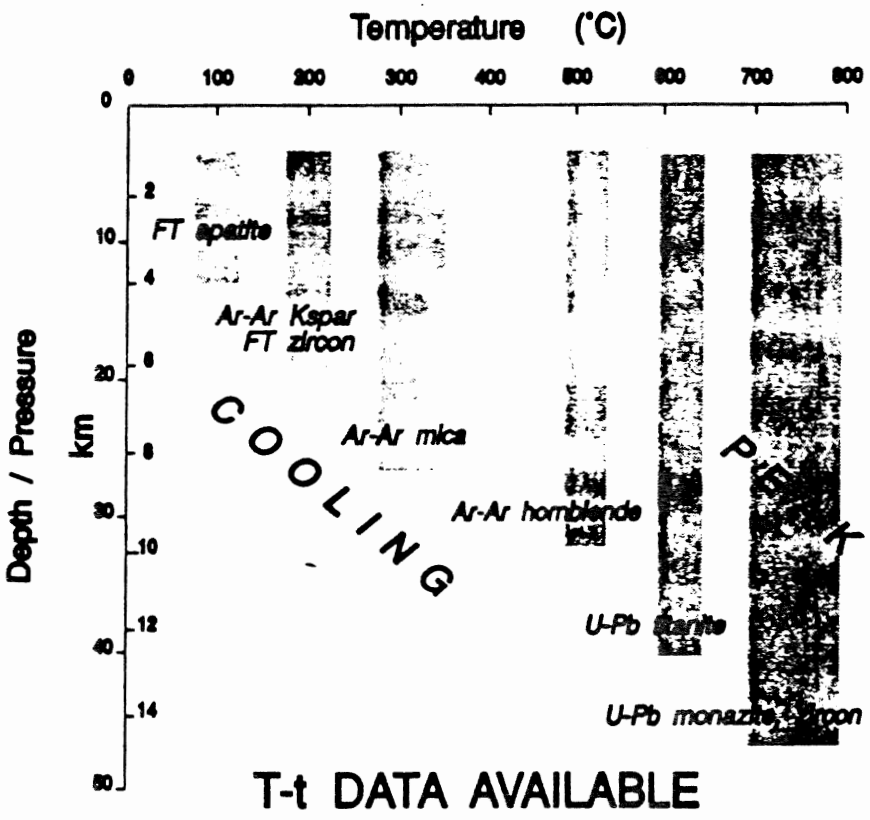

Fig. 1. T-t data can potentially be acquired over the full spectrum of metamorphic temperatures, if suitable minerals are present. The vertical shaded zones represent the range of »closure temperatures« for the specified thermochronometric systems; the cut-off depths are arbitrary. (Jamieson, 1991)

In southwestern Ontario, three main subdivisions of the Grenville Province were proposed by Wynne-Edwards (1972) (Figure 2). The Central Gneiss Belt (CGB), consists primarily of quartzofeldspathic gneisses of the Laurentian craton that were deformed and metamorphosed during the Grenville Orogeny. The Central Gneiss Belt has been further divided into domains based on rock type, structures, metamorphic grade and geophysical characteristics. North of the Central Gneiss Belt, the Grenville Front Tectonic Zone (GFTZ), a crustal-scale shear zone separates Archean rocks of the Southern Province from the Central Gneiss Belt. South of the Central Gneiss Belt, the Central Medisedimentary Belt (CMB) represents a composite magmatic arc which was thrust over what is now the Central Gneiss Belt during the Grenville Orogeny. Thrusting occurred along a southeast dipping crustal-scale thrust belt, termed the Central Metasedimentary Belt boundary thrust zone (Hanmer and McEachern, 1992). The timing of this thrusting has been variously interpreted as *ca.*1190-1180 Ma by McEachern and van Breemen (1993) or *ca.* 1080 Ma (Culshaw *et al.*, 1997).

The Muskoka domain, in the southernmost CGB, represents the footwall of this thrust. A better understanding of the thermal and structural history of the Muskoka domain and surrounding rocks is central to resolving uncertainty about Grenvillian convergence history. The present study complements work in progress on high temperature metamorphism and deformation of the Muskoka domain and adjacent units. U/Pb mineral data for zircon and monazite have produced both concordant and discordant ages which suggest protolith ages of 1457 to 1394 Ma, with metamorphic ages of ca. 1080 Ma to ~1064 Ma, supporting the hypothesis that the Central Metasedimentary Belt

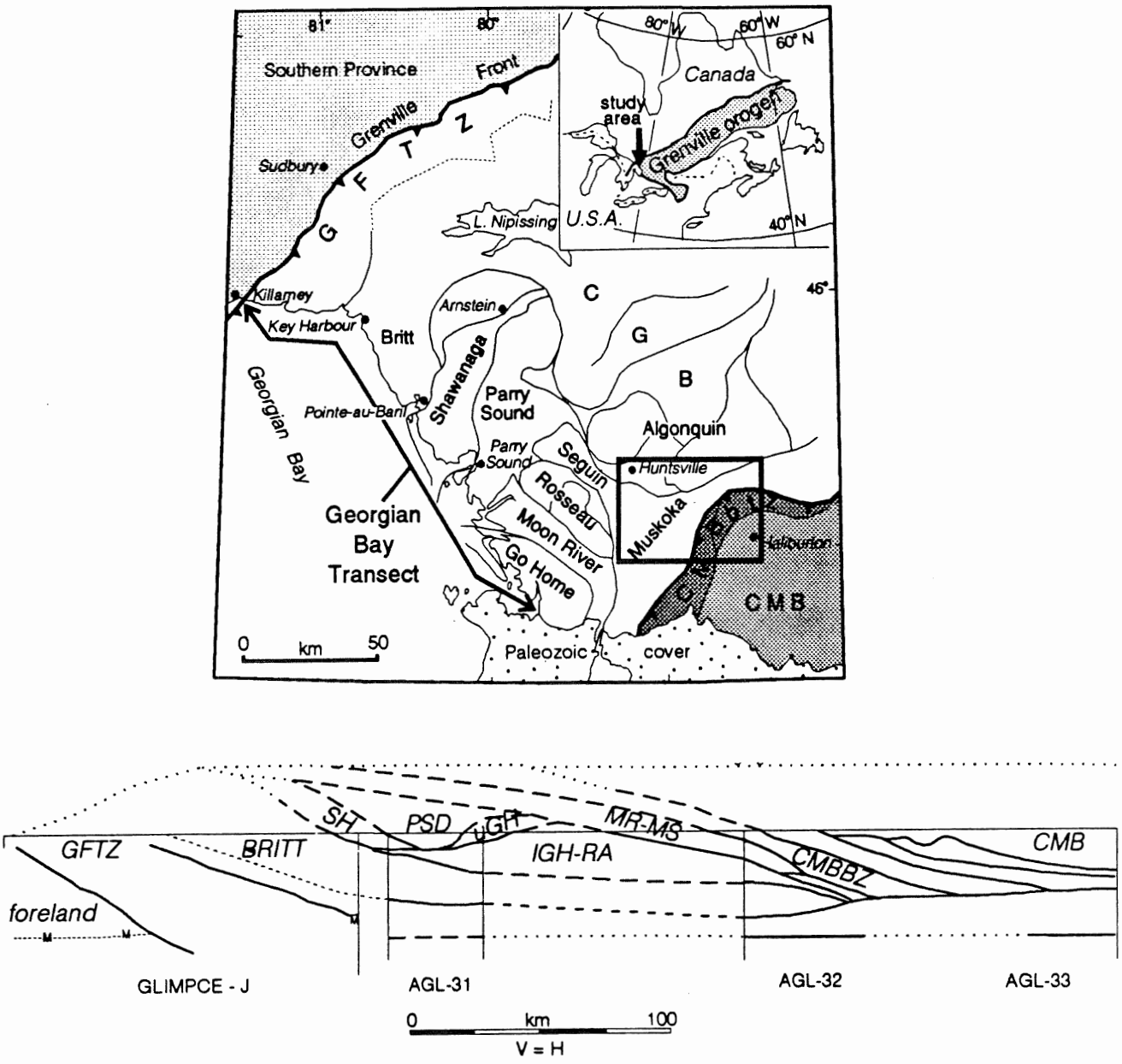

Fig. 2. Location map showing the position of the study area at the western end of the Grenville orogen (inset) and locations of major tectonic subdivisions of the orogen in Ontario (Wynne-Edwards, 1972), including the Grenville Front Tectonic Zone (GFTZ), Central Gneiss Belt (CGB), Central Metasedimentary Belt boundary thrust zone (CMBbtz), and Central Metasedimentary Belt (CMB). Lithotectonic subdivisions in the CGB are from Davidson (1984, 1986) and Culshaw *et al.* (in press). The heavy box outlines the area discussed in this study, which lies mainly in the Muskoka domain of the CGB. Cross-section (Culshaw *et al.*, in press) is slightly oblique to the Georgian Bay Transect line shown on the map. Crustal-scale distribution of lithotectonic units is based on geological, structural, and seismic data (profile line numbers noted below section), as discussed by Culshaw *et al.* (in press). Note in particular the relationship of the Central Metasedimentary Belt boundary thrust zone (CMBBZ in cross-section) to the underlying Muskoka and Algonquin domains (MR-MS and lGH-RA, respectively, in cross-section). The study area lies in the immediate footwall of the CMBBZ.

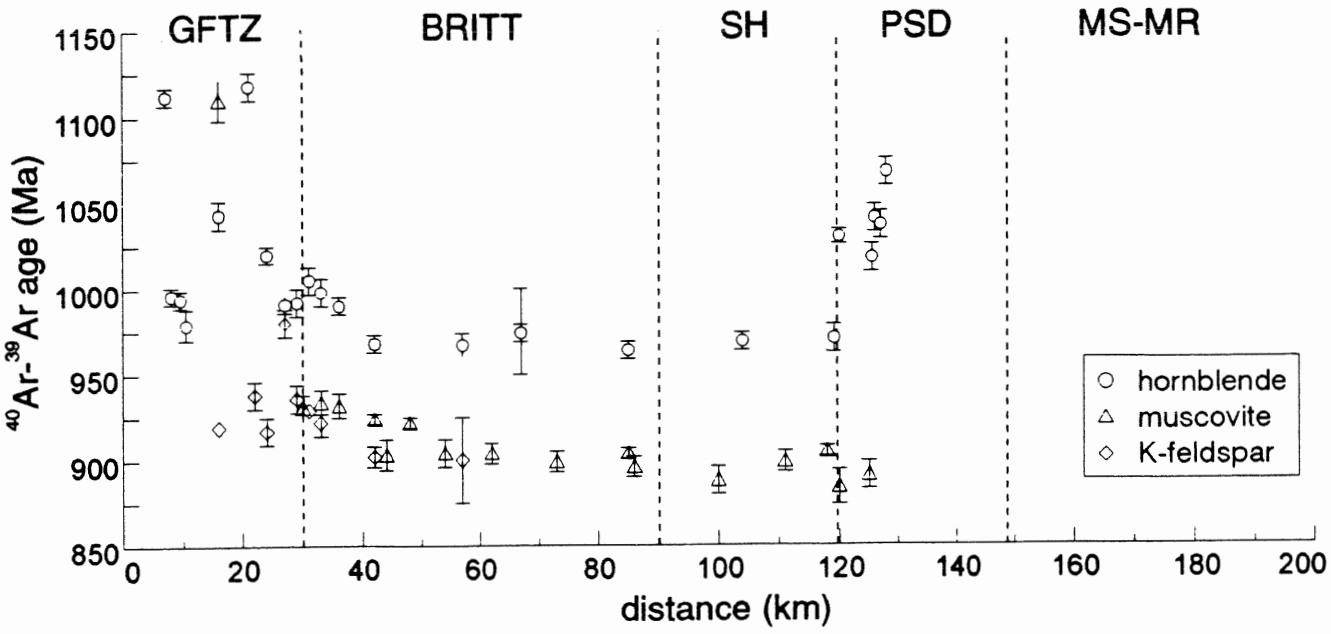

Fig. 3. Compilation of $^{40}Ar/^{39}Ar$ data from the western Central Gneiss Belt; distance refers to distance southeast of the Grenville Front along the cross-section shown in Fig. 2. Dashed vertical lines show domain boundaries from Fig. 2; SH = Shawanaga domain; PSD = Parry Sound domain; MS-MR = Moon River- Muskoka domains. Data from Culshaw *et al.* (1991), Haggart *et al.* (1993), Reynolds *et al.* (1995), and Culshaw *et al.* (in press). The study area lies at the southeastern end of this transect, approximately 200-240 km southeast of the Grenville Front. Note the consistency of hornblende, muscovite, and K-feldspar ages between about 40 and about 120 km; this is interpreted to reflect slow, post-orogenic unroofing of the Central Gneiss Belt in this area. The scatter of ages between 0 and 40 km is related to a combination of excess argon problems and rapid cooling in the Grenville Front Tectonic Zone, as discussed by Haggart (1991) and Reynolds *et al.* (1995). The old hornblende ages between 120 and 150 km are related to early transport and subsequent rapid cooling of the Parry Sound domain between 1080 and 1060 Ma (Culshaw *et al.*, in press).

1.2 Previous $^{40}Ar/^{39}Ar$ geochronology

Previous $^{40}Ar/^{39}Ar$ geochronological studies have indicated considerable differences in cooling history across the Grenville Province. Figure 3 summarizes the results of previous $^{40}Ar/^{39}Ar$ studies across a transect of the Grenville Orogen (Figure 2). Data from the GFTZ show rapid cooling to ~350°C, interpreted in terms of tectonically-controlled exhumation (Haggert *et al.*, 1993). This contrasts with results for the Britt domain, where cooling ages for hornblende (970 ± 10 Ma) and muscovite (900 ± 20 Ma) are remarkably uniform (Reynolds *et al.*, 1995). These data have been interpreted to reflect slow, erosionally controlled cooling at ~1-3°C/M.y. (Culshaw *et al.*, 1991). Several regional studies (e.g. Cosca 1991, 1992) indicate cooling rates across the CGB and CMB of ~1-4 °C /M.y.

Very little data exist to constrain the cooling history of the CGB - CMB boundary, an area crucial to the understanding of the Grenville orogen (Figure 3). Hornblende data from a regional study by Cosca *et al.* (1991), show considerable scatter in the vicinity of the CMBbtz - Muskoka domain boundary. However, since few samples were analysed, no mineral pairs were dated, and the geological context of samples was not documented, it is unclear whether this variation reflects systematic or geological differences.

1.3 Purpose of this study

The purpose of this study was to acquire hornblende and K-feldspar $^{40}Ar/^{39}Ar$ data to complement recent U/Pb dating by Timmermann *et al.* (1997). Where possible, the same samples were dated. This study presents $^{40}Ar/^{39}Ar$ data from 5 hornblende and 4 K-feldspar samples from the Muskoka domain and adjacent units, including Kawagama shear zone, McClintock subdomain, and footwall and immediate boundary of the CMBbtz. The study was undertaken to determine whether regional variations in the timing or rate of cooling exist in the footwall to the CMBbtz.

Chapter II - Local Geology and Sampling

2.1 Local geology

The geology of the study area, which includes rocks in the Muskoka domain, the Kawagama shear zone, the McClintock subdomain, and the CMBbtz is shown in Figure 4. The first three units are parts of the Central Gneiss Belt, while the last is the lowest structural level of the composite arc terrane accreted to the Central Gneiss Belt.

2.1.1 The Muskoka Domain

The Muskoka domain forms the immediate footwall to the CMBbtz. The typical rock type of the domain is medium-grained migmatitic orthogneiss (Timmermann *et al.*, 1997). The quartzofeldspathic migmatites are pink to dark-gray, depending on the mafic mineral content. Two generations of leucosome, which may constitute up to 35% of the rock, are present. The migmatites are also associated with coarse-grained, pink granitic orthogneiss and yellow-green to gray-green charnockitic gneiss. The rocks of the Muskoka domain contain numerous mafic bodies including coronitic metagabbro and amphibolite, and are also cut by pegmatites in many locations. Metamorphic grade is for the most part amphibolite facies, with local granulite facies. Thermobarometric analysis of mafic inclusions within the orthogneiss suggests peak-metamorphic conditions of approximately 10-11 kbar and 750-820°C. Rocks in the Muskoka domain occur in

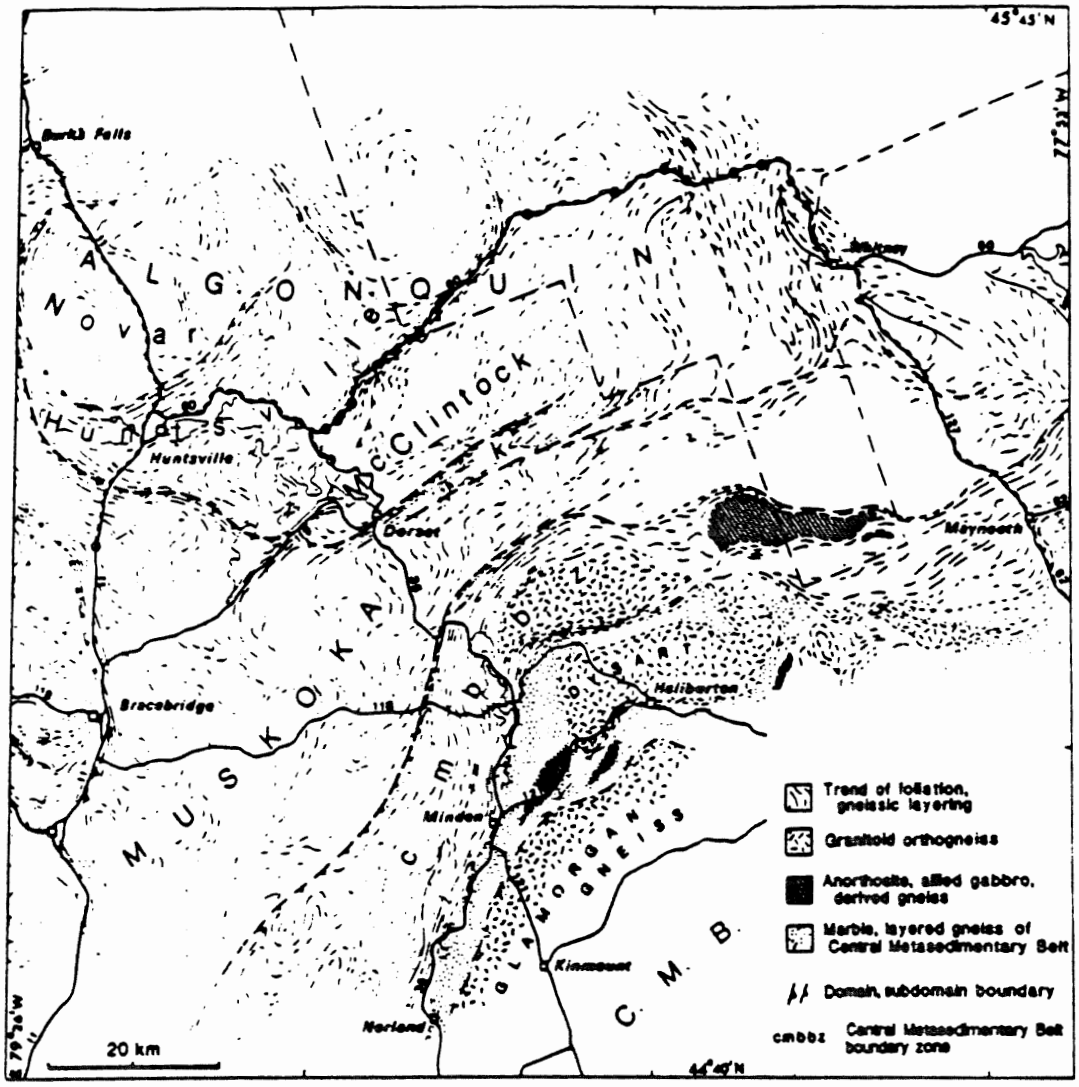

Fig. 4. General geology of the southwestern Central Gneiss Belt (area outlined in Fig. 2), showing foliation trends, domain boundaries, and dominant lithologies (Schau *et al.* 1986). Most samples investigated in this study come from the McClintock and Muskoka domains, in the vicinity of Dorset, along highways 35 and 118. See Fig. 5 for details.

various states of deformation. Penetrative ductile deformation, associated with NW-directed thrusting, produced amphibolite facies shear zones. Late-stage extensional kinematic indicators are also widespread.

2.1.2 The Kawagama Shear Zone

The Muskoka domain is separated from the structurally underlying Algonquin domain by a southeast-dipping zone of highly deformed rocks, the Kawagama shear zone (Timmermann, 1996). All of the rock types are highly deformed; mylonite zones are common. The Kawagama shear zone contains an individual lithologic package distinct from the overlying and underlying domains. The assemblage includes metapelitic migmatite, migmatitic orthogneiss, megacrystic orthogneiss, grabbroic anorthosite and hornblende-feldspar gneiss. The kinematics of the Kawagama shear zone are not yet fully understood. Subhorizontal lineations indicate transcurrent motion across the zone; however, extensional fabrics are also present (H. Timmermann, pers. communication, 1997).

2.1.3 The McClintock Subdomain

The McClintock subdomain, to the north of the Kawagama shear zone, forms the uppermost structural level of the Algonquin domain (Nadeau, 1990). The lithology is dominated by granulite facies paragneisses and orthogneisses. However, near the boundary with the Muskoka domain, metamorphic grade is in the amphibolite facies. Other rock types include megacrystic granitoids, migmatitic orthogneisses and coronitic

metagabbros. Metapelites are characteristic of the subdomain, with pelitic gneiss, calcsilicates, and marbles present (Nadeau, 1990). Peak-metamorphic pressures of approximately 6-11 kbar and temperatures of 675-775°C have been estimated using thermobarometry (Timmermann, 1996). Strong deformation due to thrusting from the southeast is indicated by isoclinal folding and thinning of the mafic bodies and layers. Kinematic indicators show northwest-directed thrusting and later southwest-directed extension.

2.1.4 The Central Metesedimentary Belt Boundary Thrust Zone

The study area is bounded to the southeast by the CMBbtz, which is the crustal-scale shear zone separating the Central Gneiss Belt from the Central Medisedimentary Belt. Within the study area, the geology of the CMBbtz is dominated by strongly deformed, quartzofeldspathic gneisses, locally containing anorthosite sheets. Three major thrust sheets which consist primarily of granitoid orthogneiss are shown in Figure 4 (Davidson, 1986). Kinematic indicators show both thrusting and extension. Late-stage extension is evident from narrow, low-angle, biotite-rich shear zones containing rotated pegmatite blocks and rotated feldspar porphyroclasts (Davidson, 1984).

2.2 Samples

The minerals dated in this study were sampled from outcrops within 30 km of the northern boundary of the CMBbtz (Figure 5). The dated rocks come from the Muskoka domain, the McClintock subdomain, Kawagama shear zone and CMBBtz, and were collected in 1994 and 1995 by H. Timmermann. Minerals suitable for $^{40}Ar/^{39}Ar$ analysis selected from a variety of rock types including quartzofeldspathic gneiss, amphibolite, anorthosite and calcsilicate. Sample reference numbers used in this study have been abbreviated from the names assigned by H. Timmerman during fieldwork. Appendix A lists the full sample names, rock types, and UTM coordinates. Where possible, minerals were separated from samples for which U/Pb data exist. Other samples were then selected to provide better data density across the study area.

Samples were studied in thin section to assess the suitability of minerals for $^{40}Ar/^{39}Ar$ dating. Hornblende and K-feldspar grains with a minimum degree of alteration and few inclusions were desired. Particular care was taken to avoid hornblende intergrown with biotite, because biotite (K_20 ~10%) is much greater than that of hornblende (K_20~0.5-2%) so that very small quantities of biotite can dominate the $^{40}Ar/^{39}Ar$ results.

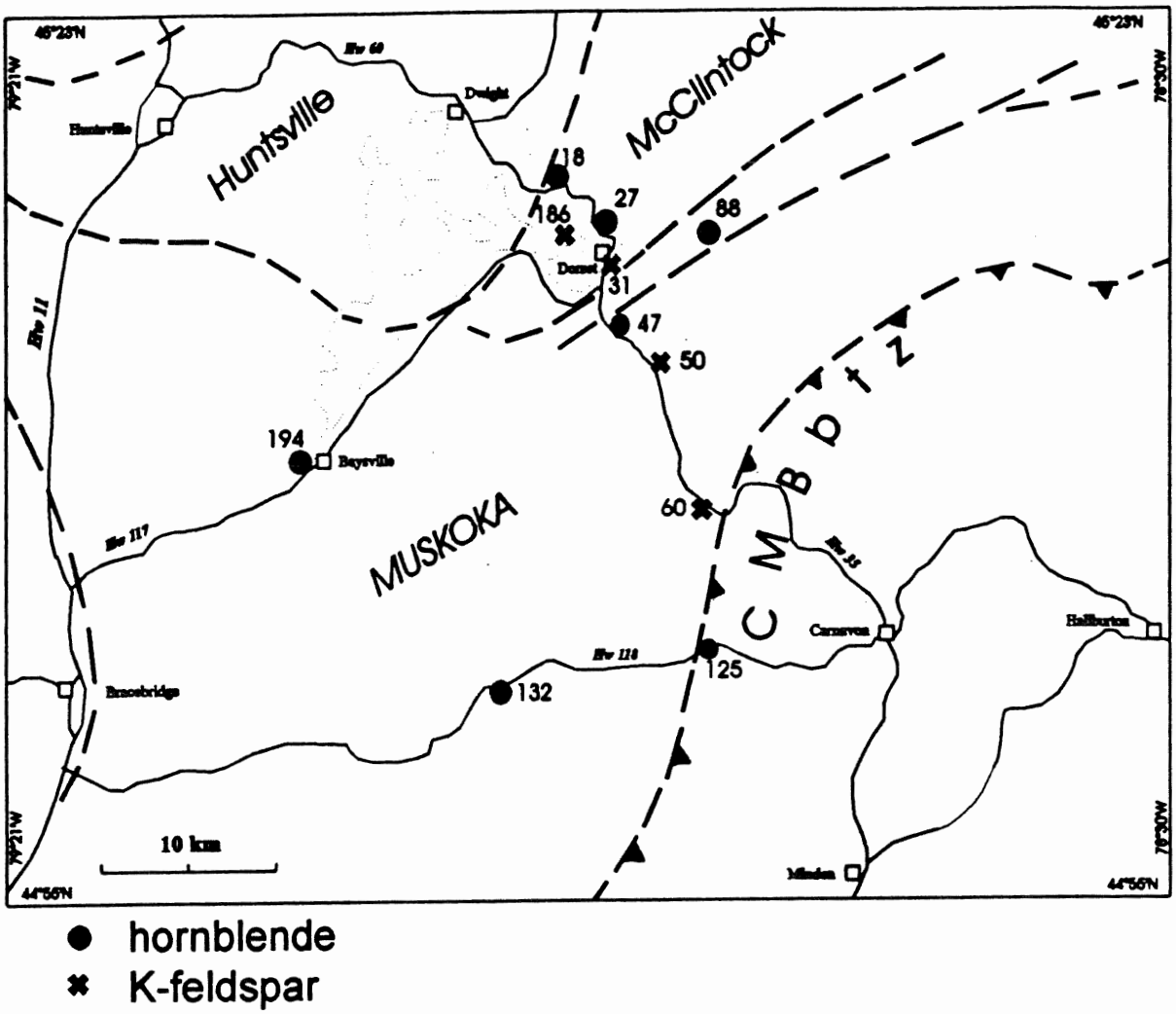

Fig. 5. Locations of the hornblende and K-feldspar samples dated in this study, relative to the major lithotectonic units in the study area. Huntsville and McClintock subdomains lie within the Algonquin domain (Fig. 2, 4); Muskoka domain and Central Metasedimentary Belt boundary thrust zone (CMBbtz) as shown in Fig. 2, 4. Dashed lines show positions of ductile shear zones corresponding to domain and subdomain boundaries; the Kawagama shear zone lies between the Muskoka and McClintock (sub)domains, as discussed in the text. Dashed line with barbs shows the position of the basal thrust in the CMBbtz; barbs on upper plate. Boxes show the positions of towns and villages; highways shown with solid lines; Lake of Bays outlined in light dots. The distribution of samples was designed to complement a recent U/Pb dating study (Timmermann *et al.*, in press).

Chapiter III - Methods

3.1 K-Ar and $^{40}Ar/^{39}Ar$ dating

Thompson first reported the radioactivity of potassium in 1905. Other researchers suggested that the weak radioactivity was attributible to trace amounts of francium (in Korenman, 1969). The debate was not settled until the radioactive content of potassium-bearing minerals was shown to be proportional to the potassium content. Although ^{40}K accounts for only 0.0117% of naturally occurring potassium, it is of extreme importance because it is a significant source of the radiogenic heat within the earth and is used for radiometric dating.

The decay of ^{40}K is branched, decaying to both ^{40}Ca and ^{40}Ar with a half-life of 1.28×10^9 years. The majority of ^{40}K (~89%) decays to ^{40}Ca by position emission releasing 1.35 MeV of energy. The remaining 11% decays by electron capture to ^{40}Ar releasing γ-quanta and 1.51 MeV of energy (Bowen, 1988). The decay of ^{40}K to ^{40}Ar is used to determine the age of K-bearing rocks and minerals. As argon is an atmosphile element, it is not normally incorporated into minerals during crystallization. Therefore any ^{40}Ar present in a rock is assumed to be due to the radioactive decay of potassium. The ratio of daughter ^{40}Ar parent ^{40}K is therefore a function of time and can be used to determine the age of a sample. The derivation of the equations needed for both K/Ar and $^{39}Ar/^{40}Ar$ dating is included in Appendix B.

One important disadvantage of K/Ar dating is that a sample must be divided such that the ^{40}K content can be found using wet chemistry and the ^{40}Ar using mass spectrometry. The $^{40}Ar/^{39}Ar$ dating method is a variation of the K/Ar method whereby the sample does not need to be split. The sample to be dated is irradiated in a nuclear reactor. The stream of fast neutrons transforms a portion of the ^{39}K in the sample to ^{39}Ar. The amount of ^{39}Ar is proportional to the amount of ^{39}K, which is in turn is proportional to the concentration of ^{40}K parent atoms. The sample is heated to release the argon and its age calculated from the ratio of $^{39}Ar/^{40}Ar$ measured by mass spectrometry.

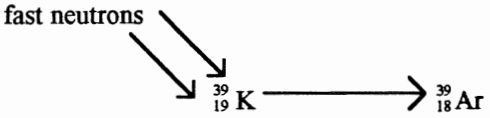

The amount of ^{39}Ar produced depends upon several irradiation parameters that are difficult to measure directly. Minerals of known age ("flux-monitors") are therefore irradiated along with the samples to define values for the general irradiation parameter, *J*.

An important advantage of $^{40}Ar/^{39}Ar$ dating is that samples can be outgassed through a series of increasing temperature steps, a technique known as step-wise heating. The argon 40/39 isotope ratio for each step is measured and an apparent age calculated. A plot of the apparent age for each step againt the cumulative percentage of ^{39}Ar released is known as an age spectrum. The shape of an age spectrum can reveal irregularities due to experimental effects (e.g. loss of argon during irradiation or breakdown of the sample during heating) or geological events (e.g. reheating of the sample). Selected steps can be eliminated from the calculation of a mean age, to give a result that is more likely to have a geological significance.

The $^{40}Ar/^{39}Ar$ ages of minerals are generally interpreted to record the time at which the mineral cooled through its "closure temperature" (also known as blocking temperature). Ideally, this is the temperature at which the mineral became a closed system with respect to the diffusion of argon (Dodson 1973). Assigning closure temperatures is complicated because the diffusion of argon (and thus these temperatures) for a given mineral depend on a number of parameters, including grain size, microstructures, cooling rate, and composition (e.g. McDougall and Harrison, 1988). The closure temperature of anhydrous minerals (such as K-feldspar) can be calculated by modelling the data obtained from step-wise heating analyses (e.g. Lovera *et al.*, 1991). Based on assumed diffusion behaviour of Ar in K-feldspar, estimates of closure temperature for K-feldspar vary widely, within the range of ~175-400 °C. For this study a closure temperature for the most retentive part of K-feldspar of 350 ±75°C is assumed based on modelling experiments on K-feldspars from the Central Gneiss Belt (Reynolds *et al.*, 1995). As hornblende is a hydrous mineral, it breaks down during *in vacuo* heating and its closure temperature cannot be calculated from diffusion stepwise-heating information. Estimates for its closure temperature vary from 450 to 550°C; a temperature of 500 ± 50°C for hornblende (Harrison, 1981; Onstott and Peacock, 1987) has been adopted for this study.

3.2 Sample preparation technique

3.2.1 Hornblende

The rock samples from which mineral separates were desired were processed as follows. The samples were first crushed in a tungsten-carbide shatterbox and then sieved, washed and dried to obtain a 60 - 120 mesh fraction (25 -12.5 μm). A Frantz magnetic separator was used to divide the grains into fractions of decreasing magnetic susceptibility. The more magnetic, mafic fractions consisted primarily of biotite and hornblende, which were separated by "paper-panning". The grains were poured on an inclined piece of paper that was gently shaken. Whereas the hornblende grains were typically blocky and quickly rolled off the sheet, the platy biotite grains tended to adhere to the paper. To ensure optimal purity, the hornblende grains were then examined using an optical microscope and hand-picked.

3.2.2 K-feldspar

Whereas all hornblende samples used in this study were prepared using conventional mineral separation techniques, two different methods were used to obtain K-feldspar samples. Feldspar separates are commonly obtained by density separation. However, study of the samples in thin section revealed the presence of both perthite and plagioclase. It was suspected that due to the presence of exsolution lamellae, the K-feldspar grains would show a density much closer to that of plagioclase, and these two grain types could not be distinguished optically in mineral separates. A somewhat unorthodox method for obtaining single grains of K-feldspar was devised such that the

composition of the individual grain could be known. This method proved successful, but unfortunately could only be used for coarse-grained samples. Mineral separates of the fine-grained samples from which K-feldspar was desired were prepared in the same way. Magnetic separation removed mafic minerals leaving felsic fractions which consisted primarily of K-feldspar, plagioclase and quartz; these were separated by immersion in a sodium poly-tungstate solution that had a density of approximately 2.65g/cm^3. Quartz and plagioclase, denser than the solution, sank to the bottom of the flask and were drained off. The feldspar grains floating on top of the remaining liquid were collected, washed and dried. The composition of the feldspar grain separates were then analyzed using X-ray diffraction. The X-ray diffraction spectra, included in Appendix C, indicate the likely presence of both plagioclase and K-feldspar; however, samples were judged acceptable as no further separation could be achieved using density separation techniques.

To obtain single grains of K-feldspar, polished thin sections were prepared somewhat thicker than normal (approximately 70-90 μm), using an acetone-soluble glue. The slides were examined under optical microscope and possible grains to be dated were selected. The slides were photographed and the chemical compositions of the target grains were then analyzed using the electron microprobe, to ensure that they were indeed K-feldspar. The slides were then placed in acetone to detach the section of rock from the glass. To remove the desired grains the sections were carefully broken using tweezers.

3.3 $^{40}Ar/^{39}Ar$ lab procedures

Each sample was wrapped in aluminum foil and placed in an aluminum irradiation canister. Samples of hornblende standard MMHb-1, which has been accurately dated as 519.4 ± 3.2 Ma using K-Ar dating (Sampson and Alexander, 1987), were interspersed with the samples in the canister to serve as a flux monitors. The samples were irradiated for ten hours in position 5C of the nuclear reactor at McMaster University. Upon their return to Dalhousie, the samples were allowed to "cool" for two weeks, time enough for many short-lived interfering radionuclides to decay.

The samples were then loaded, eleven at a time, into a disk-shaped cassette and introduced into the fully automated Ar-extraction system. The extraction furnace and all of the pneumatic valves are connected to a computer, so that the number and duration of temperature steps can be pre-programmed and the system run unattended.

The samples were introduced one at a time into the extraction furnace, a double-vacuum tantalum resistance furnace. Each sample was heated from ~500-1500°C through a series of up to 18 temperature steps, during which the temperature within the furnace was maintained constant by a thermocouple-regulated power supply. The samples were outgassed at each step for 20 minutes. After each step, all of the gas produced was pumped from the furnace to a VG3600 mass spectrometer. Before reaching the spectrometer, the gas was passed through a GP50 (Ti-Al alloy) getter to remove impurities.

The data acquisition system, also fully automated, measured the relative amounts of ^{36}Ar, ^{37}Ar, ^{39}Ar and ^{40}Ar in the mass spectrometer. The gas from each time step was

analyzed for 30 minutes, during which time the argon isotope ratios were measured sixteen times. Correction for contamination by argon absorbed from the atmosphere, or produced by the irradiation of elements other than K (so-called interfering isotopes), were based on the measured ratios of the argon isotopes and were made by the data reduction software. A summary printout listing the relevant data for each step was produced. The flux monitors were outgassed in the same manner and values for the parameter *J* ranged from 0.002274 to 0.002294. The *J*-values used for individual samples were interpolated from the closest standards to it during irradiation and this interpolated value was used to calculate an apparent age for each temperature step of a sample. Age spectra were produced by plotting the apparent age (in Ma) versus the cumulative percentage of gas released. All age spectra and data summaries are included in Appendix D.

Chapter IV - Results

4.1 Hornblende

4.1.1 Interpretation of hornblende spectra

Hornblende interpretation generally is based on the recognition of broad, flat portions of the age spectra, often called plateaux. A weighted average of the ages of the steps comprising the plateau is generally thought to give the best estimate of the age at which the sample passed through its closure temperature (McDougall and Harrison, 1988). Objective criteria proposed for the recognition of plateau are based on the number and size of steps required and the age variation among them. Among the definitions proposed, that of Fleck *et al.* (1977) has been adopted in many studies. A "plateau" according to this definition must consist of contiguous steps, that together represent more than 50% of the total ^{39}Ar released. No difference in age can be detected between any two fractions at the 95% level of confidence. However, with increasing analytical precision, many spectra that are nearly concordant do not meet this strict definition of a plateau. In many cases the shape of the spectra can yield meaningful age information, and the presence of a plateau in itself does not guarantee geological significance.

In this study, along with the apparent age spectra, the $^{37}Ar/^{39}Ar$ ratio of samples were also considered. During irradiation, ^{37}Ar is produced from ^{40}Ca, so that the $^{37}Ar/^{39}Ar$ ratio of a step is a function of the Ca/K ratio of the phase being outgassed.

Discordance in the $^{37}Ar/^{39}Ar$ spectra can indicate the presence of a phase with a different Ca/K content.

To determine the "preferred age"of a given sample, both the apparent age spectrum and the $^{37}Ar/^{39}Ar$ spectrum were examined. The weighted average was calculated for the most concordant part of the age spectrum over which the $^{37}Ar/^{39}Ar$ ratio was constant. Errors estimates are given at the 2σ level, and include the error in *J*.

4.1.2 Hornblende results

Five of the seven hornblende samples dated yielded relatively concordant, simple spectra. The other two samples exhibit more complex patterns and their interpretation is discussed separately.

Figure 6 shows the first set of concordant, "well-behaved" age spectra. They have similar shapes, with low ages for the up to 6 small low temperature steps, rising to a series of large steps with consistent ages, followed by a series of small high-temperature steps of somewhat variable age. The $^{37}Ar/^{39}Ar$ spectra follow the general pattern of the apparent age spectra, and are concordant over much of the release, indicating that the hornblende separates are of relatively uniform chemical composition and uncontaminated .

The first 3-6 small low-temperature steps account for no more than 12% of the gas released. This effect is present in all samples and is slightly more pronounced in samples 194 and 125, which show a staircase pattern for the first 10-12 % of the release. This effect may be due to slow cooling through the closure temperature, or may reflect the escape of small amounts of loosely trapped argon.

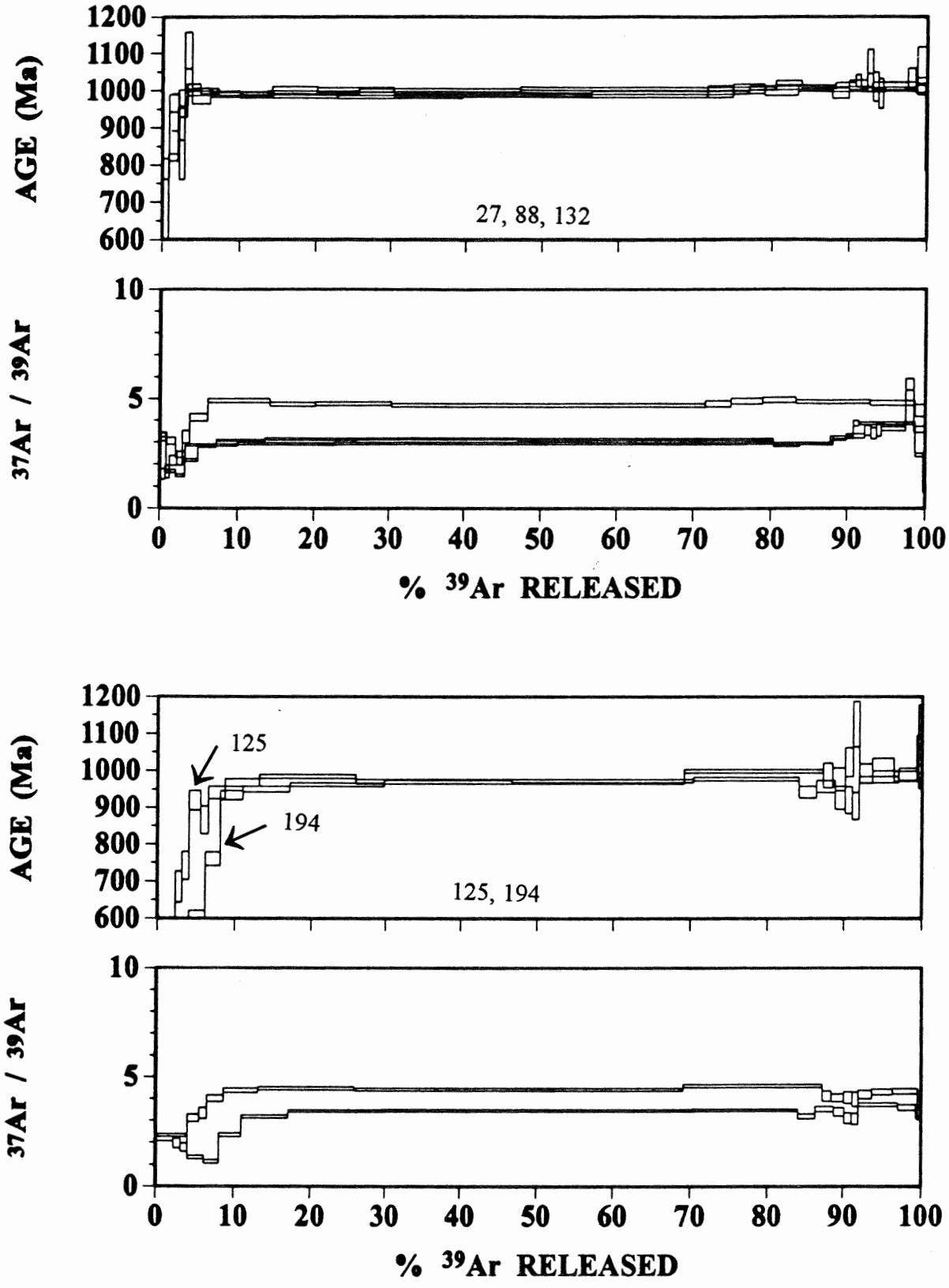

Fig. 6. Apparent age spectra from hornblende samples 27, 88, 125, 132, and 194.

Apparent age values for the highest temperature steps generally fall within approximately 2% of the mean age. Variability in the age of these small steps is likely related to changes in the diffusion behavior of the hornblende, due to breakdown of the mineral *in vacuo*. The central concordant parts of the spectrum, which account for 72-85% of the gas released, were used to determine the preferred age for each sample. The mean ages were determined by taking a weighted average of the concordant steps. The error, expressed at the 2σ level, was calculated from the individual errors of the constituent steps, and includes the error in the irradiation parameter, *J*. Although all five spectra are relatively concordant, only 132 meets the criteria for a plateau age as defined by Fleck *et al.* (1977). As explained above, the critical value by which two age steps can differ in a plateau depends on their error at the 95% confidence level. The absence of plateaux in these samples is a function of high precision, rather than poor data quality.

The preferred ages calculated for these samples exceed the total gas ages in all cases and range from a minimum of 967 ± 9 Ma for sample 194 to a maximum of 1001 ± 9 Ma for sample 132. Preferred ages of 983 ± 9 Ma , 991 ± 6 Ma and 995 ± 9 Ma were calculated for samples 125, 88 and 27, respectively.

Sample 47 yielded a U-shaped age spectrum, with older ages calculated from the gas released at low and high temperature steps and younger ages calculated for steps in between (Figure 7). Similar concave-upwards or "saddle-shaped" patterns have been recognized in many previous $^{40}Ar/^{39}Ar$ studies and are often produced by samples containing excess argon (Harrison, 1990). An isotope correlation calculation was used to try to detect trapped excess argon.

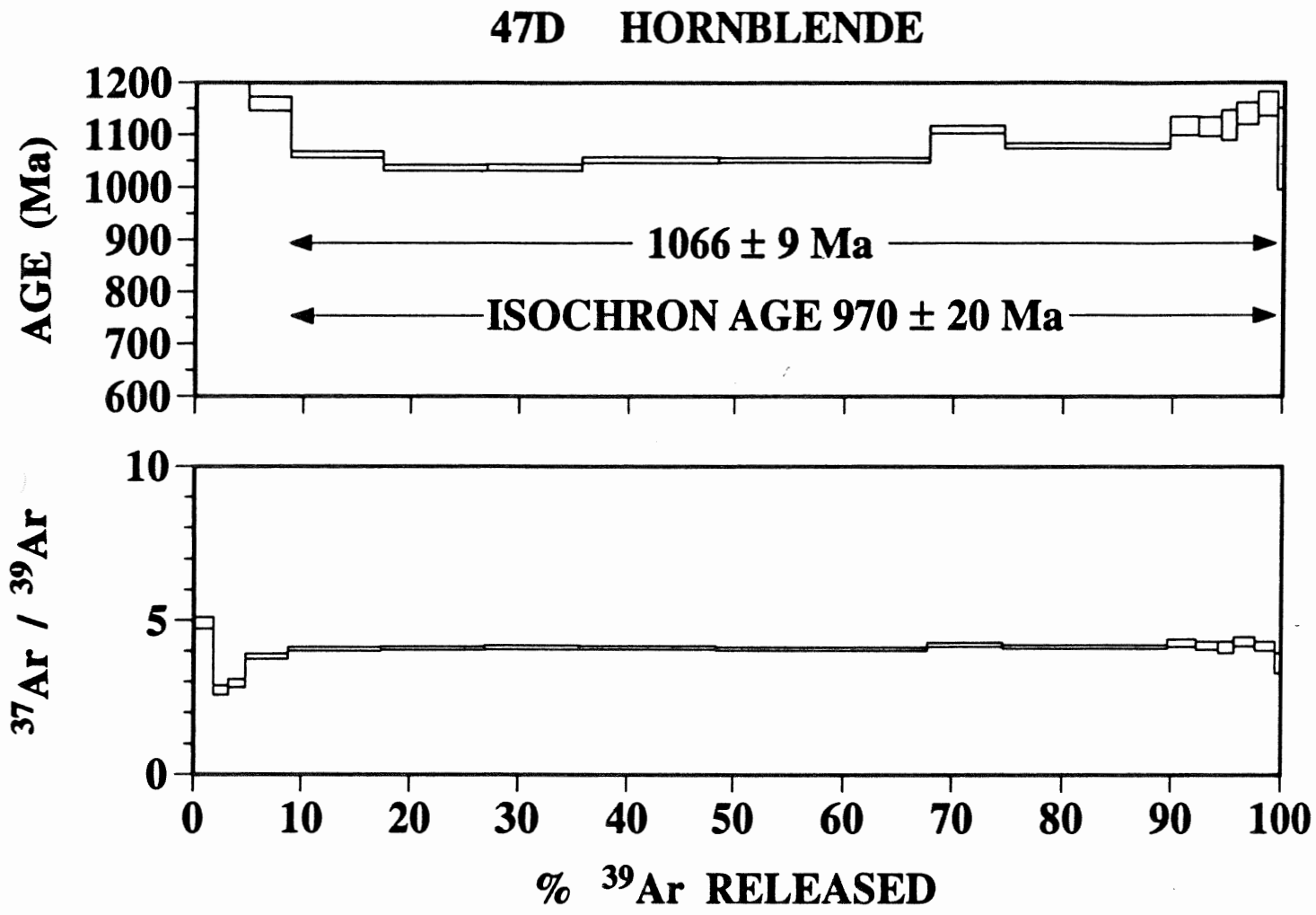

Fig. 7. Apparent age spectrum for hornblende sample 47, shown with $^{37}Ar/^{39}Ar$ spectrum, which is related to Ca/K ratio.

The plot, presented in Appendix D, indicates an initial $^{40}Ar/^{36}Ar$ ratio of approximately 5000 for the trapped gas, well above the atmospheric value (295.5) assumed for the other age spectrum calculations. Unfortunately, the line (and therefore its intercepts) is poorly constrained because, due to low ^{36}Ar content, the values for the various steps cluster near the horizontal axis. A preferred age of 970 Ma was nonetheless calculated using the $^{40}Ar/^{39}Ar$ ratio determined from the horizontal intercept. An error estimate is difficult to determine accurately, but is expected to be higher than the others. Another method of interpreting saddle-shaped spectra is to take the lowest-age steps of the spectrum as a maximum possible age for the sample. Using this approach, a four-step mean age of 1046 ± 8 Ma is taken as a maximum age for this sample.

Sample 18, a calcsilicate from the McClintock subdomain, yielded an extremely discordant release spectrum from which no meaningful age information could be interpreted. The unreasonably low ages calculated are due to the absence of significant quantities of both radiogenic argon ($^{40}Ar^*$) and neutron-induced argon (^{39}Ar) in the sample, indicating that the mineral phase dated has an extremely low K content. The phase dated may be a low-potassium amphibole or another mineral (possibly a pyroxene). The remaining fraction of the irradiated sample has been submitted for analysis using X-ray diffraction to determine whether the highly pleochroic, green, moderately birefringent mineral identified in thin section is indeed amphibole. If so, its composition will be analyzed using electron microprobe.

4.2 K-Feldspar

4.2.1 Interpretation of K-feldspar spectra

The interpretation of K-feldspar data is generally more complicated than for hornblende. K-feldspar age spectra can show a wide variety of shapes that may reflect argon loss during slow cooling, microstructural differences, or resetting due to late thermal events. In addition to apparent age and $^{37}Ar/^{39}Ar$ spectra, it is normal to consider Arrhenius plots in data interpretation. These are plots of D/a^2 as a function of 1/T where D is the diffusion coefficient, 'a' the effective diffusion radius and T the laboratory release temperature (in Kelvin). They can be constructed from the data obtained in standard step-heating experiments. Under ideal conditions, a mineral should show a linear Arrhenius plot. However, K-feldspar Arrhenius plots commonly have one or more kinks. The significance of these kinks is highly debated, but they are probably related either to changes in microstructures during gas extraction (e.g. Harrison, 1983), changes in the size of the domain from which gas is released (e.g. Lovera *et al.*, 1991) or changes in the diffusion mechanism (Lee, 1995). For this study, the general shapes of the Arrhenius plots were considered, and ages selected where possible from contiguous steps which correspond to linear patterns on the Arrhenius plots.

4.2.2 K-feldspar results

K-feldspar samples from four localities were analyzed in this study with one sample (186) run in duplicate. The five spectra produced very different patterns and their interpretation is discussed individually.

Sample 60, from within 2 km of the CMBbtz, shows a rise in age over the first 5% of the spectrum followed by a series of concordant steps in the middle part of the spectrum (Figure 8). The ages increase again over the last 40 % of gas realease, reaching a maximum of ~850 Ma. The $^{37}Ar/^{39}Ar$ ratio is relatively flat over the middle part of the spectrum. This pattern could represent partial resetting of the sample by a late thermal event or slow cooling. A mean age of 807 ± 5 Ma has been calculated for the part of the spectrum over which $^{37}Ar/^{39}Ar$ is constant.

The other K-feldspar analyzed from the Muskoka domain is a separate of fine-grained microcline from a vein of intermediate composition at location 50. The apparent ages for the sample rise gradually over the first half of the release to a ten-step plateau representing 53% of the gas volume (Figure 9). The $^{37}Ar/^{39}Ar$ spectrum is concordant over much of the release. The mean age of 821 ± 6 Ma is a plateau that corresponds to a straight part of the Arrhenius plot.

Sample 186, from a McClintock domain porphyroclastic gneiss, was run in duplicate to assess the reproducibility of the K-feldspar results. The two orthoclase grains, designated 186 FA-1 and 186 FA - 3, were separated from a single thick section and showed similar microstructural characteristics including small exsolution blebs. The age spectra, $^{37}Ar/^{39}Ar$ spectra, and Arrhenius plots produced for the two grains are very similar (Figures 10 & 11). The $^{37}Ar/^{39}Ar$ spectra from both grains show peaks at approximately 10% ^{39}Ar released. This is caused by the outgassing of Ca-rich phase, likely plagioclase, which was observed in thin section as irregular-shaped inclusions and exsollution lamellae.

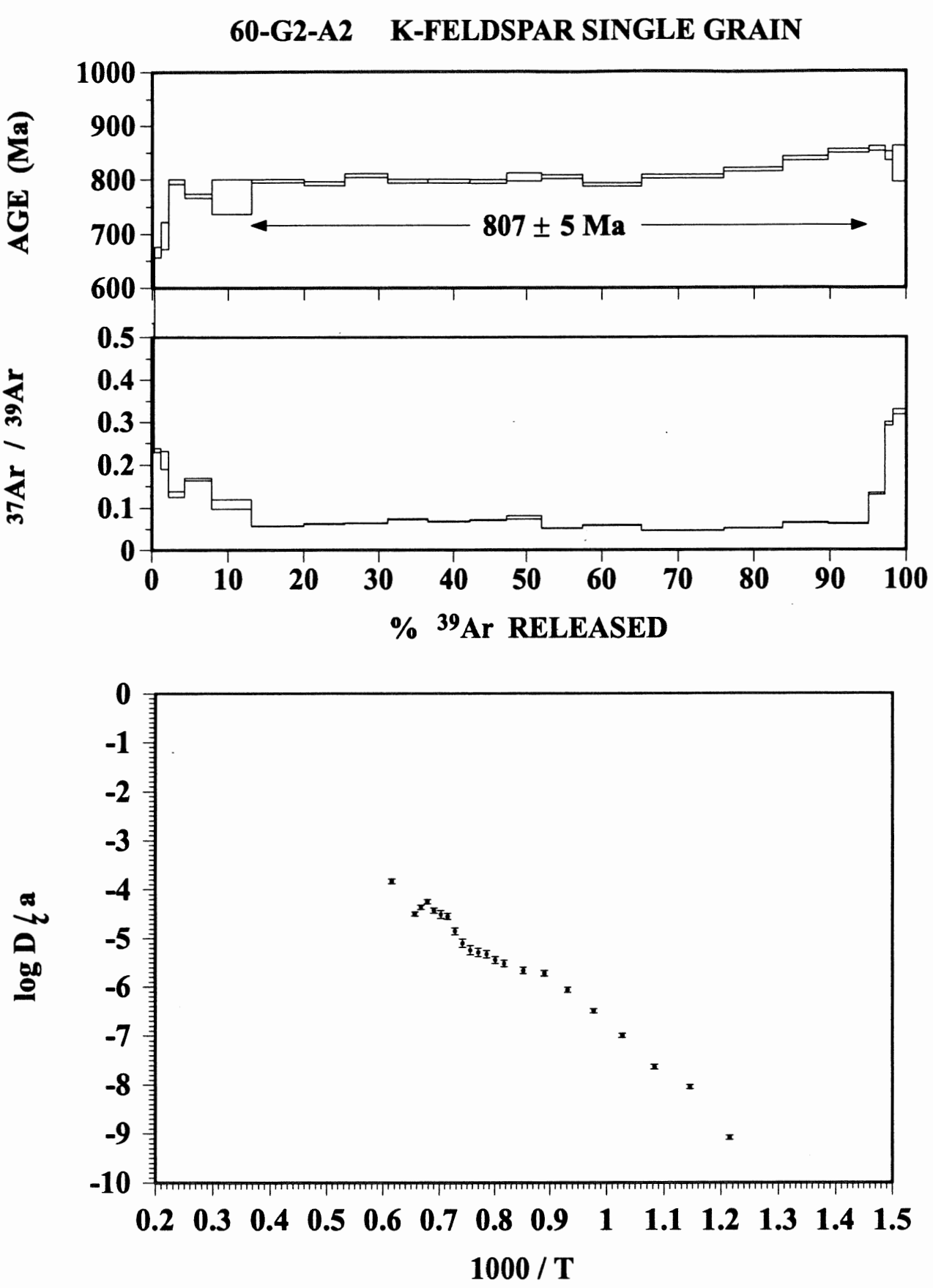

Fig. 8. Results from K-feldspar sample 60. Upper panel shows $^{40}Ar/^{39}Ar$ apparent age spectrum and preferred age, middle panel shows $^{37}Ar/^{39}Ar$ spectrum (related to Ca/K), bottom panel shows Arrhenius plot. See text for further discussion.

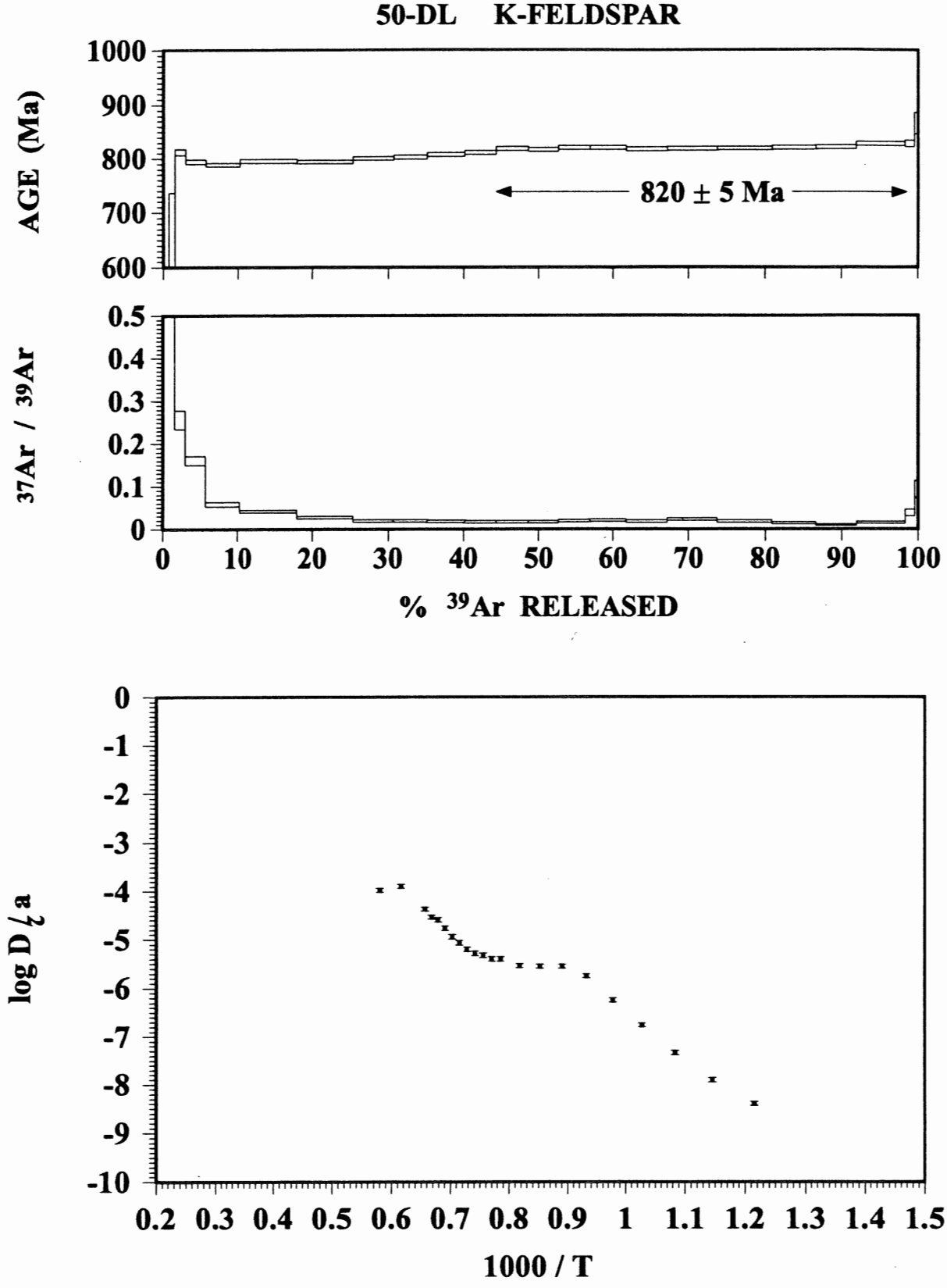

Fig. 9. Results from K-feldspar sample 50. Upper panel shows $^{40}Ar/^{39}Ar$ apparent age spectrum, middle panel shows $^{37}Ar/^{39}Ar$ spectrum (related to Ca/K), bottom panel shows Arrhenius plot. See text for further discussion.

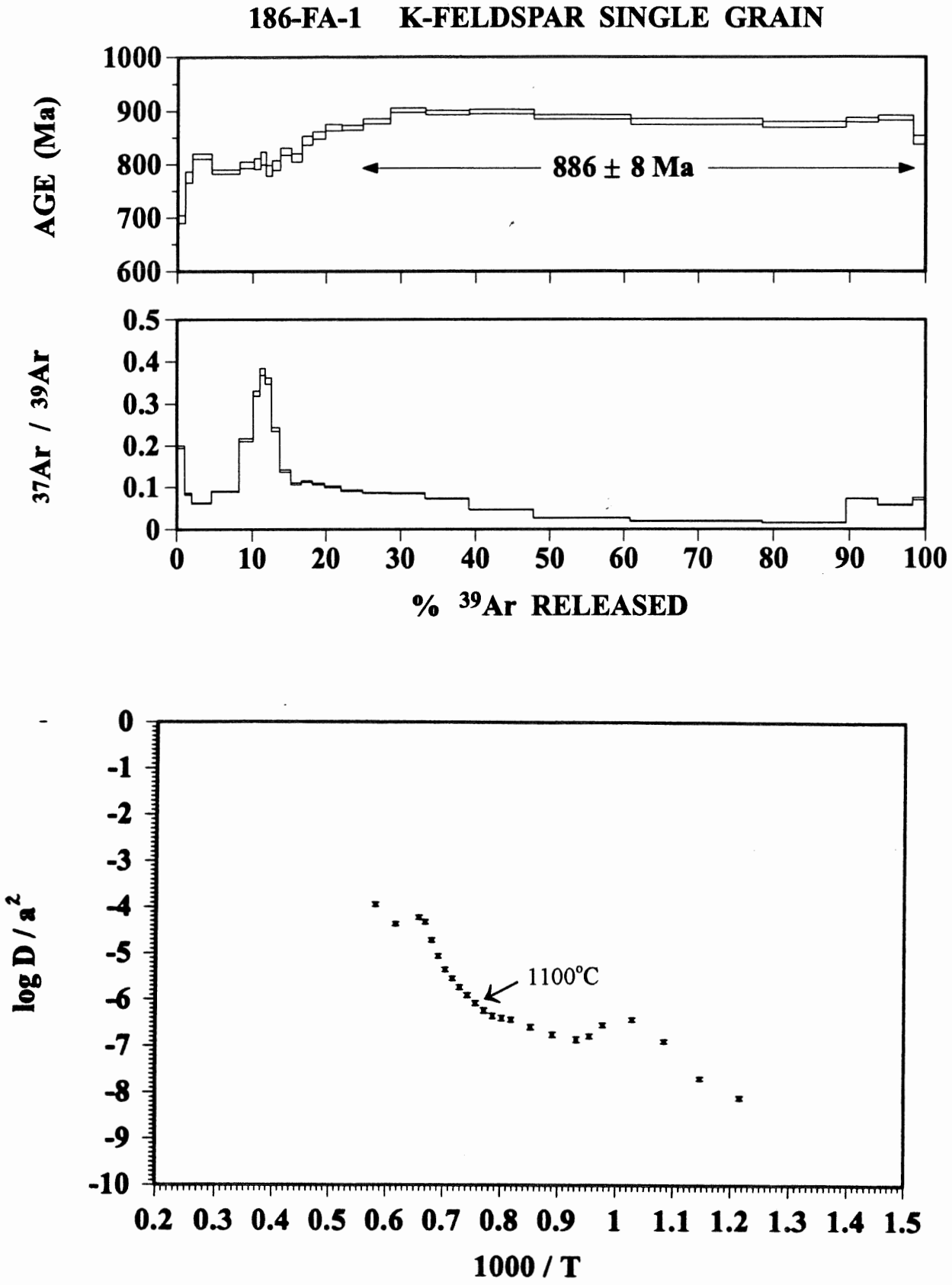

Fig. 10. Results from single grain K-feldspar sample 186-FA-1. Upper panel shows $^{40}Ar/^{39}Ar$ apparent age spectrum, middle panel shows $^{37}Ar/^{39}Ar$ spectrum (related to Ca/K), bottom panel shows Arrhenius plot. See text for further discussion.

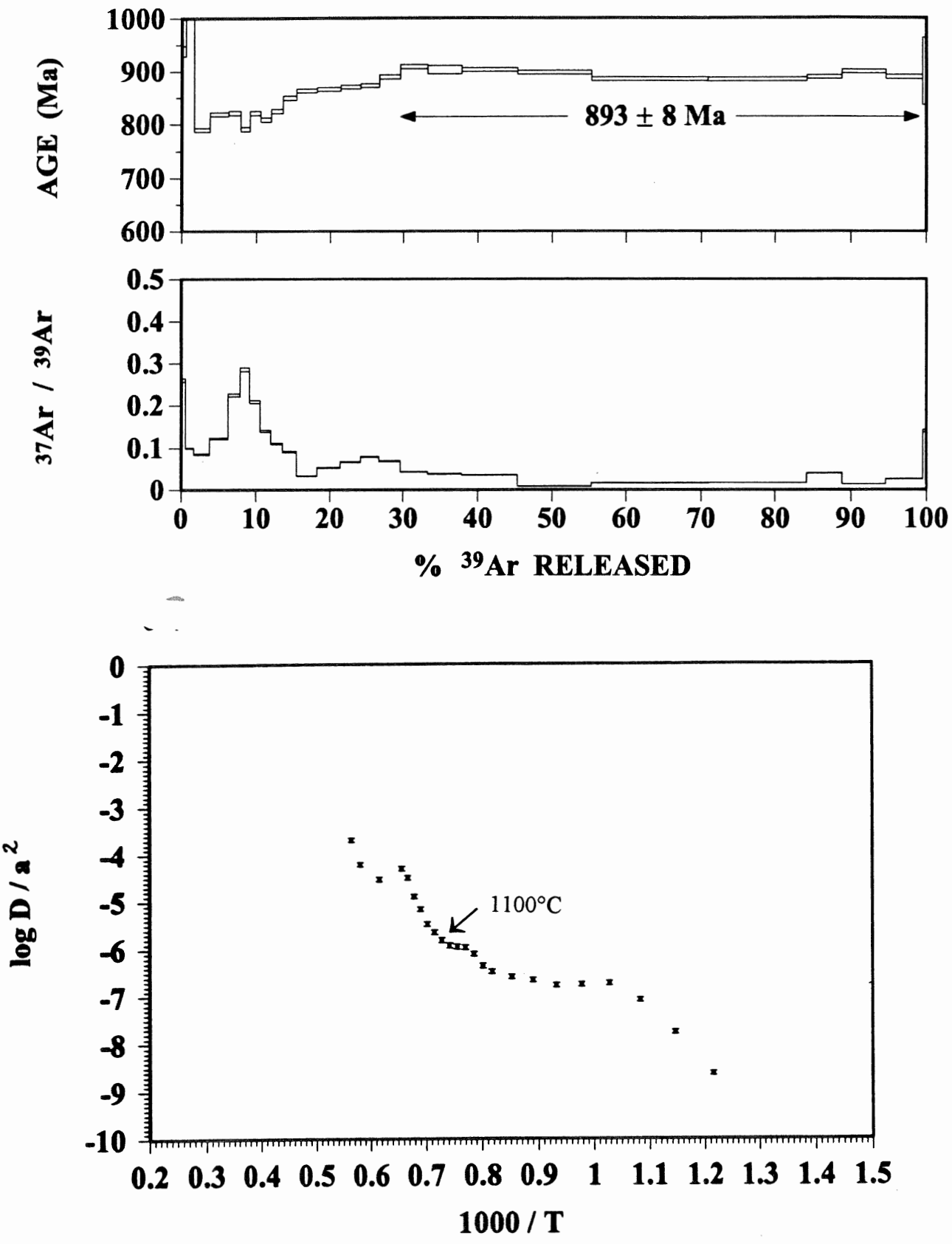

Fig. 11. Results from single grain K-feldspar sample 186-FA-3, a duplicate of 186-FA-1. Upper panel shows $^{40}Ar/^{39}Ar$ apparent age spectrum, middle panel shows $^{37}Ar/^{39}Ar$ spectrum (related to Ca/K), bottom panel shows Arrhenius plot. See text for further discussion.

The Arrhenius plots both showed complex patterns with multiple kinks. However, the points representing the gas released above 1100°C form a relatively linear array corresponding to the most concordant steps of the age spectra. A weighted average for these high-temperature, concordant steps (which comprise 73% of the release gas in both cases), was calculated. The two ages, 886 ± 8 Ma for grain 186-FA-1 and 893 ± 8 for grain 186-FA-3, are indistinguishable within error. The average of the two ages, 890 ± 8 Ma is used in all subsequent discussion.

The other K-feldspar sample from the McClintock subdomain, a microcline grain separate from 31, yielded a highly discordant age spectrum (Figure 12). The $^{37}Ar/^{39}Ar$ ratio is also highly variable and does not mimic the pattern of the age spectrum. This suggests the presence of a contaminating phase, likely plagioclase. Contamination by plagioclase is supported by X-ray diffraction analysis results, included in Appendix C. A preferred age of 904 ± 6 Ma was calculated from six high-temperature steps, and selection based on the linear portion of the Arrhenius plot. Although a concordant spectrum is normally a prerequisite for the selection of a plateau-type mean age, an estimate for the high-temperature/large domain age of the sample was desired for comparison with the other samples. The other alternative would have been to use the total gas age of 886 Ma, which would not have changed the present interpretation of the data.

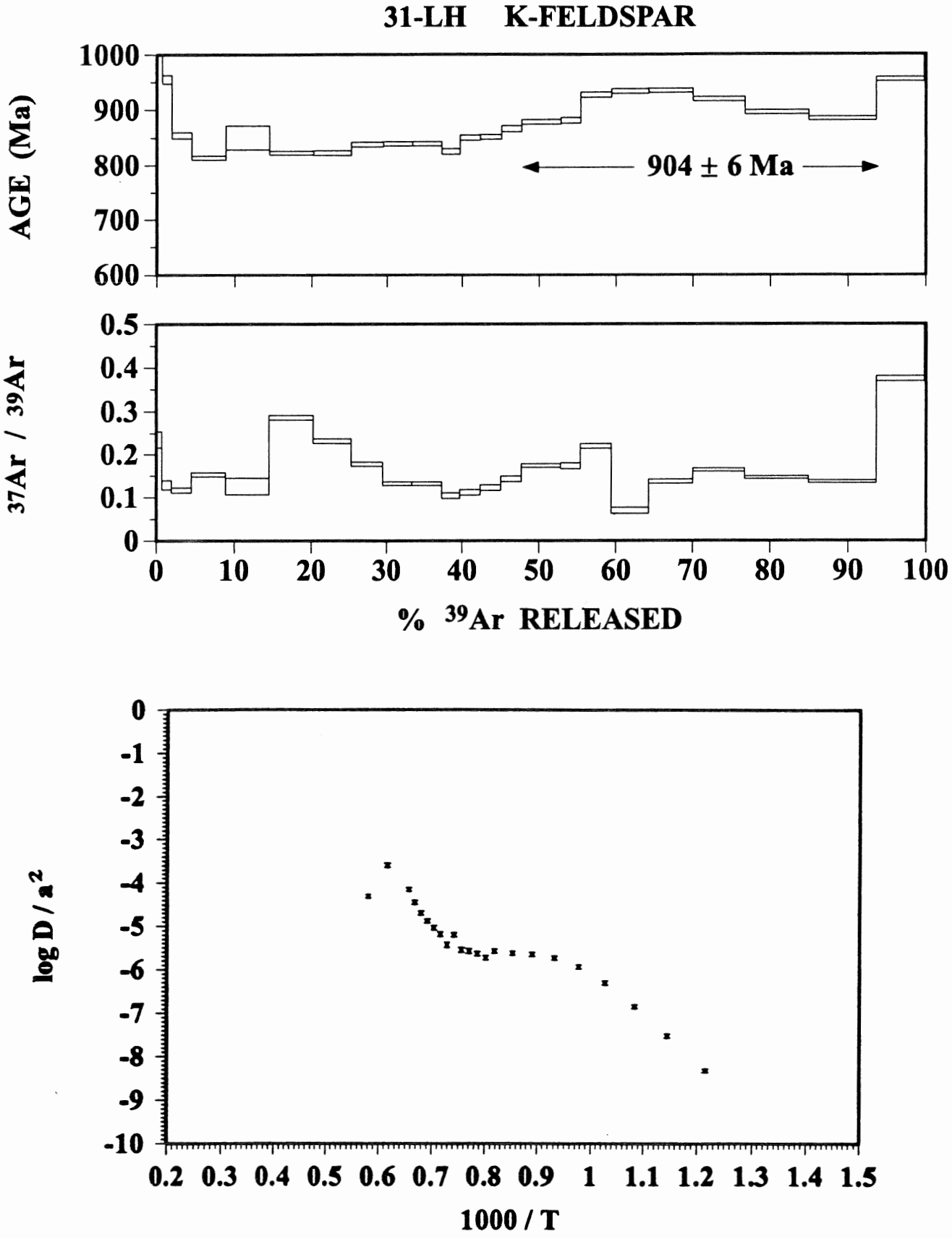

Fig. 12. Results from K-feldspar sample 31. Upper panel shows $^{40}Ar/^{39}Ar$ apparent age spectrum, middle panel shows $^{37}Ar/^{39}Ar$ spectrum (related to Ca/K), bottom panel shows Arrhenius plot. See text for further discussion.

Chapter V - Interpretation

5.1 Introduction

The location and preferred ages of all of the samples dated are shown in Figure 13. Three hornblende ages from the study area obtained by Cosca *et al.* (1991) have also been added to the data set. The three samples, which have ages of 971 ± 8, 948 ± 8 and 977 ±8 (errors at the 2σ level) are from the McClintock subdomain, Muskoka Domain and the the CMBbtz respectively. All three ages were calculated from concordant spectra, and "plateau ages" were selected based on similar criteria to those used in this study. Interlaboratory accuracy is expected to be high because the $^{40}Ar/^{39}Ar$ apparent ages were calculated using the same standard, hornblende MMhb-1. All three hornblende ages determined by Cosca *et al.* (1991) are younger than their closest neighbouring sample from this study, however the age differences fall within the range of differences observed between neighbouring samples from this study.

Figure 14 presents a cross-sections of the study area that shows the approximate position of the samples projected to the line A-A' (Figure 13). This approximately NE-SW trending line is roughly perpendicular to local structural boundaries and to the general strike of the Grenville Orogen. All major tectonic boundaries are also shown. Samples were projected to the line A-A' along perpendiculars.

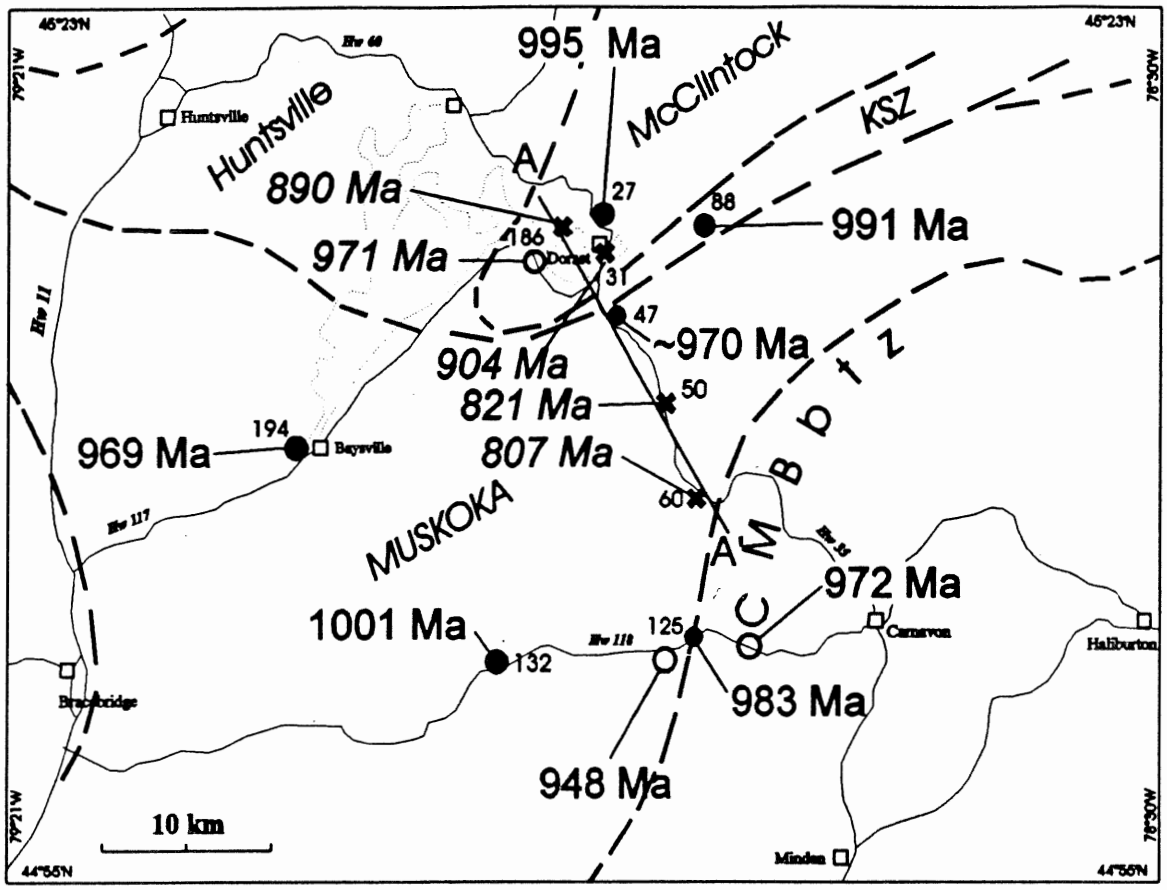

Fig. 13. Summary of preferred $^{40}Ar/^{39}Ar$ ages for the analysed samples; numbers in italics are K-feldspar ages. Also shown are hornblende ages presented by Cosca *et al.* (1991). As discussed in the text, the preferred ages represent concordant plateau or near-plateau ages that also correspond to concordant $^{37}Ar/^{39}Ar$ (related to Ca/K) ratios. For simplicity, errors are not shown, but are generally in the range ± 5 Ma. See text for futher details.

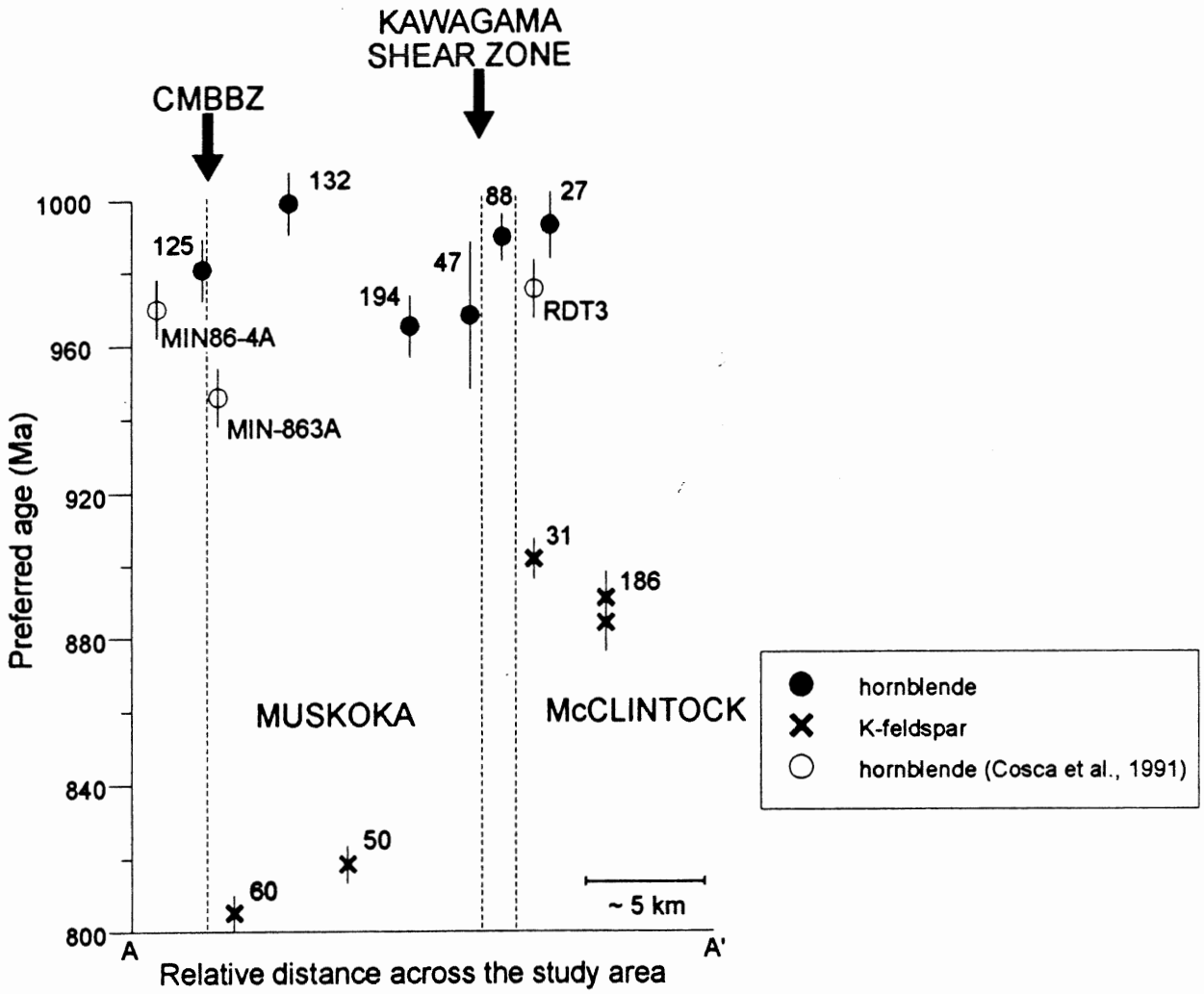

Fig. 14. Preferred ages plotted relative to position along line A-A' (Fig. 13), along with hornblende data from Cosca *et al.* (1991; open circles). Data from samples lying off line A-A' have been projected into the line. The hornblende data show considerable scatter with no clear relationship to lithotectonic unit or structural boundary (cf. data shown in Fig. 3). The reasons for this variation are not yet known. K-feldspar ages from the Muskoka domain are significantly younger than those from the McClintock domain. This could reflect either microstructural variation or contrasting cooling histories, as discussed in the text.

Because the boundaries are curved, the position of some of samples in the western part of the Muskoka domain (194, 125 and the two samples of Cosca *et al.*, 1991) were adjusted to place them within the correct domain.

The apparent ages for both hornblende and K-feldspar show differences between samples at the 95% (2σ) confidence interval that cannot be explained by random variation due to analytical techniques. In any $^{40}Ar/^{39}Ar$ study, two possibilities exist to explain apparent age differences between samples. The first is that the samples have behaved differently with respect to Ar retention and/or diffusion. As discussed above, the closure temperature and diffusion characteristics of a sample depend upon a large number of variables and samples may not always behave as closed systems over geologic time. The second explanation for age differences is that samples have experienced a different cooling history, reaching their closure temperature at different times or experiencing different cooling rates. Differentiating between these two basic scenarios is not always straightforward. The evidence supporting differences in $^{40}Ar/^{39}Ar$ systematics versus differences in cooling history will be evaluated separately for the hornblende and feldspar data.

5.2 Hornblende

The preferred ages of the hornblende samples (including those of Cosca *et al.* (1991)), range from 948 ± 8 Ma (RDT-3) to 1001 ± 9 Ma (132) with an average of 979 Ma. In general, these dates fall well within the range of hornblende ages determined for

other parts of the CGB (e.g. 1005-990- Ma for the Grenville Front Tectonic Zone, 960-990 for the Britt domain, Reynolds *et al.*, 1995).

Various methods were attempted to detect regional trends in the hornblende data. As seen in Figure 14, no correlation was found between the ages of the samples and their position along a cross-section perpendicular to the regional strike. Several other ways of constructing the cross-section were attempted (including plotting the distance from the boundary along a perpendicular to strike (i.e. the distance from the CMBbtz-Muskoka domain boundary measured paralllel to the NW-SE line A-A'), and against the absolute distance from the CMBbtz boundary, and no correlation was found. In the presence of any regional trend, neighbouring samples would be expected to be more similar in age than more distant samples. However, only two pairs of neighbouring samples are indistinguishable within error (27 & 88 and 125 & MIN 86-3), and the maximum difference between apparent ages (53 My) occurs between two samples only ~12 km apart, RDT-3 in the immediate footwall of the CMBbtz and sample 132 approximately 12 km to the east. Even if the data of Cosca *et al.* is not included, no correlation with structural position exists. Without considering the Cosca *et al.* data, there is a 31 My age range within the samples with sample 132 (1001 ± 9 Ma) significantly older than the other ages determined for the Muskoka domain.

These differences in ages across the study area may be related to a difference in closure temperature between the samples. Differences in closure temperature for hornblende can be affected by grain size, microstructures (such as exsollution lamellae, or fracturing). The petrography of the samples was re-examined (see Appendix E)to

determine whether the ages recorded could be related to a systematic variation in grain size or texture, however no consistent pattern emerges.

It has also been suggested that chemical composition of hornblende, in particular the Fe/(Fe + Mg) ratio, may affect its closure temperature. Since the rocks dated come from a variety of rock types, some degree of compositional difference is likely present. However, electron microprobe analysis of the hornblende samples was not performed, it is difficult to asses to whether or not there is any correlation between composition and apparent age. Examination of the hornblende grains using electron microscopy might also reveal microtextures, (e.g. exsolution lamellae, microfractures and fission tracks) which can serve as pathways for Ar diffusion, affecting the calculated closure temperature (Lee, 1995).

The presence of excess argon was recognized in sample 47 based on its U-shaped age spectrum. However, not all samples bearing excess argon will show this pattern (Harrison, 1990). Samples with excess argon can give plateau-type ages that are unrealistically old (e.g. Haggart, 1991). The inverse isochron method was attempted on the other hornblende samples to detect the presence of excess argon, however the inverse isochron lines were poorly defined due to clustering of the data points. It is possible that a component of excess argon could be present in one or more of the samples that yielded concordant spectra.

In brief, no regional difference in cooling history is present, it cannot be detected from the present hornblende dataset. Age differences between samples may be a result of

differences in closure temperature (in turn related to textural and/or compositional differences betweeen the hornblendes) or related to the gain or loss of radiogenic argon.

5.3 Feldspar

The apparent ages of the two samples for the Muskoka domain (807 ± 5 Ma and 820 ± 5 Ma for samples 60 and 50 respectively) are significantly younger than the two apparent ages obtained from the McClintock subdomain (890 ± 8 Ma and 904 ± 15 Ma). Again, it is very difficult to distinguish the effects of differences in cooling history or differences in the argon retention.

As discussed in the Results section, the age spectra, $^{37}Ar/^{39}Ar$ spectra and Arrhenius plots for the four locations show different patterns. For example, sample 50 yieded a relatively concordant spectrum. With the exception of a single kink, the Arrhenius plot data points form a linear array. In contrast, both grains from location 186 yielded age spectra with a staircase pattern at low gas release. Their respective Arrhenius plots are complex, with multiple kinks. Although these differences are only qualitative, they indicate that Ar retention systematics may have been different for each of the samples. However, the data from the Muskoka domain (samples 60 and 50) do not appear more similar to each other than to the two samples from the McClintock domain. Modelling of the diffusion behavior of the K-feldspars should be attempted to provide better estimates of closure temperatures, and determine whether the older apparent ages for the McClintock domain are due to higher closure temperature. The differences in

step-heating data may also relate to differences in diffusion related to the microtextures present, and further study of these textures is necessary.

The other explanation for these data is that the ~70 M.y. age difference between the Muskoka and McClintock K-feldspar ages reflects a genuine difference in cooling history, with samples from the McClintock domain passing through closure temperature (~350°C) before those in the Muskoka domain. This is inconsistent with the present structural position of the two domains.

As seen in Figure 2, the McClintock subdomain is presently located at a greater structural depth as it is more deeply buried beneath the CMBbtz than the Muskoka domain. Assuming no major difference in exhumation rate was present across the area, the McClintock subdomain would therefore be expected to have cooled later than the Muskoka domain. That is, the McClintock subdomain would be expected to have younger K-feldspar ages than the overlying Muskoka domain. However, the opposite is true, with the Muskoka domain reaching the K-feldspar closure temperature ~70 M.y. later than the McClintock subdomain.

This age difference may indicate that differential unroofing occurred between the McClintock subdomain and Muskoka domain between ~ 970 Ma and ~900 Ma (i.e., between the time at which the units passed though the closure temperature for hornblende and K-felspar respectively). This offset would therefore indicate tectonic activity such that rocks with different cooling histories were juxtaposed. The units may have been offset along the Kawagama Shear Zone. The structural relationships across this zone are

poorly understood. Further investigation of this area are warranted to determine whether differential unroofing occurred.

5.4 Cooling history

Cooling histories for the two domains have been constructed on the assumption that these differences in age are real, and not a function of the $^{40}Ar/^{39}Ar$ artifacts. The hornblende and K-feldspar ages obtained from the Muskoka and McClintock domain were plotted versus assumed closure temperatures of 500 ± 50 °C and 350 ± 75°C in order to produce cooling curves. Estimates for the timing and temperature of peak metamorphism are based on thermobarometry and U/Pb dating by Timmermann (1996).

Estimates of the cooling rate over the ~500-200°C range were calculated for each domain. A mean estimate for cooling rate was calculated by taking the mean ages at the assumed closure temperatures of 500°C to 350°C. An estimate for the maximum rate based on these data was calculated using the youngest possible age estimate for hornblende (including error), at the maximum closure temperature (550°C), to the the minimum K-feldspar age at maximum closure temperature (and vice versa to calculate the maximum rate).

In the McClintock domain, estimates for cooling rate range from ~0.2-5.3°C My with a mean of cooling rate of 1.5 °C/M.y. In the Muskoka domain, estimated cooling rates range from approximately 0.1°C to 2.4°C, with a mean of 0.7°C/M.y.

Two U/Pb age determinations on titanite from location 194 provide and estimate for cooling through ~600° C at ~990 Ma (H. Timmermann, unpublished data). Based on

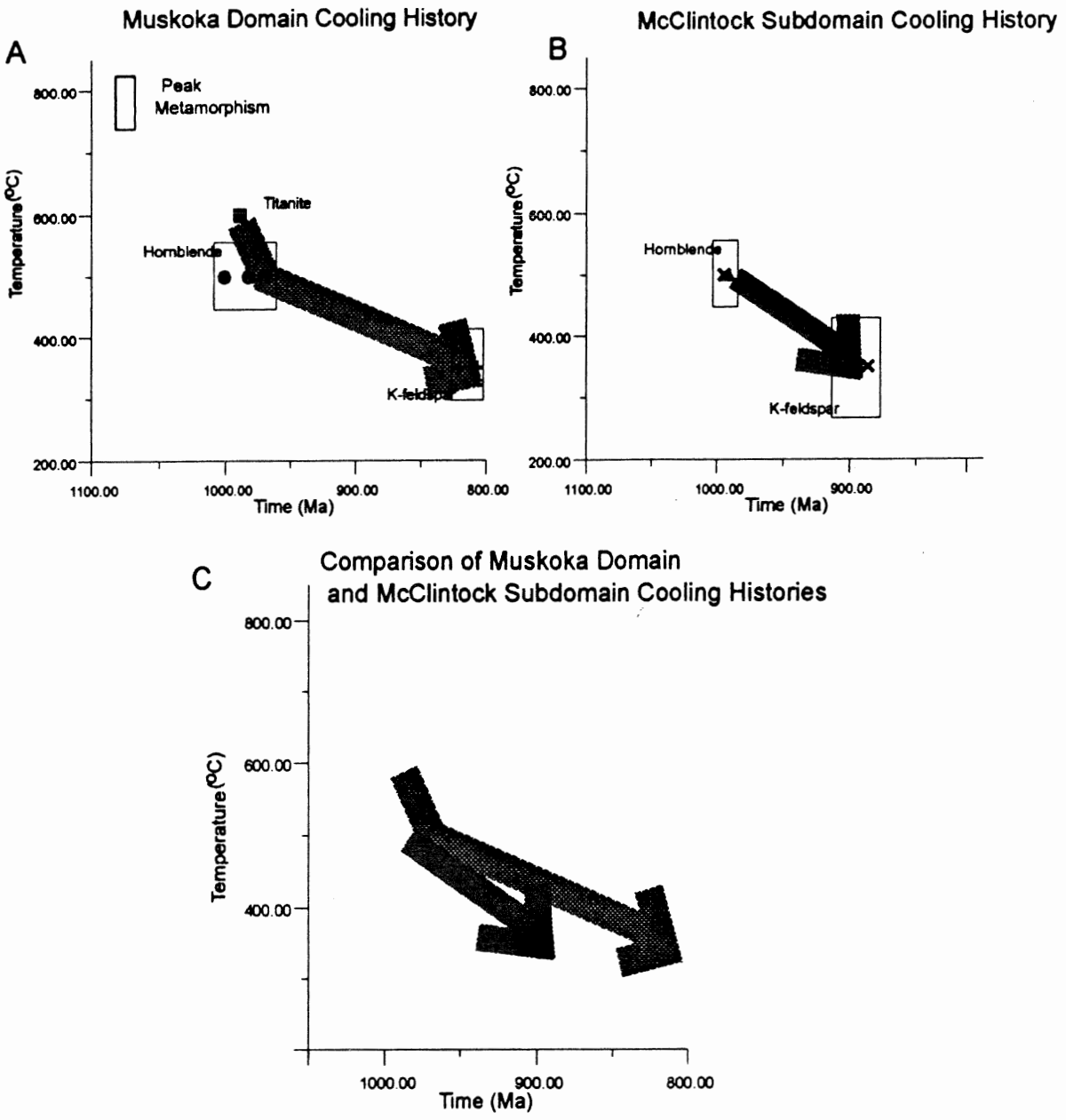

Fig. 15. Temperature-time plots for the Muskoka (A) and McClintock (B) (sub)domains, assuming that the contrasting K-feldspar ages from these two domains are related to cooling history and not microstructural differences. Heavy arrows join data from coexisting minerals in single samples, assuming mean closure temperatures discussed in the text. Muskoka domain plot includes estimate of peak metamorphic temperature at ca. 1080 Ma (Timmermann *et al.*, in press) and unpublished titanite data from sample 194 (Timmermann, 1996). These data suggest that cooling over the range 600-500°C was more rapid than cooling over the range 500-350°C. Comparable data are not yet available from the McClintock subdomain. (C) Comparison of cooling histories from the two regions, showing that the McClintock domain apparently cooled more rapidly and somewhat earlier than the Muskoka domain over the temperature range 500-350°C. This is inconsistent with its present structural position, since the McClintock subdomain is more deeply buried beneath the CMBbtz.

this age and the hornblende $^{40}Ar/^{39}Ar$ age for this location, cooling over the range of ~600-500°C is estimated to have taken place at ~4-5°C / M.y., indicating a decrease in cooling rate over time.

5.5 Future work

Future work is necessary in order to better constrain the cooling history of the footwall of the CMBbtz. Study of the hornblende samples under optical microscope, and the local geology failed to produce conclusive reasons for the variation in hornblende ages across the study area. More samples should be dated to provide higher data density. More data is necessary to reveal regional trends in the data, so that anomalies due to sample composition or excess Ar can be detected. Future work on the hornblende samples dated in this study should include electron microprobe work to determine whether the apparent ages are correlated to chemical composition.

Further work on K-feldspars dated in this study should include modelling of the diffusion results to provide a better estimate for the closure temperature. More samples should be obtained from accross the study area. As the microtextures may play a role in the age obtained, similar grains should be sought. The method used to prepare the coarse-grained samples (removing them from thick-sections), can be used to document the texture and composition of the grain before dating, and may be useful for dating grains in which more than one type of grains are present. If possible, samples of other minerals from the locations in this study should be dated to permit the calculation of cooling rates at a given location, and to check the consistancy of results.

Chapter VI - Conclusions

1. Results for hornblende show a 31 My age difference within the study area, ranging from a minimum of 969 ± 9 Ma for sample 194 to a maximum of 1001 ± 9 Ma for sample 132. Excess argon is present in one of the samples. No correlation with structural position is evident from the present dataset.

2. Results from K-feldspar analyses from the McClintock subdomain are ~70 My older than those in the Muskoka domain. Qualitative comparison of the results suggests the samples behaved differently during the step-wise heating experiments. These differences may be related to differences in microstructures.

3. Approximate cooling rates for the Muskoka and McClintock domain were calculated based on the available data. Co-existing titanite and hornblende from one location in the Muskoka domain suggest more rapid cooling (~5°C/My) over the temperature interval 600-500°C followed by slower cooling (~0.7°C/My). McClintock domain cooling rates calculated between hornblende and K-feldspar closure are on average faster than in the Muskoka domain, however they overlap within error.

4. Further work should include modelling of the K-feldspar spectra. More $^{40}Ar/^{39}Ar$ data are necessary to constrain the cooling history of this area.

References

Alexander, E.C., Michelson, G.M., and Lanphere, M.A., MMHb-1: A new $^{40}Ar/^{39}Ar$ dating standard, Short Paper, 4th International Conference on Geochronology, Cosmochronology and Isotope Geology, *United States Geological Survey, Open File Report 78-701*, 6-8, 1978.

Bowen, M. Isotopes in the Earth Sciences, Elsevier, London, 1988.

Cliff, R.A., Isotopic dating in metamorphic belts, *Geological Society of London Journal, 142*, 97-110, 1985.

Cosca, M.A., Sutter, J.F., and Essene, E.J., Cooling and inferred uplift/erosion history of the Grenville orogen, Ontario: Constraints from $^{40}Ar/^{39}Ar$ thermochronology. *Tectonics, 10*, 959-977, 1991.

Cosca, M.A., Essene, E.J., Kunk, M.J., and Sutter, J.F., Differential unroofing within the Central Metasedimentary Belt of the Grenville orogen: Constraints from $^{40}Ar/^{39}Ar$ thermochronology, *Contributions to Mineralogy and Petrology, 110*, 211-225, 1992.

Culshaw, N., Jamieson, R.A., Ketchum, J.W.F., Wodicka, N., Corrigan, D., and Reynolds, P.H., Transect across the northwestern Grenville orogen, Georgian Bay, Ontario: Polystage convergence and extension in the lower orogenic crust, *Tectonics*, in press.

Culshaw, N., Reynolds, P.H., and Check, G., A $^{40}Ar/^{39}Ar$ study of post-tectonic cooling in the Britt domain of the Grenville Province, Ontario, *Earth and Planetary Science Letters, 105*, 405-415, 1991.

Davidson, A., Identification of ductile shear zones in the southwestern Grenville Province of the Canadian Shield, in *Precambrian Tectonics Illustrated*, edited by A. Kröner and R. Greiling, Schweizerbart'sche Verlagsbuchhandlung, Stuttgart, 263-279, 1984.

Davidson, A., New interpretations in the southwestern Grenville Province, in *The Grenville Province*, edited by J.M. Moore, A. Davidson, and A.J. Baer, *Geological Association of Canada, Special Paper 31*, 61-74, 1986.

Dodson, M.H., Closure temperatures in cooling geochronological and petrological systems, *Contributions to Mineralogy and Petrology, 40*, 250-274, 1973.

Easton, R.M., The Grenville Province and the Proterozoic history of central and southern Ontario, in *Geology of Ontario,* edited by P.C. Thurston, H.R. Williams, R.H. Sutcliffe, and G.M. Stott, *Ontario Geological Survey, Special Volume 4*, Part 2, 715-904, 1992.

Fleck, R.J., J.F. Sutter, Elliot, D.H., Interpretation of discordant $^{40}Ar/^{39}Ar$ age spectra of Mesozoic tholeiites from Antarctica, *Geochimica et Cosmochimica Acta, 41*, 15-32, 1977.

Haggart, M.J., Thermal history of the Grenville Front Tectonic Zone, Central Ontario, M.Sc. thesis, Dalhousie University, Halifax, Nova Scotia, 1991.

Haggart, M.J., Jamieson, R.A., Reynolds, P.H., Krogh, T.E., Beaumont, C., and Culshaw, N.G., Last gasp of the Grenville orogeny: Thermochronology of the Grenville Front Tectonic Zone near Killarney, Ontario, *Journal of Geology, 101*, 575-589, 1993.

Hanmer, S., and McEachern, S., Kinematical and rheological evolution of a crustal-scale ductile thrust zone, Central Metasedimentary Belt, Grenville orogen, Ontario, *Canadian Journal of Earth Sciences, 29,* 1779-1790, 1992.

Harrison, T.M., Diffusion of ^{40}Ar in hornblende, *Contributions to Mineralogy and Petrology, 78,* 324-331, 1981.

Harrison, T.M., Some observations on the interpretation of $^{40}Ar/^{39}Ar$ age spectra, *Isotope Geoscience, 1,* 319-338, 1983.

Harrison, T.M., Some observations on the interpretation of feldspar $^{40}Ar/^{39}Ar$ results, *Chemical Geology (Isotope Geoscience Section), 80,* 219-229, 1990.

Jamieson, R.A., P-T-t paths of collisional orogens, *Geologische Rundschau, 80,* 321-332, 1991.

Korenman, I.M., Analytical Chemistry of Potassium, Humphrey Science Publishers, Ann Arbour, 1969.

Lee, J.K.W., Multipath diffusion in geochronology, *Contributions to Mineralogy and Petrology, 120,* 60-82, 1995.

Lovera, O.M., Richter, F.M., and Harrison, T.M., Diffusion domains determined by ^{39}Ar release during step-heating, *Journal of Geophysical Research, 96,* 2057-2069, 1991.

McDougall, I., and Harrison, T.M., Geochronology and Thermochronology by the $^{40}Ar/^{39}Ar$ Method, Oxford University Press, New York, 1988.

McEachern, S.J., and van Breemen, O., Ages of deformation within the Central Metasedimentary Belt boundary thrust zone, southwest Grenville orogen:

Constraints on the collision of the mid-Proterozoic Elzevir terrane, *Canadian Journal of Earth Sciences, 30*, 1155-1165, 1993.

Nadeau, L., Tectonic, thermal and magmatic evolution of the Central Gneiss Belt, Huntsville region, southwestern Grenville orogen, Ph.D. thesis, Carleton University, Ottawa, Ontario, 1990.

Onstott, T.C., and Peacock, M.W., Argon retentivity of hornblendes: A field experiment in a slowly cooled metamorphic terrane, *Geochimica et Cosmochimica Acta, 51*, 2891-2903, 1987.

Reynolds, P.H., Culshaw, N.G., Jamieson, R.A., Grant, S.L., and McKenzie, K., $^{40}Ar/^{39}Ar$ traverse: Grenville Front Tectonic Zone to Britt Domain, Grenville Province, Ontario, Canada, *Journal of Metamorphic Geology, 13*, 209-221, 1995.

Rivers, T., Martignole, J., Gower, C.F., and Davidson, A., New tectonic divisions of the Grenville Province, southeast Canadian Shield, *Tectonics, 8*, 63-84, 1989.

Sampson, S.D., and Alexander, E.C., Calibration of the interlaboratory $^{40}Ar/^{39}Ar$ dating standard, *Chemical Geology, 66*, 27-34, 1987.

Schau, M., Davidson, A., and Carmichael, D.M., Granulites and granulites, Field Trip 6 Guidebook, Geological Association of Canada - Mineralogical Association of Canada - Canadian Geophysical Union, Joint Annual Meeting, Ottawa, 1986.

Timmermann, H., Petrology and geochronology of the Muskoka domain, Grenville Province, Ontario, Canada, Unpublished report to Deutscher Akademischer Austauschdienst, 1996.

Timmermann, H., Parrish, R.R., Jamieson, R.A., and Culshaw, N.G., Time of metamorphism beneath the Central Metasedimentary Belt boundary thrust zone, Grenville orogen, Ontario: Accretion at 1080 Ma?, *Canadian Journal of Earth Sciences*, in press.

Wynne-Edwards, H.R., The Grenville Province, in *Variations in Tectonic Styles in Canada*, edited by R.A. Price, and R.J.W. Douglas, *Geological Association of Canada, Special Paper 11*, 263-334, 1972.

Appendix A - Samples

Sample	Full Sample Name	Rock type	Locality	Domain	Northing	Easting
194	HT-95-194-G1	leucosome-free protolith of migmatitic orthogneisses	194a; Hw117 SW of Baysville	Muskoka Domain	5000200	647550
50	HT-94-50d-G2	leucocratic granulite vein, cuts amph.-facies migmatitic orthogneisses	50d; Hw35 S of Raven Lake	Muskoka Domain	5006280	668090
60	HT-95-60-G2	pink, coarse, foliated granitoid	60b; Hw 35 St. Nora's Lake	Muskoka Domain	4998160	671670
18	HT-94-18a-6	Gt-rich calcsilicate layer	Hw 35; Birkendale	McClintock Subdomain of Algonquin Domain	5016600	661300
186	HT-95-186f-G1	megacrystic granitoid	Sea Breeze Road NW of Dorset	McClintock Subdomain of Algonquin Domain	5013250	663270
27	HT-94-27-8	foliated Gt-rich mafic band	Hw 35, NW of Dorset	McClintock Subdomain of Algonquin Domain	5014200	664400
132	HT-95-132b-G2	nonmigmatitic granulite (associated with amph.facies migm. orthogneisses)	Hw118 West	Muskoka Domain	4988490	659430
47	HT-47d-2	amphibolite lense in pink felsic gneiss	Hw 35, S of Dorset	Muskoka Domain	5007600	667000
31	HT-95-31-G2	intermediate grey, foliated vein, cuts leucosomes of p.g./metapelitic host	31; Hw 35 Dorset	McClintock Subdomain of Algonquin Domain	5012740	665720
88	HT-94-88j-3	Gt-bearing amphibolite lense	Kawagama Lake Rd, NE of Dorset	Kawagama Shear Zone	5012700	669800
125	HT-94-125d-2	anorthosite	Hw 118 W, Hindon Hill	Central Metasedimentary Belt boundary thrust zone	4989700	670500

Appendix B - Radiogenic Dating theory and equations

(modified from McDougall and Harrison, 1988)

A-1 Derivation of general radiometric dating equations

The decay of radioactive "parent" atoms to radiogenic "daughter" atoms has been observed to take place at a rate that is proportional to the number of parent atoms present (N). Expressed mathematically:

$$- dN/ dt = \lambda N \qquad (A.1.1)$$

where dN/dt represents the rate of decay of parent atoms (negative as the rate decreases with time) and λ is a constant, characteristic of the radionuclide in question. Called the decay constant, λ represents the probability that an atom will decay in one time unit.

In radiometric dating, we are interested in the total number of atoms which have decayed as this is dependant on the amount of time elapsed, i.e. the age of the sample. This can be obtained by integrating equation A.1.1:

$$\int_{No}^{N} \frac{dN}{dt} = -\int_{0}^{t} \lambda \, dt \qquad (A.1.2)$$

where N_o is the original number of atoms present, and N is the number remaining at time t. If no daughter product is initially present, this integration is equivalent to:

$$\ln (N/N_o) = -\lambda t$$

(A.1.3)

which can be rewritten:

$$N = N_o \cdot e^{-\lambda t} \qquad (A.1.4)$$

If each parent atom decays to produce one daughter atom (D) the sum of parent and daugthter isotopes at any given time will be equal to the original number of parent (N_o), i.e.,

$$N_o = N + D \tag{A.1.5}$$

Substituting this relationship into equation A.1.4 we find:

$$N = (N + D) \cdot e^{-\lambda t} \tag{A.1.6}$$

which can also be expressed in terms of the total number of daughter atoms produced:

$$D = N \cdot (e^{\lambda t} - 1) \tag{A.1.7}$$

By taking the natural logarithm of both sides and rearranging to solve for t , one obtains the basic radiometric age equation. This equation can be used for any closed system where the number of daughter (D) and parent (N) atoms have been measured and the decay constant is accurately known.

$$t = \frac{1}{\lambda} \ln (D/N + 1) \tag{A.1.8}$$

The decay of a radionuclide is often discussed with respect to its half-life ($t_{½}$). The half-life is the length of time required for the decay of a given number of parent atoms to half of its original number. After one half-life has elapsed, the number of parent atoms is equal to the number of daughter atoms such that D/N ratio of equation A.1.7 will be equal to 1 and the equation can be rewritten:

$$t_{½} = \frac{\ln 2}{\lambda} \tag{A.1.9}$$

A-2 K-Ar dating

K-Ar and $^{40}Ar/^{39}Ar$ dating are based on the branched decay of ^{40}K to two stable daughter products ^{40}Ar and ^{40}Ca. The total number of daughter atoms will be equal to the sum of radiogenic ^{40}Ar and ^{40}Ca. Asterisks are used to denoted the radiogenic isotopes (i.e. those produced by the decay of ^{40}K), to differentiate them from ^{40}Ar and ^{40}Ca which were either present initially, or introduced through contamination. As expressed in equation A.1.7, the total number of daughter atoms ($^{40}Ar^*$ and $^{40}Ca^*$) produced is a function of the initial number of parent atoms (^{40}K), the decay constant (λ) and the time elapsed (t):

$$^{40}Ar^* + {}^{40}Ca^* = {}^{40}K \cdot e^{\lambda t} - 1 \qquad (A.2.1)$$

Each branch of the decay can be expressed by a different partial decay constant, with the sum of the partial decay constants equal to λ. The branch of the decay series which produces ^{40}Ar by electron capture has the partial decay constant λ_e. The fraction of ^{40}K that decays to produce ^{40}Ar is equal to the ratio of the partial decay constant (λ_e) to the total decay constant, i.e., λ_e/λ. This fraction can be used to modified equation A.2.1 to express only the $^{40}Ar^*$ produced.

$$^{40}Ar^* = \lambda_e/\lambda \cdot {}^{40}K \cdot e^{\lambda t} - 1 \qquad (A.2.2)$$

Rearranging this equation gives the general age equation used for K/Ar dating:

$$t = \frac{1}{\lambda} \ln \left| \frac{\lambda \cdot {}^{40}Ar^* \cdot e^{\lambda t} + 1}{\lambda_e \, {}^{40}K} \right| \qquad (A.2.3)$$

A-3 $^{40}Ar/^{39}Ar$ dating

During $^{40}Ar/^{39}Ar$ dating the sample is irradiated with both thermal and fast neutrons such that a given proportion of the ^{39}K atoms are tranformed into ^{39}Ar. The number of ^{39}Ar atoms produced from a given sample is given by:

$$^{39}Ar_K = {}^{39}K\ DT \int \phi(\varepsilon)\ \sigma(\varepsilon)\ d\varepsilon \qquad (A.3.1)$$

Where: $^{39}Ar_K$ - numberof atoms of ^{39}Ar produced from ^{39}K; i.e. corrected for interfering isotopes
^{39}K - original number of ^{39}K atoms present in the sample
DT - duration of irradiation
$\phi(\varepsilon)$ - neutron flux density at energy ε
$\sigma(\varepsilon)$ - neutron capture cross-section of at energy ε
$d\varepsilon$ - indicates that the equation is integrated over the whole energy spectrum of the neutrons

In order to determine the age of the sample, we require the ratio of daughter isotopes to parent isotopes. As given in equation A.2.2 the amount of radiogenic Ar ($^{40}Ar^*$) produced by the decay of ^{40}K is expressed by:

$$^{40}Ar^* = \lambda_e/\lambda \cdot {}^{40}K \cdot (e^{\lambda t} - 1) \qquad (A.2.2)$$

Dividing this equation by equation A.3.1 gives the ratio of daughter to parent isotopes i.e., $^{40}Ar^*/^{39}Ar$:

$$\frac{^{40}Ar^*}{^{39}Ar_K} = \frac{\lambda_e/\lambda \cdot {}^{40}K \cdot e^{\lambda t} - 1}{{}^{39}K\ DT \int \phi(\varepsilon)\ \sigma(\varepsilon)\ d\varepsilon} \qquad (A.3.2)$$

In order to simplify calculations a new term J is introduced. It incompasses the irradiation parametres ϕ and σ, which are difficult to measure as well as the duration of irradiation. J also includes the decay constant ratio (λ_e/λ) and the $^{40}K/^{39}K$ ratio, both of which are

constants, such that J is expressed:

$$J = \frac{\lambda_e/\lambda \cdot {}^{40}K}{{}^{39}K} \cdot DT \int \phi(\varepsilon)\, \sigma(\varepsilon)\, d\varepsilon \qquad (A.3.3)$$

In practice, J is determined by irradiating a sample (known as the flux moniter or simply the standard), of known age (t_m) along with the samples of unknown age. The ratio of $^{40}Ar^*$ to ^{39}Ar measured i.e., $(^{40}Ar^* / ^{39}Ar_K)_m$, and age (t_m) of the standard are substituted into the following equation to yield the J value used to calculate the age of all samples with which it was irradiated.

$$J = \frac{e^{\lambda t m} - 1}{(^{40}Ar^* / ^{39}Ar_K)_m} \qquad (A.3.4)$$

The equation expressing the ratio of parent to daughter isotopes (equation A.3.2) can now be simplified and rewritten:

$$\frac{^{40}Ar^*}{^{39}Ar_K} = \frac{e^{\lambda t} - 1}{J} \qquad (A.3.5)$$

Equation 3.2 can be rearrranged to give the $^{40}Ar / ^{39}Ar$ age equation:

$$t = \frac{1}{\lambda} \ln (^{40}Ar^* / ^{39}Ar_K \cdot J + 1) \qquad (A.3.6)$$

Similar in form to the general radiometric dating age equation (A.1.8), this equation permits the calculation of the age of a sample knowing only the ratio of argon isotopes produced, provided the J value has been determined.

Error estimates for the preferred ages of samples in this study are based on the error in J. To obtain the error in J, the measured J-values were plotted versus their position in the irradiation cannister. A regression line is calculated, and the error in J is based on the goodness of fit of the points to this line.

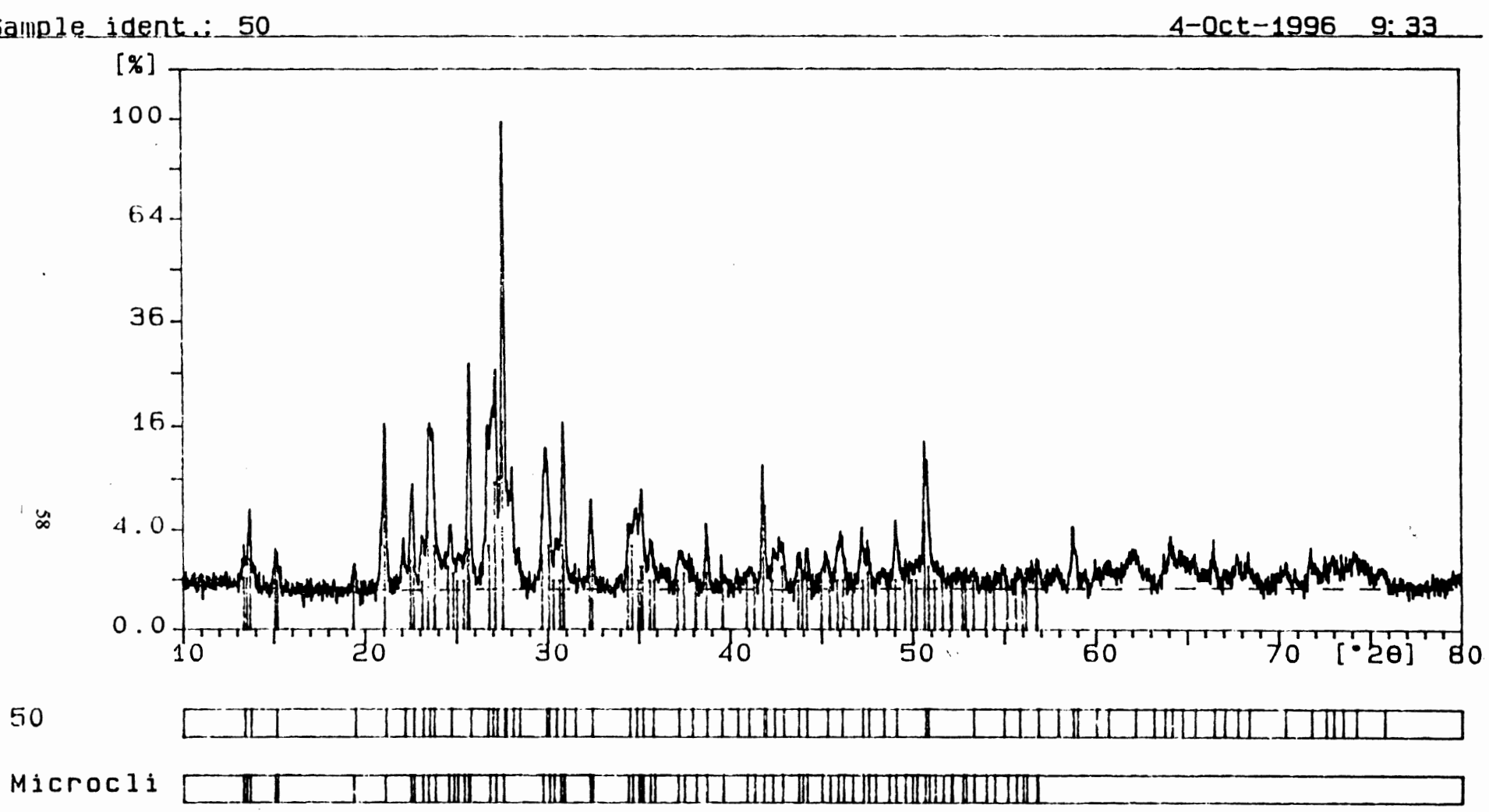
Sample ident.: 50
4-Oct-1996 9:33
[%]
100
64
36
16
4.0
0.0
10
20
30
40
50
60
70
[°2θ]
80
50
Microcli

Analyzed DI file : C:\APD\DATA\50 DI
Sample identification : 50
Last update of results file : 3-Oct-1996 15:21

Database used : C:\IDENTDB

MEASUREMENT PARAMETERS

Diffractometer : PW3710
Start angle [x2i] : 9.995
Final angle [x2f] : 80.005
Step size [x2f] : 0.010
Time per step [s] : 0.5
Anode material : Cu

Date and time of measurement : 2-Oct-1996 16:08

PEAK SEARCH PARAMETERS

Minimum peak width : 0.00
Maximum peak width : 1.00
Peak base width : 2.00
Minimum significance : 0.75

Number of peaks detected : 75

SEARCH-MATCH PARAMETERS

Number of strong lines of the
reference patterns used in SEARCH : 5
Intensity threshold : 3.02
Confidence threshold : 20
Minimum specimen displacement : -40
Maximum specimem displacement : 35
Step size in specimen displacement: 75

Restrictions file : FELD

Results:

	Card. ident.	Match score	Rel m score	I [%]	Name
1	22-0540	5.03	0.84	2	50.Tazheranite
2	31-0966	62.11	0.65	16	110.Orthoclase
3	19-0931	50.99	0.65	16	119.Orthoclase
4	22-1212	35.70	0.61	13	76.Orthoclase
5	10-0353	13.53	0.59	19	144.Sanidine, h n. syn
6	19-0002	25.91	0.54	16	119.Orthoclase ovarian
7	19-0932	40.27	0.51	16	117.Microcline, intermediate
8	38-0353	10.69	0.49	4	73.Dompeaarite

Sample ident.: 31 3-Oct-1996 16:43

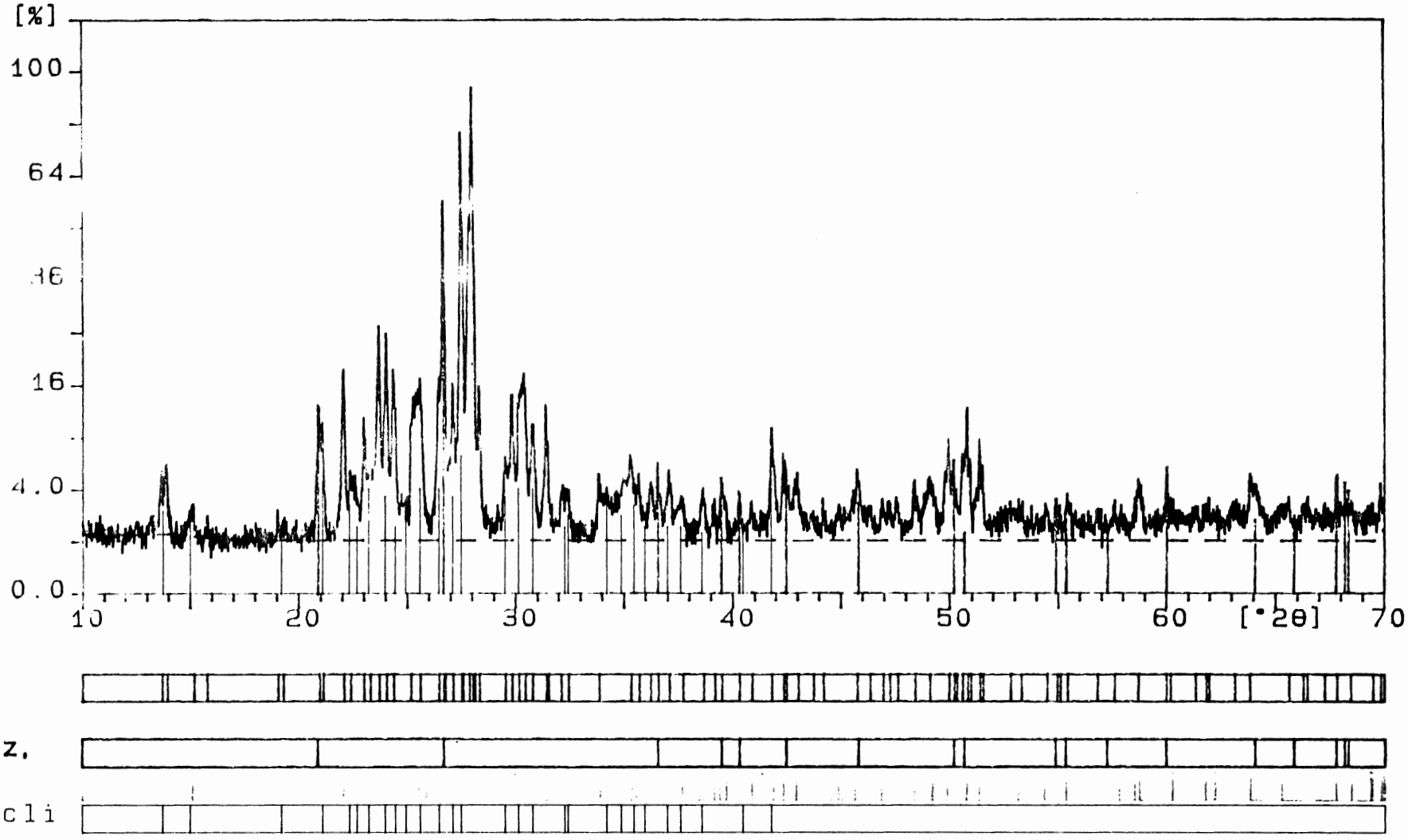

Sample identification: 31
Data measured at: 3-Oct-1996 15:27:00

Diffractometer type: PW3710 BASED
Tube anode: Cu
Generator tension [kV]: 40
Generator current [mA]: 45
Wavelength Alpha1 []: 1.54060

Results:

	Card. ident.	Match score	Rel m score	I [%]	Displ [fm]	Name
1	22-0540	4.27	0.85	4	86	Tazheranite
2	33-1161	14.59	0.81	48	45	Quartz, syn
3	05-0490	14.55	0.81	33	103	Quartz, low
4	42-1417	2.26	0.75	16	-4	Fahleite
5	41-1480	46.04	0.72	48	45	Albite, calcian, ordered
6	09-0457	12.90	0.65	13	65	Albite, calcian, ordered
7	09-0462	19.42	0.61	5	-3	Orthoclase
8	10-0359	12.53	0.60	11	126	Andesine, low

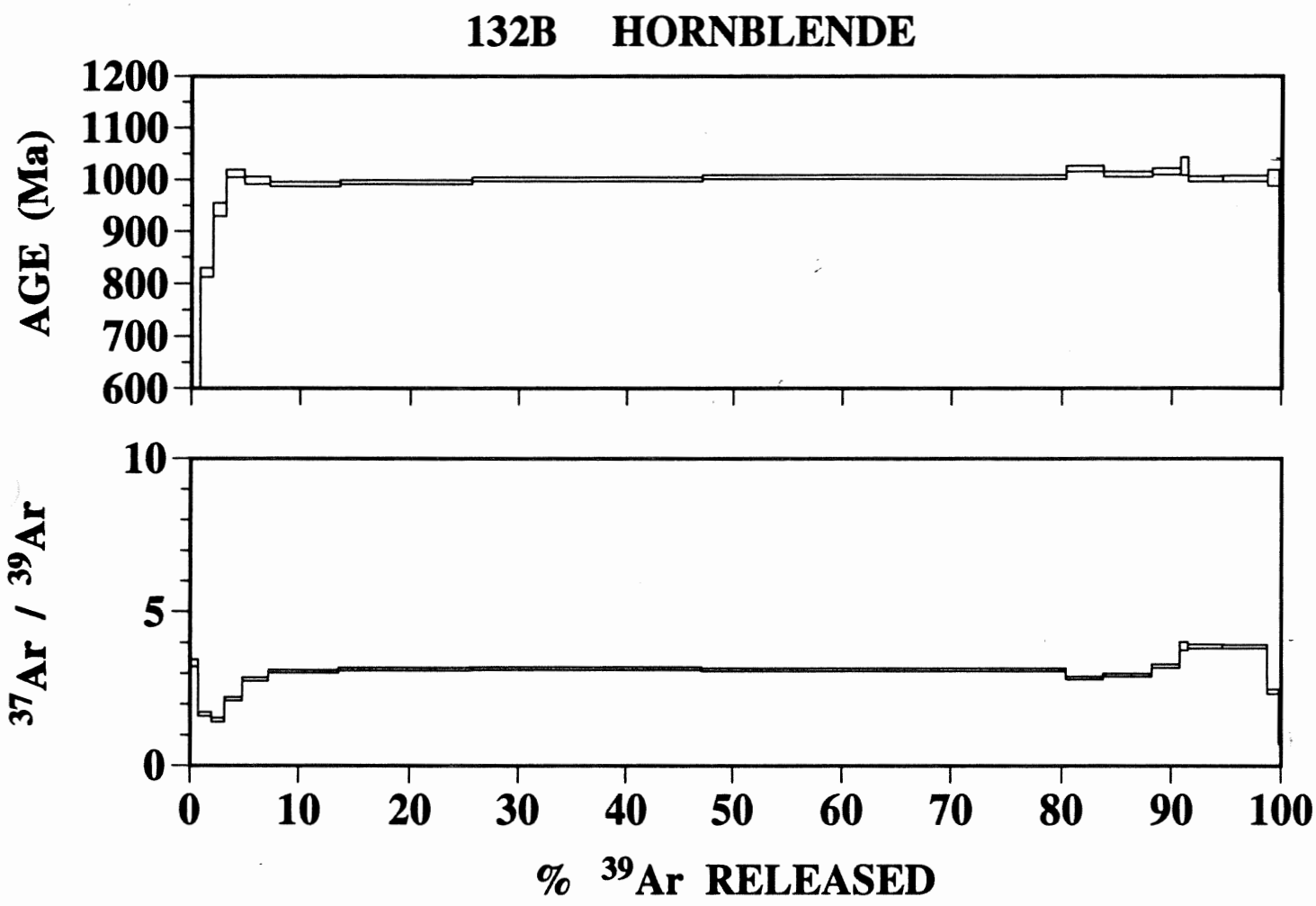
132B HORNBLENDE
AGE (Ma)
1200
1100
1000
900
800
700
600
^{37}Ar / ^{39}Ar
10
5
0
0
10
20
30
40
50
60
70
80
90
100
% ^{39}Ar RELEASED

132B HORNBLENDE SUMMARY

C	mV 39	% 39	AGE (Ma) 1σ	% ATM	37/39	36/40	39/40	% IIC
750	8.7	.8	512 ± 13.9	19.4	3.33	.00066	.005547	.39
850	12.5	1.1	820.7 ± 9	5.5	1.67	.000187	.003709	.15
950	12.4	1.1	942.2 ± 12.5	2.1	1.49	.000074	.003225	.13
1000	17.6	1.6	1012 ± 6.9	.7	2.17	.000027	.002981	.19
1025	25.1	2.3	998.7 ± 6.7	.3	2.81	.000014	.003046	.24
1050	67.3	6.3	991 ± 4.3	.1	3.06	.000005	.003085	.27
1075	127.1	12	995 ± 3.9	.1	3.14	.000005	.003068	.27
1100	226.7	21.4	1000.6 ± 3.8	0	3.15	.000002	.003049	.27
1125	352.4	33.3	1005.2 ± 4	.6	3.12	.000021	.003014	.27
1150	36.2	3.4	1021 ± 5.5	0	2.85	.000003	.002969	.25
1175	46.6	4.4	1010.6 ± 4.8	.1	2.94	.000006	.003006	.25
)0	27.4	2.5	1016.1 ± 5.9	.3	3.23	.000014	.002977	.28
1225	7.4	.7	1026 ± 16.8	2.1	3.88	.000072	.002889	.33
1250	33.4	3.1	1001.6 ± 5.1	.5	3.86	.00002	.003029	.34
1350	43.1	4	1002.7 ± 5.2	1.2	3.86	.000041	.003005	.34
1450	11	1	1003.6 ± 15.2	13.8	2.42	.000469	.002618	.21
1500	2.5	.2	862.8 ± 77.9	53.5	.86	.001813	.001711	.08

TOTAL GAS AGE = 996.3 Ma

MEAN AGE(1050°C-1125°C)= 1000.9 ± 8.899999 Ma (2σ UNCERTAINTY,INCLUDING ERROR IN J)

J = .00228 ± .0000228 (1 %)

ERROR ESTIMATES AT ONE SIGMA LEVEL

37/39,36/40 AND 39/40 Ar RATIOS ARE CORRECTED FOR INTERFERING ISOTOPES

IIC - INTERFERING ISOTOPES CORRECTION

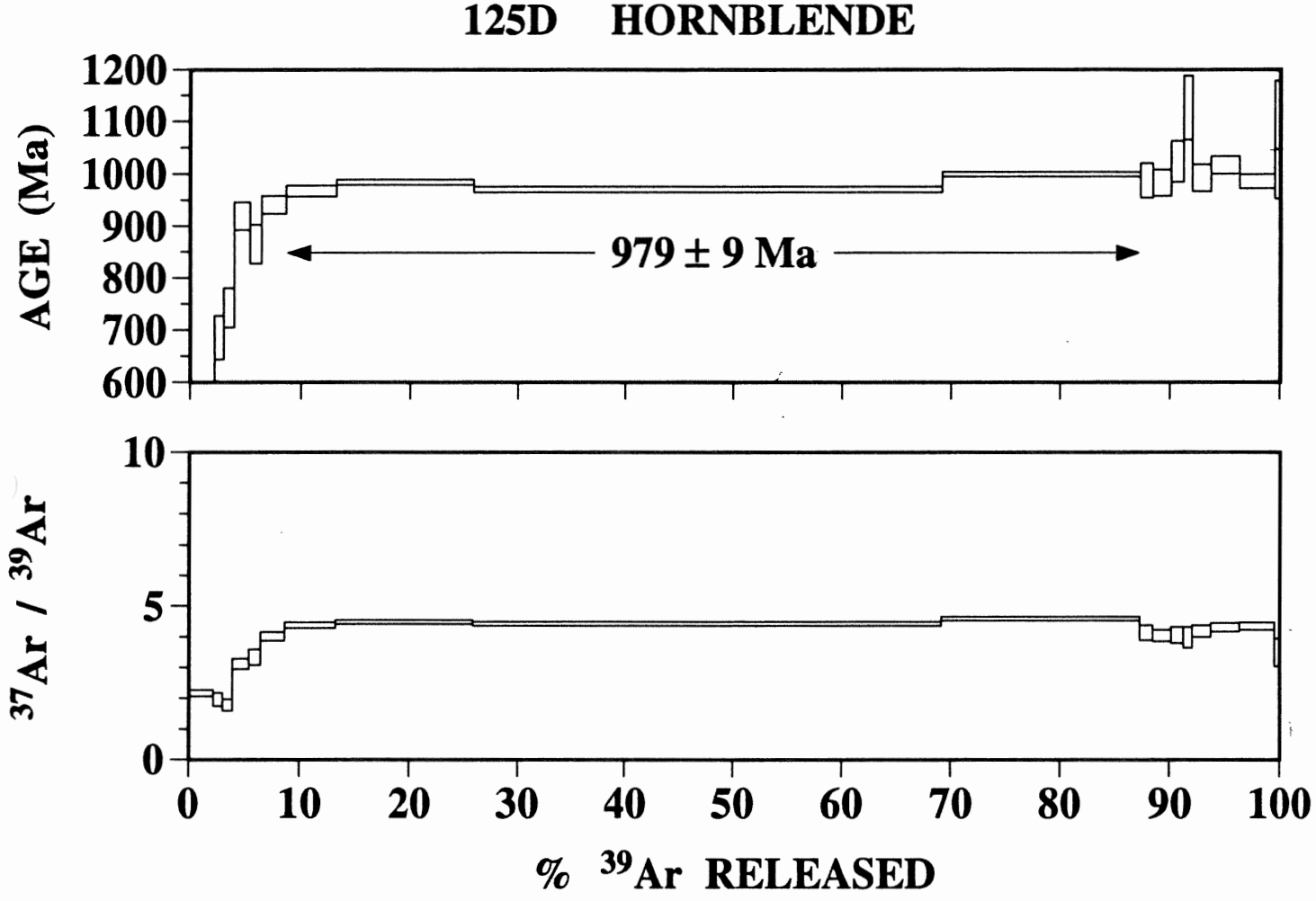
125D HORNBLENDE
AGE (Ma)
1200
1100
1000
900
800
700
600
979 ± 9 Ma
37Ar / 39Ar
10
5
0
0
10
20
30
40
50
60
70
80
90
100
% 39Ar RELEASED

125D HORNBLENDE SUMMARY

°C	mV 39	% 39	AGE (Ma) 1σ	% ATM	37/39	36/40	39/40	% IIC
750	20.4	2.2	361.2 ± 14.2	24.1	2.17	.000817	.007759	.3
850	7.4	.8	685.3 ± 41.3	18.4	1.96	.000623	.004002	.2
950	8.2	.9	742.2 ± 37.4	6.9	1.77	.000235	.004145	.17
1000	13.2	1.4	919.1 ± 26.3	3.2	3.11	.000112	.0033	.28
1025	9	1	865.3 ± 37.6	2.6	3.33	.000092	.003585	.3
1050	19.8	2.2	940.7 ± 17.2	.8	4	.000032	.003283	.36
1075	40.8	4.5	967.6 ± 10.2	.4	4.37	.000018	.003178	.39
1100	113.8	12.6	984.3 ± 5.1	.2	4.46	.00001	.003116	.39
1125	389.5	43.2	970.3 ± 5.9	.3	4.41	.000012	.003172	.39
1150	162.8	18	998.7 ± 4.5	.2	4.58	.000009	.003059	.4
1175	10.7	1.1	987.8 ± 32.7	2.9	4.11	.0001	.003019	.36
1200	14.9	1.6	983.4 ± 24.7	2.6	4.03	.000089	.003047	.35
1225	9.8	1	1023.2 ± 38.8	8.9	4.05	.000303	.002705	.35
1250	7.1	.7	1125.9 ± 61.3	17.7	3.96	.000601	.002152	.33
1300	15.1	1.6	992.4 ± 25.6	5	4.18	.00017	.002936	.37
1350	23.8	2.6	1016.9 ± 17	3.2	4.3	.00011	.002898	.37
1450	28.5	3.1	985.6 ± 13.5	6.4	4.33	.00022	.002917	.38
1500	4.5	.4	1065.2 ± 112	31.5	3.49	.001066	.001929	.3

TOTAL GAS AGE = 963.7 Ma

MEAN AGE(1075°C-1150°C)= 979 ± 8.8 Ma (2σ UNCERTAINTY,INCLUDING ERROR IN J)

J = .002286 ± .000016 (.69 %)

ERROR ESTIMATES AT ONE SIGMA LEVEL

37/39,36/40 AND 39/40 Ar RATIOS ARE CORRECTED FOR INTERFERING ISOTOPES

IIC - INTERFERING ISOTOPES CORRECTION

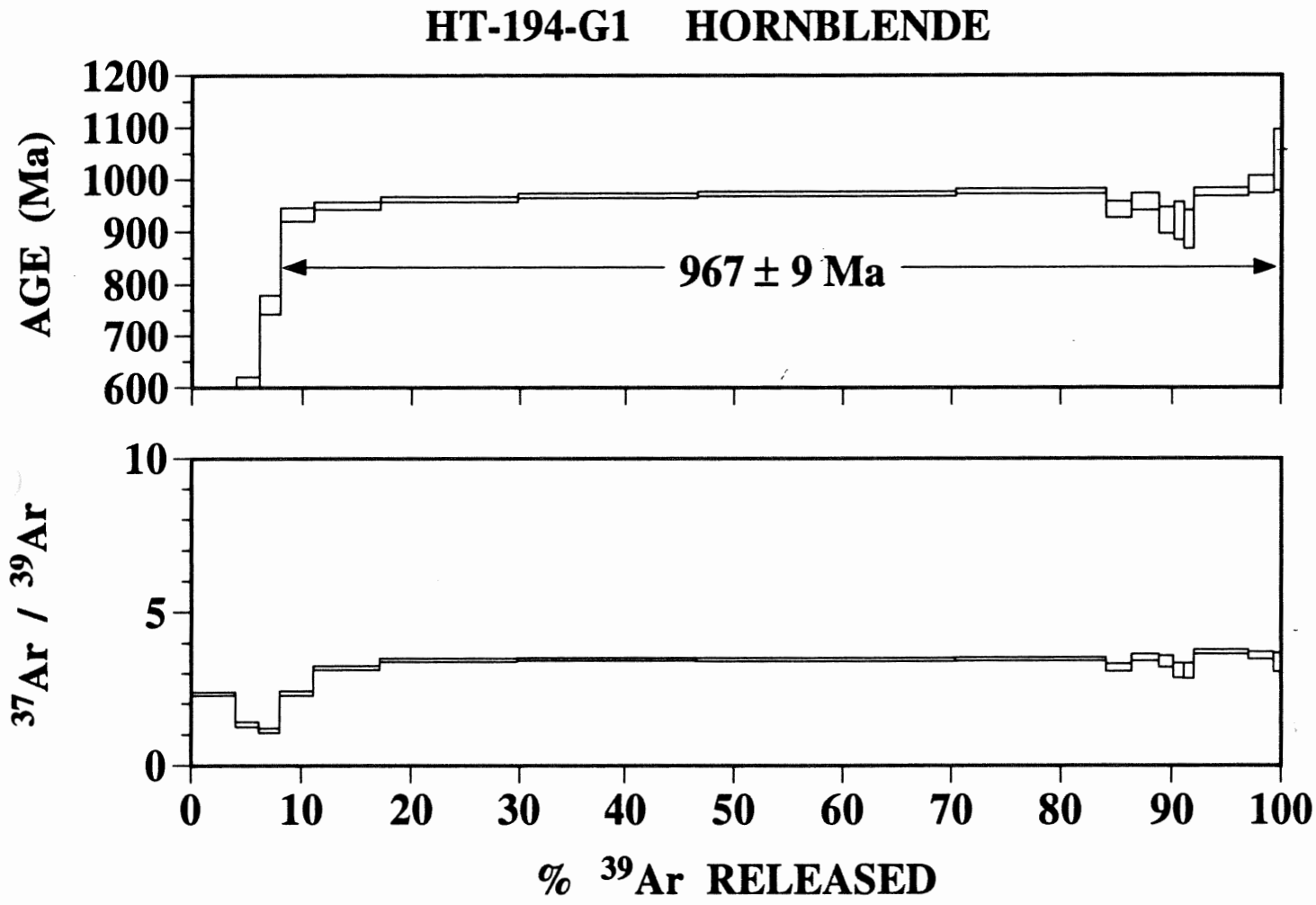
HT-194-G1 HORNBLENDE
AGE (Ma)
1200
1100
1000
900
800
700
600
967 ± 9 Ma
^{37}Ar / ^{39}Ar
10
5
0
0
10
20
30
40
50
60
70
80
90
100
% ^{39}Ar RELEASED

HT-194-G1 HORNBLENDE SUMMARY

C	mV 39	% 39	AGE (Ma) 1σ	% ATM	37/39	36/40	39/40	% IIC
750	40.2	4	423.6 ± 8.9	11.5	2.32	.000391	.007558	.3
850	21	2.1	605.4 ± 15.2	6.9	1.32	.000236	.005275	.14
950	19.1	1.9	760.5 ± 18.1	2.8	1.12	.000095	.004192	.1
1000	30.1	3	933.5 ± 12.5	.8	2.34	.000028	.003309	.21
1025	60.6	6	950 ± 7	.1	3.17	.000007	.003257	.28
1050	125.7	12.5	961.9 ± 4.8	0	3.43	.000003	.003209	.3
1075	168.2	16.8	969.2 ± 4.5	0	3.45	.000003	.003178	.3
1100	237.1	23.7	972.3 ± 4.1	0	3.44	.000002	.003165	.3
1125	137	13.7	977.6 ± 4.7	0	3.46	.000002	.003144	.3
1150	22.7	2.2	942.6 ± 15.4	0	3.19	.000003	.003294	.28
1175	24.4	2.4	957.7 ± 15.8	0	3.52	.000004	.003227	.31
)0	13.5	1.3	922 ± 25.1	.1	3.39	.000008	.003384	.3
1225	9.2	.9	921 ± 36.3	.5	3.1	.000021	.003375	.28
1250	8.9	.8	905 ± 36.8	.4	3.07	.000018	.003454	.28
1300	50	5	975.7 ± 8.1	0	3.71	.000005	.003149	.33
1400	23.2	2.3	990.3 ± 16.8	1.2	3.58	.000042	.003054	.31
1500	6.9	.6	1036.7 ± 58.1	15.8	3.36	.000537	.00245	.29

TOTAL GAS AGE = 936.7 Ma

MEAN AGE(1025°C-1400°C)= 967.1 ± 8.5 Ma (2σ UNCERTAINTY,INCLUDING ERROR IN J)

J = .00228 ± .0000228 (1 %)

ERROR ESTIMATES AT ONE SIGMA LEVEL

37/39,36/40 AND 39/40 Ar RATIOS ARE CORRECTED FOR INTERFERING ISOTOPES

IIC - INTERFERING ISOTOPES CORRECTION

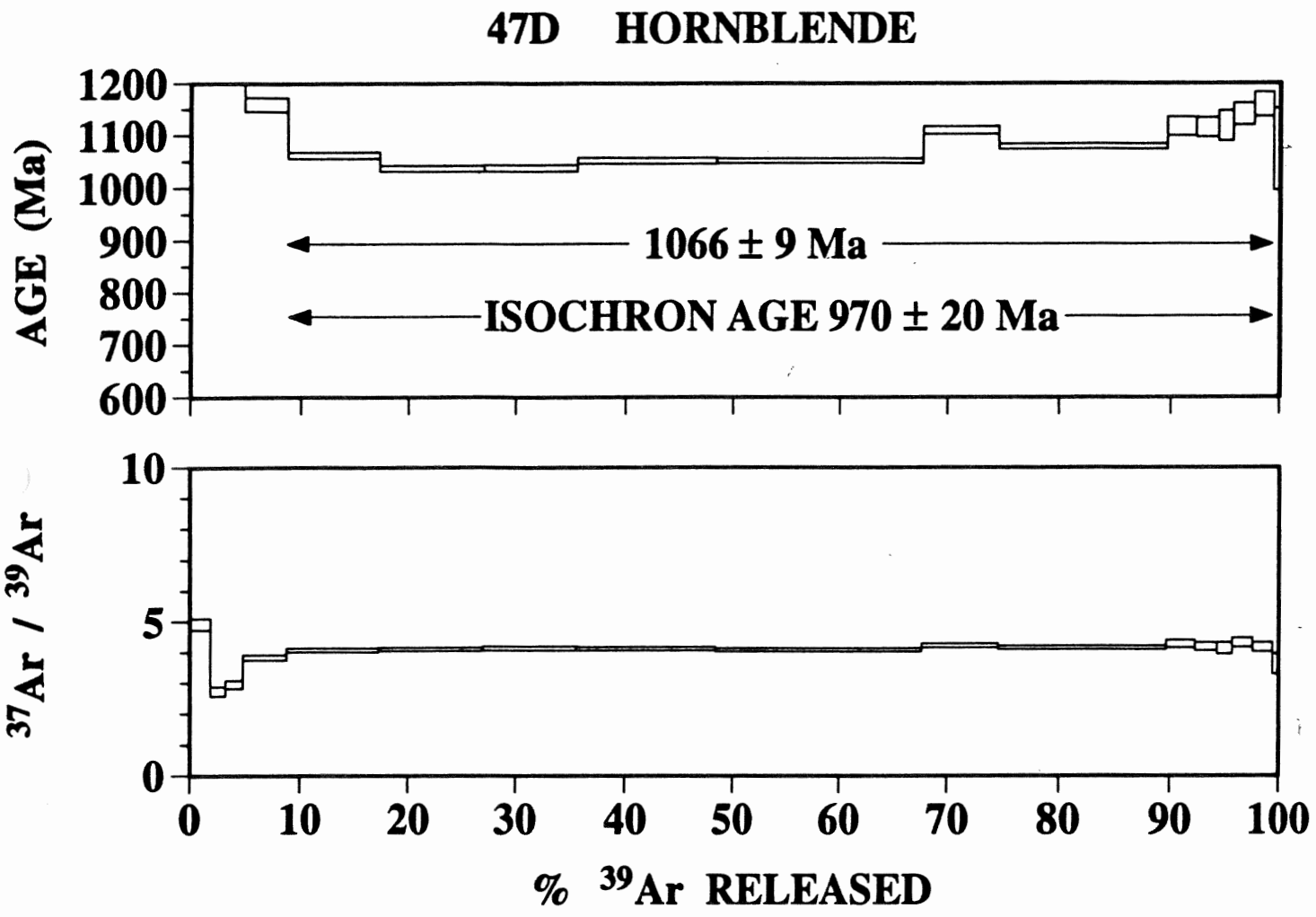
47D HORNBLENDE
AGE (Ma)
1200
1100
1000
900
800
700
600
1066 ± 9 Ma
ISOCHRON AGE 970 ± 20 Ma
37Ar / 39Ar
10
5
0
0
10
20
30
40
50
60
70
80
90
100
% 39Ar RELEASED

47D HORNBLENDE SUMMARY

T°C	mV 39	% 39	AGE (Ma) 1σ	% ATM	37/39	36/40	39/40	% IIC
750	18.6	1.8	1959.6 ± 34.3	3.2	4.91	.000111	.001115	.36
850	13.6	1.3	1466.7 ± 35.6	2.7	2.71	.000093	.001755	.21
950	16	1.5	1413 ± 27.7	1.7	2.94	.000059	.001871	.23
1000	39.6	3.9	1158.4 ± 12.9	.8	3.81	.000028	.002493	.32
1025	85.8	8.5	1061.8 ± 6.4	.3	4.05	.000013	.002814	.35
1050	97.3	9.6	1037 ± 5.5	.1	4.08	.000007	.002909	.35
1075	86.3	8.5	1037.3 ± 5.7	.1	4.1	.000006	.002908	.35
1100	128.2	12.7	1051 ± 5.1	0	4.1	.000004	.00286	.35
1125	194.3	19.3	1050.8 ± 4.4	.1	4.06	.000005	.00286	.35
1150	69	6.8	1109 ± 7	.2	4.2	.000008	.00266	.35
1175	151.2	15	1078.1 ± 4.9	.1	4.13	.000005	.002764	.35
1200	26.3	2.6	1116.3 ± 17.8	.2	4.26	.000009	.002636	.36
1225	20.4	2	1114.9 ± 18.1	0	4.17	.000005	.002644	.35
1250	13.8	1.3	1117.4 ± 28.6	.1	4.12	.000007	.002634	.35
1300	19.4	1.9	1139.7 ± 20.9	.2	4.31	.00001	.002563	.36
1400	18	1.8	1158.5 ± 22.6	1.3	4.15	.000045	.00248	.34
1500	5.9	.5	1073.8 ± 77.5	17.1	3.6	.00058	.002306	.31

TOTAL GAS AGE = 1103.6 Ma

MEAN AGE(1050°C-1125°C)= 1045.9 ± 7.6 Ma (2σ UNCERTAINTY,INCLUDING ERROR IN J)

J = .002282 ± .000016 (.7 %)

ERROR ESTIMATES AT ONE SIGMA LEVEL

37/39,36/40 AND 39/40 Ar RATIOS ARE CORRECTED FOR INTERFERING ISOTOPES

% IIC - INTERFERING ISOTOPES CORRECTION

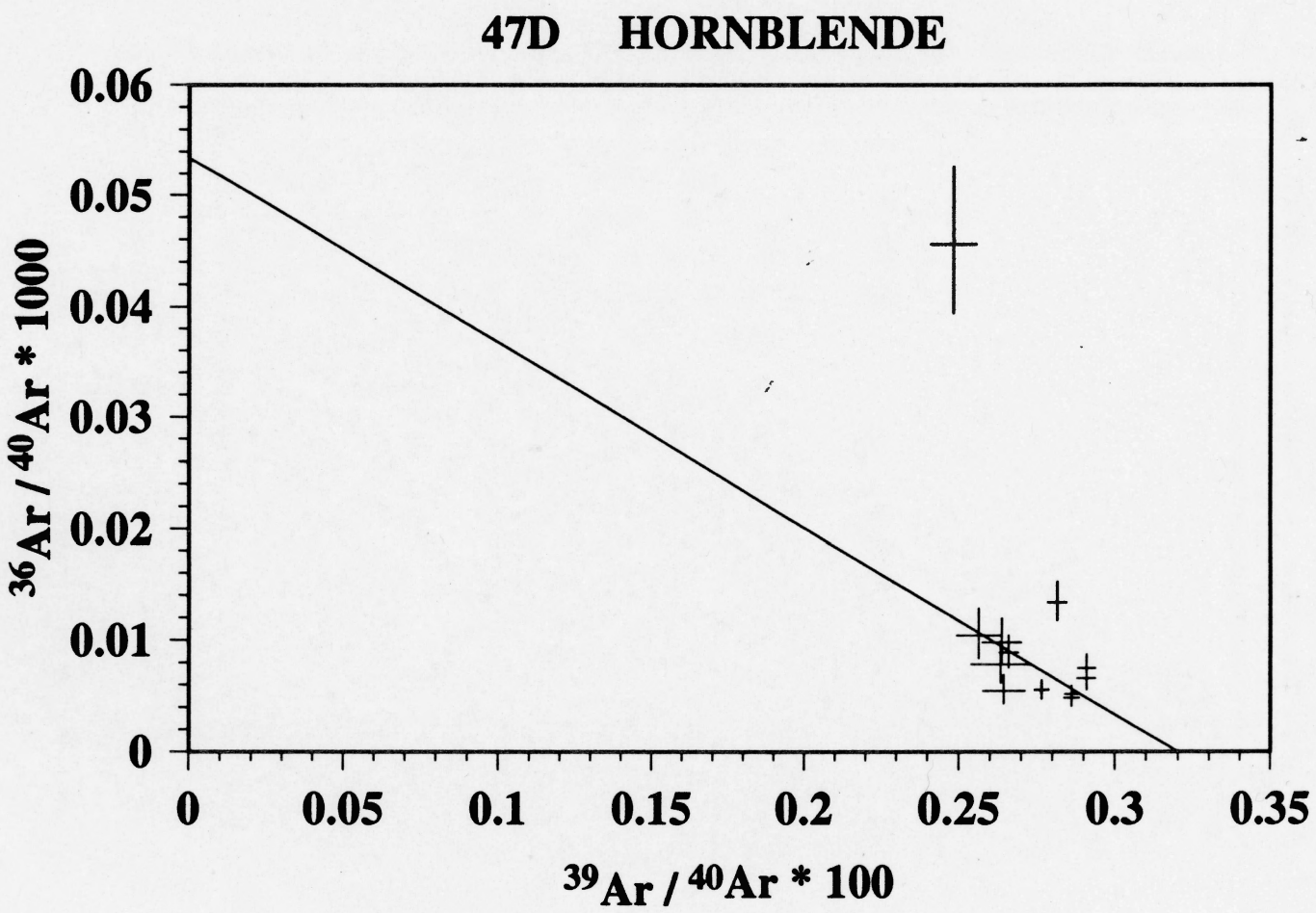
47D HORNBLENDE
0.06
0.05
0.04
0.03
0.02
0.01
0
$^{36}Ar / ^{40}Ar * 1000$
0
0.05
0.1
0.15
0.2
0.25
0.3
0.35
$^{39}Ar / ^{40}Ar * 100$

47D HORNBLENDE ISOCHRON FIT

	T	39Ar/40Ar	%ERR	36Ar/40Ar	%ERR
1	1025	.281468	1.026682	1.334367E-02	13.52467
2	1050	.2909125	.9508921	7.471858E-03	16.13507
3	1075	.2908922	1.002894	6.576719E-03	18.08592
4	1100	.2860429	.8473698	4.835271E-03	17.39238
5	1125	.2860755	.7239285	5.209512E-03	13.52993
6	1150	.2660159	1.126094	8.848449E-03	17.20882
7	1175	.2764763	.7910842	5.546788E-03	15.39669
8	1200	.263674	2.366913	9.728772E-03	22.19854
9	1225	.2644459	2.566507	5.45457E-03	25.24619
10	1250	.2634758	3.77578	7.812631E-03	26.10836
11	1300	.2563655	2.784236	1.034313E-02	23.50711
12	1400	.2480882	2.924669	4.555887E-02	15.50557

BLANK CORRECTIONS APPLIED (ALL STEPS)

36Ar (VOLTS)= .0004 +/- 25 %

39Ar (VOLTS)= .0015 +/- 25 %

40Ar/36Ar (ATM)= 100 +/- 25 %

ITERATIONS = 12

SLOPE =-.1670331

INTERCEPT = 5.345933E-02

XBAR = .2810419

YBAR = 6.516038E-03

SUM S = 51.02449

INTERCEPT ERROR WITHOUT SUM S = 1.161629E-02
WITH SUM S = 2.623958E-02

SLOPE ERROR WITHOUT SUM S = 4.130971E-02
WITH SUM S = 9.331284E-02

X = .3200524
(Y=0)

Y = 5.345933E-02
(X=0)

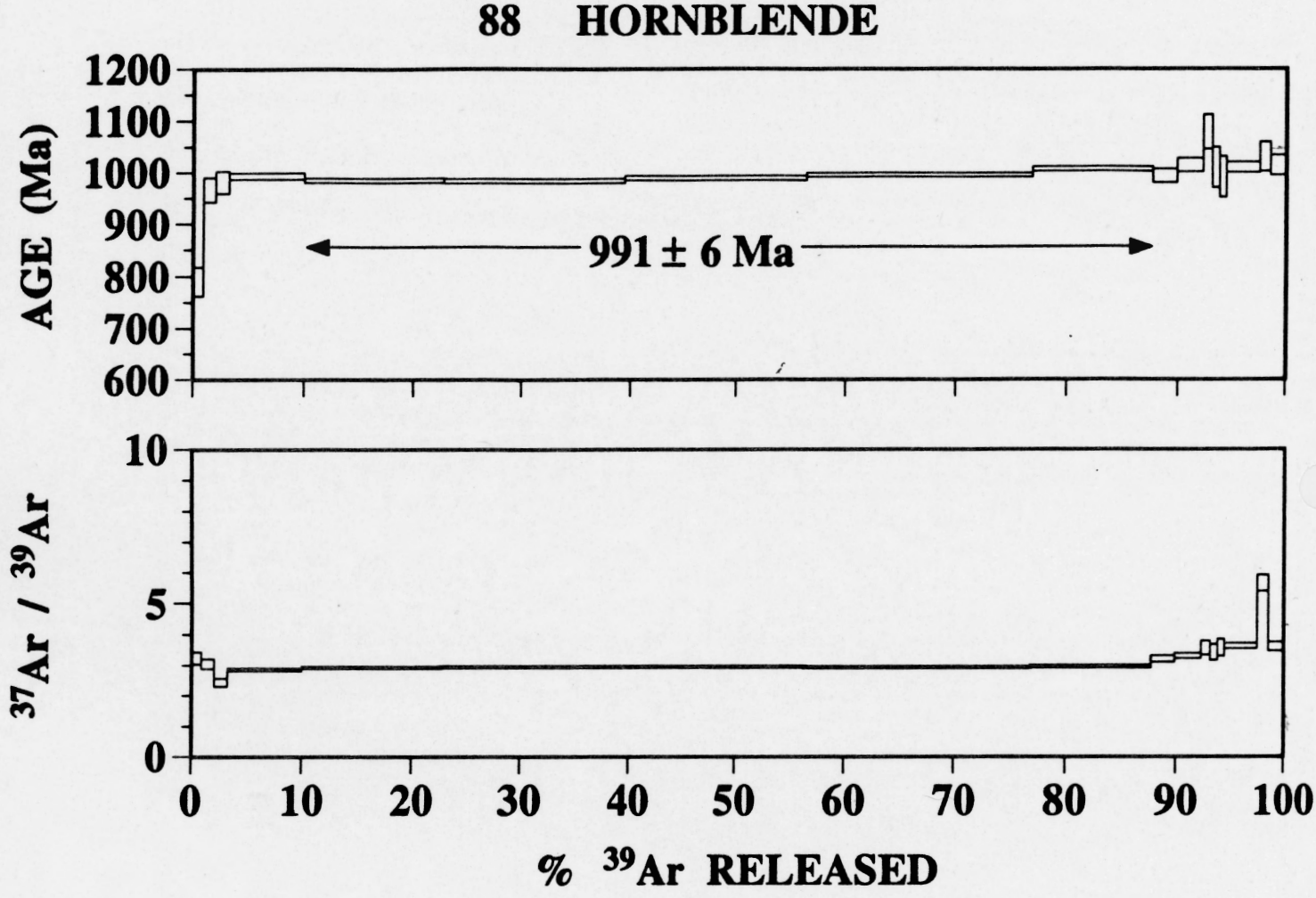
88 HORNBLENDE
AGE (Ma)
1200
1100
1000
900
800
700
600
991 ± 6 Ma
37Ar / 39Ar
10
5
0
0
10
20
30
40
50
60
70
80
90
100
% 39Ar RELEASED

88 HORNBLENDE SUMMARY

°C	mV 39	% 39	AGE (Ma) 1σ	% ATM	37/39	36/40	39/40	% IIC
750	12.4	.9	789.6 ± 27.3	6.6	3.23	.000224	.003855	.31
850	15.1	1.1	966.2 ± 23.6	5.2	3.05	.000178	.003032	.27
950	15.9	1.1	981 ± 21.7	.3	2.43	.000013	.003127	.21
1000	90.6	6.7	992.6 ± 5.8	.3	2.85	.000011	.003081	.25
1025	170.4	12.7	984.3 ± 4.4	0	2.92	.000004	.003121	.25
1050	224.4	16.7	983.2 ± 4.1	0	2.94	.000002	.003128	.26
1075	227.5	16.9	989.3 ± 4.1	0	2.94	.000002	.003103	.26
1100	274.2	20.4	995 ± 4.1	0	2.92	.000002	.00308	.25
1125	145.8	10.8	1007 ± 4.7	0	2.95	.000001	.003033	.26
1150	28.5	2.1	993.6 ± 13.7	0	3.19	.000003	.003085	.28
1175	31.9	2.3	1015.1 ± 13.1	.1	3.28	.000006	.002998	.28
[illegible]00	11.1	.8	1077.9 ± 32.5	.5	3.53	.000019	.002759	.3
1225	9.3	.6	1009.7 ± 39.3	.8	3.4	.000029	.002998	.29
1250	8.4	.6	991.1 ± 39.8	1	3.54	.000036	.003065	.31
1300	41.1	3	1010.1 ± 10.4	.4	3.61	.000016	.003008	.31
1350	13.3	.9	1030.8 ± 28.2	1.6	5.65	.000056	.002895	.49
1450	20.1	1.5	1014 ± 19.6	4.3	3.58	.000148	.002874	.31

TOTAL GAS AGE = 991.9 Ma

MEAN AGE(1000°C-1125°C)= 991.3 ± 6.4 Ma (2σ UNCERTAINTY,INCLUDING ERROR IN J)

J = .002286 ± .000016 (.6999126 %)

ERROR ESTIMATES AT ONE SIGMA LEVEL

37/39,36/40 AND 39/40 Ar RATIOS ARE CORRECTED FOR INTERFERING ISOTOPES

% IIC - INTERFERING ISOTOPES CORRECTION

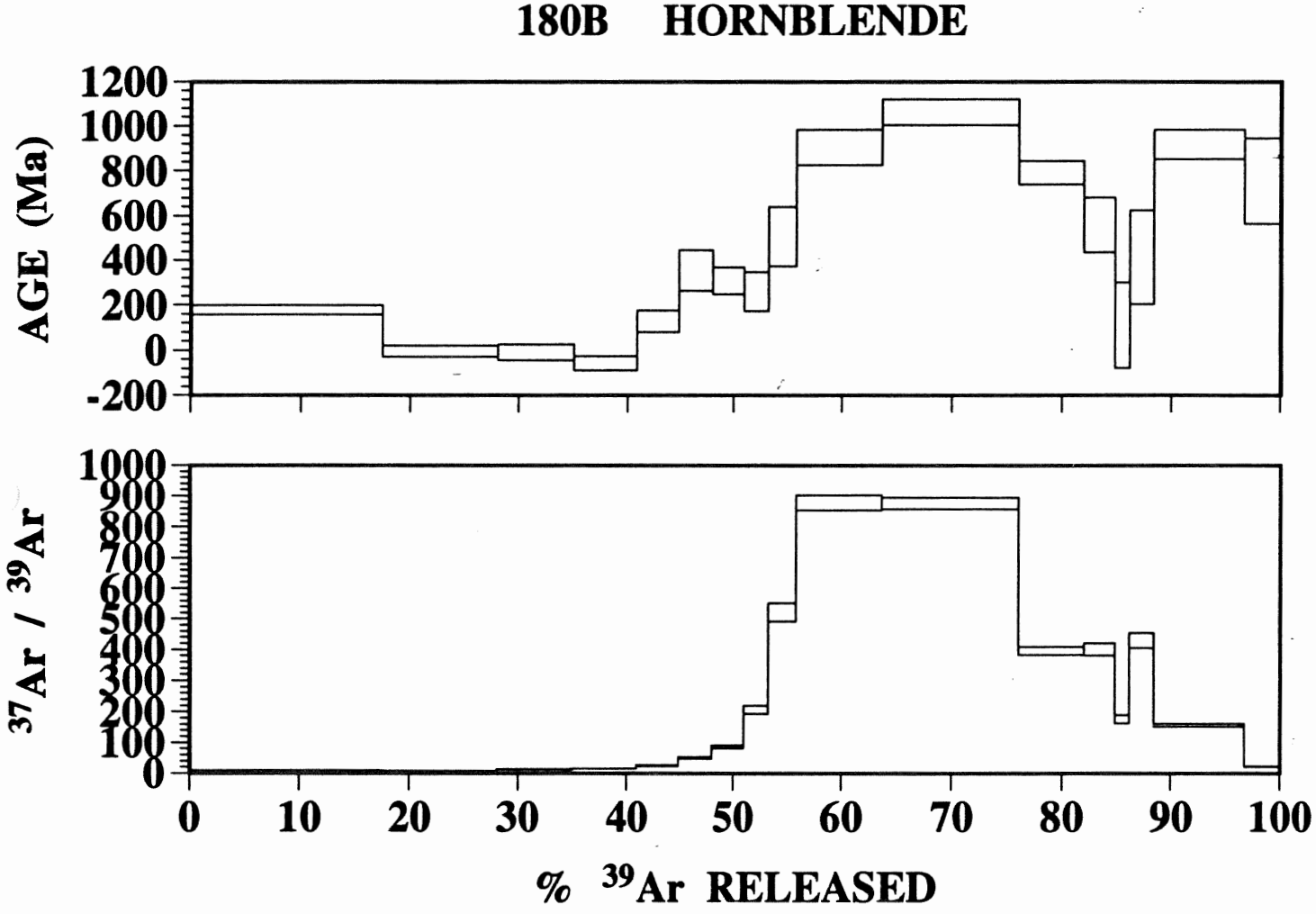
180B HORNBLENDE
AGE (Ma)
1200
1000
800
600
400
200
0
-200
^{37}Ar / ^{39}Ar
1000
900
800
700
600
500
400
300
200
100
0
0
10
20
30
40
50
60
70
80
90
100
% ^{39}Ar RELEASED

180B HORNBLENDE SUMMARY

C	mV 39	% 39	AGE (Ma)	% ATM	37/39	36/40	39/40	% IIC
750	6.7	17.4	177.6 +/- 20	59.8	7.94	.002025	.008782	1.82
850	4.1	10.6	-4.5 +/--24.4	101.8	6.42	.003449	.017174	44.45
950	2.6	6.9	-9.6 +/--35.4	104.1	12.41	.003532	.017686	39.39
1000	2.2	5.8	-57.2 +/--31.3	146.2	15.01	.004963	.033195	7.25
1025	1.5	3.8	127.4 +/- 46.4	56.1	24.31	.00193	.013487	7.26
1050	1.2	3.1	354.5 +/- 90.5	30.1	48.82	.001064	.007284	7.02
1075	1.1	3	306.8 +/- 59.4	35.2	85.39	.001274	.007925	13.44
1100	.8	2.3	259.9 +/- 86.6	50.7	205.85	.001877	.007386	36.12
1125	.9	2.5	504.2 +/- 133.8	44.7	521.49	.001734	.004491	61.61
1150	2.9	7.7	902.3 +/- 79.2	23.5	878.05	.001025	.003227	80.3
1175	4.8	12.4	1060.5 +/- 58.5	11.6	875.93	.000578	.002848	75.75
1200	2.2	5.9	791.5 +/- 51.7	9.8	395.84	.000519	.003885	38.06
1225	1.1	2.8	556.6 +/- 122.5	29.2	400.15	.001216	.004819	44.99
1250	.4	1.2	110.7 +/- 189.1	86	175.7	.002973	.005249	58.91
1350	.8	2.2	413.2 +/- 209.6	69.1	428.83	.002411	.003132	56.41
1450	3.2	8.3	915.7 +/- 66.5	34	156.45	.001161	.002298	14.23
1500	1.2	3.2	751.3 +/- 191	65.8	21.06	.002228	.001501	2.06

TOTAL GAS AGE = 493 Ma

J = .00228

ERROR ESTIMATES AT ONE SIGMA LEVEL

37/39,36/40 AND 39/40 Ar RATIOS ARE CORRECTED FOR INTERFERING ISOTOPES

% IIC - INTERFERING ISOTOPES CORRECTION

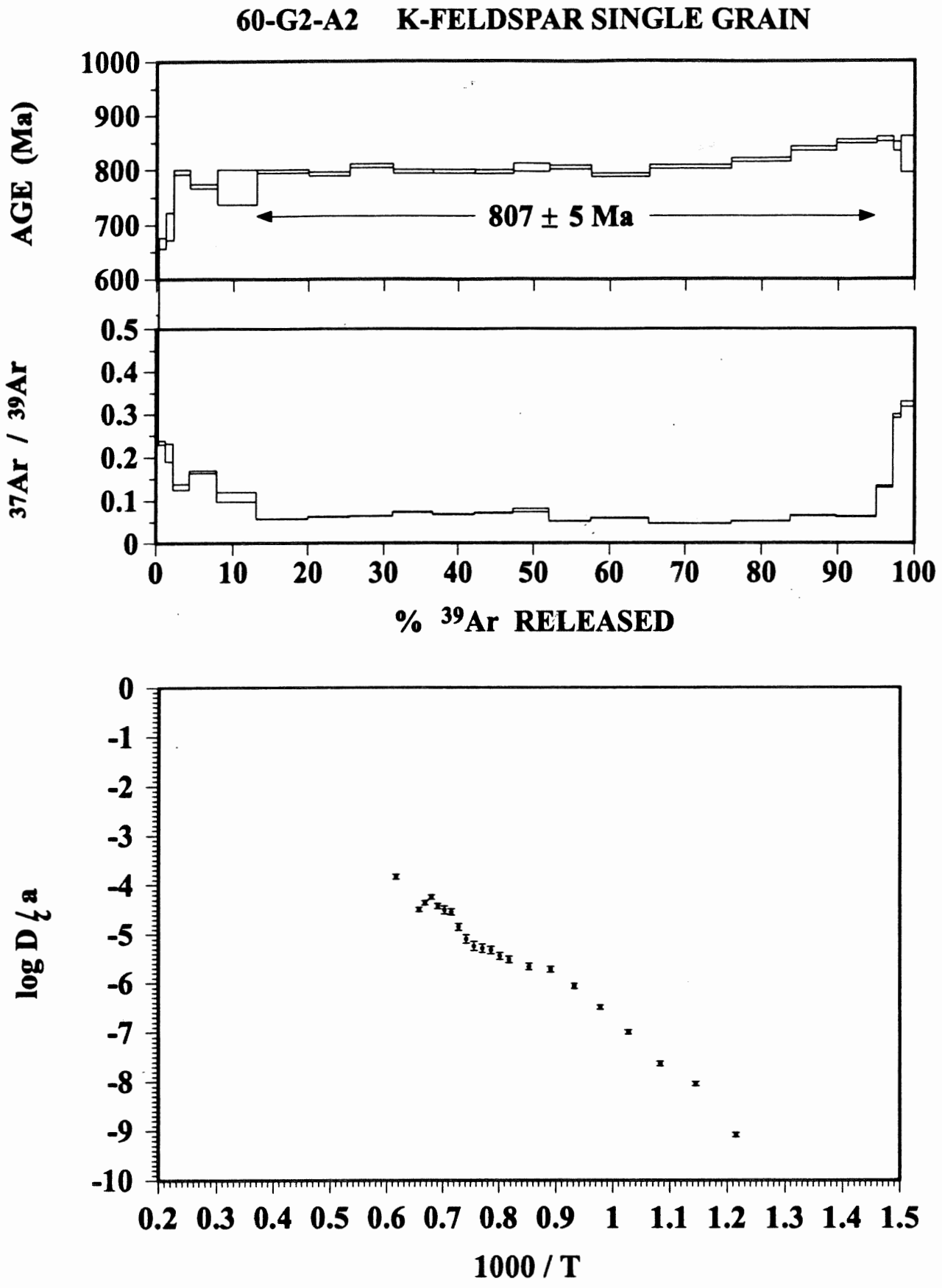

Fig. 8. Results from K-feldspar sample 60. Upper panel shows $^{40}Ar/^{39}Ar$ apparent age spectrum and preferred age, middle panel shows $^{37}Ar/^{39}Ar$ spectrum (related to Ca/K), bottom panel shows Arrhenius plot. See text for further discussion.

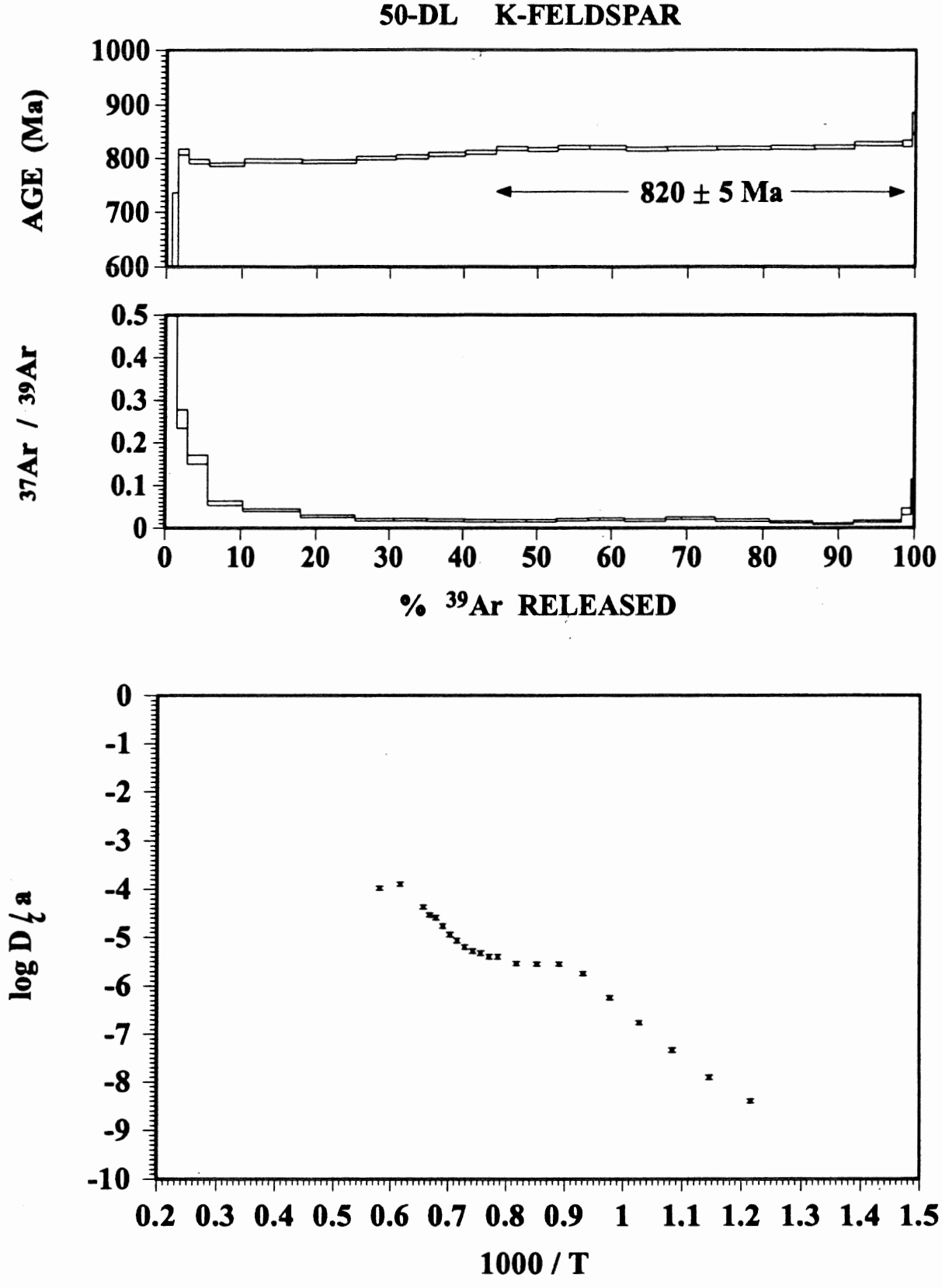

Fig. 9. Results from K-feldspar sample 50. Upper panel shows $^{40}Ar/^{39}Ar$ apparent age spectrum, middle panel shows $^{37}Ar/^{39}Ar$ spectrum (related to Ca/K), bottom panel shows Arrhenius plot. See text for further discussion.

60-G2-A2 K-FELDSPAR SUMMARY

°C	mV 39	% 39	AGE (Ma) 1σ	% ATM	37/39	36/40	39/40	% IIC
550	3.6	.3	448.9 ± 10.9	47	.52	.001592	.004386	.06
600	8.9	.8	665.9 ± 10	9.8	.23	.000332	.004648	.02
650	10.3	.9	697 ± 24.8	5.7	.21	.000193	.004601	.02
700	22.9	2.1	796 ± 4.7	2.7	.13	.000094	.004034	.01
750	37.7	3.5	770.5 ± 3.6	1.6	.16	.000056	.004248	.01
800	56.3	5.2	768.7 ± 31.8	1.1	.1	.000039	.004282	.01
850	73.8	6.8	797.2 ± 3.3	.8	.05	.000027	.004109	0
900	58.2	5.4	792.7 ± 3.4	.8	.06	.000029	.004134	0
950	61.4	5.7	807.7 ± 3.5	.8	.06	.000029	.00404	0
975	57.2	5.3	796.5 ± 3.4	.9	.07	.000032	.004107	0
1000	60.8	5.6	796.6 ± 3.4	1.1	.06	.000039	.004097	0
1025	54.1	5	795.9 ± 3.5	1.2	.07	.000041	.004099	0
1050	50.5	4.7	804.1 ± 7.3	1.3	.07	.000045	.004042	0
1075	59	5.5	804.7 ± 3.5	2.8	.05	.000095	.003978	0
1100	82.5	7.7	790.3 ± 3.3	.6	.05	.000023	.004158	0
1125	115.5	10.8	805.8 ± 3.2	.5	.04	.000018	.004065	0
1150	82.7	7.7	817.5 ± 3.4	.8	.05	.000027	.003982	0
1175	64.6	6	838.1 ± 3.6	.8	.06	.000028	.003859	0
1200	56.1	5.2	851.5 ± 3.8	1	.06	.000034	.003776	0
1225	23.2	2.1	855.9 ± 4.6	3.3	.13	.000112	.003665	.01
1250	10.8	1	842.3 ± 8.1	5.6	.29	.000192	.003648	.02
1500	19	1.7	828.3 ± 32.9	45.6	.32	.001545	.002146	.03

TOTAL GAS AGE = 802.3 Ma

MEAN AGE(850°C-1200°C)= 807.3 ± 5 Ma (2σ UNCERTAINTY,INCLUDING ERROR IN J)

J = .002281 ± .000016 (.7 %)

ERROR ESTIMATES AT ONE SIGMA LEVEL

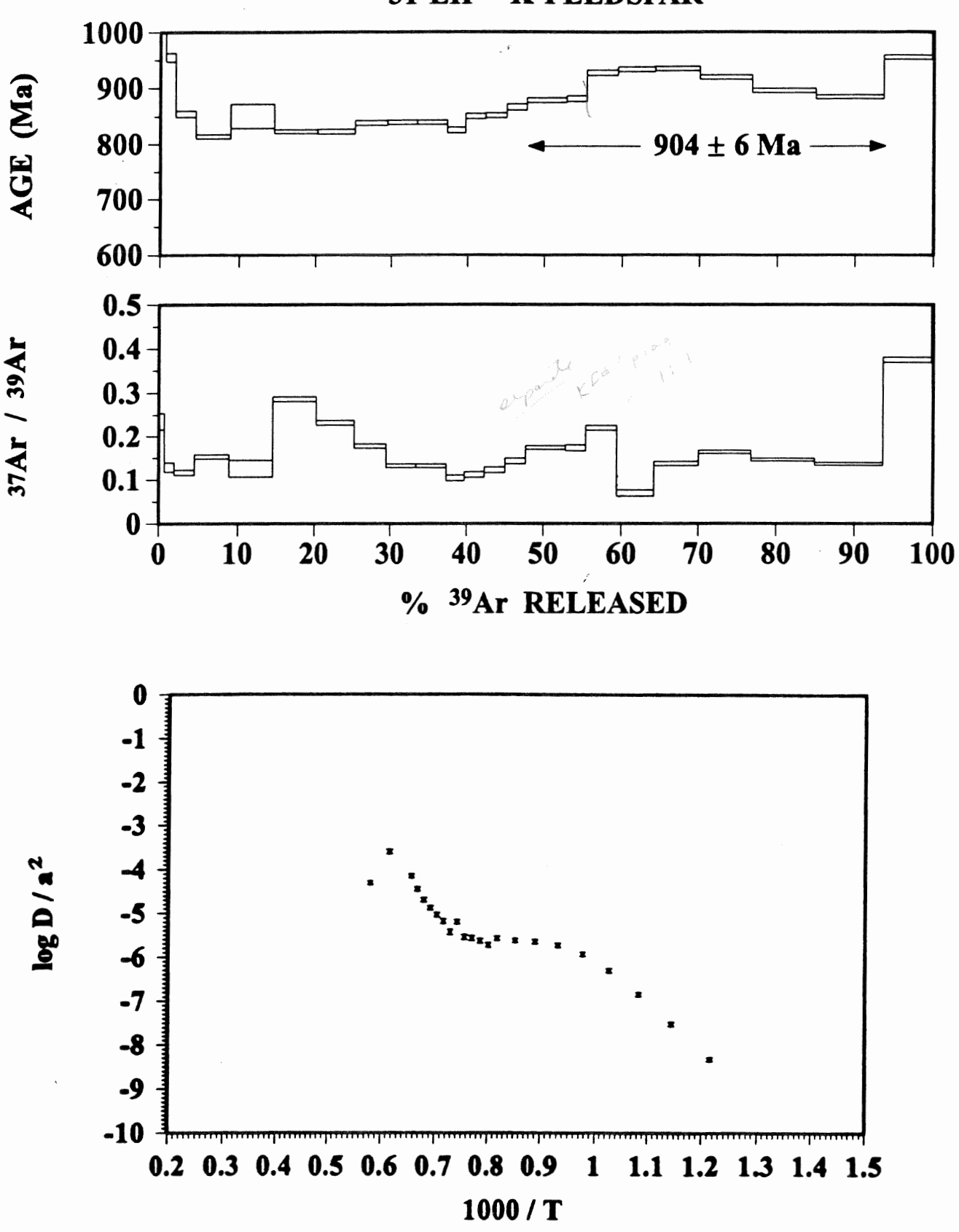

Fig. 12. Results from K-feldspar sample 31. Upper panel shows $^{40}Ar/^{39}Ar$ apparent age spectrum, middle panel shows $^{37}Ar/^{39}Ar$ spectrum (related to Ca/K), bottom panel shows Arrhenius plot. See text for further discussion.

50-DL K-FELDSPAR SUMMARY

C	mV 39	% 39	AGE (Ma) 1σ	% ATM	37/39	36/40	39/40	% IIC
550	15.3	.7	362.5 ± 7.3	12.9	1.83	.000438	.008838	.26
600	15.5	.7	726.9 ± 9.2	2	.64	.000068	.004461	.06
650	29.4	1.3	812 ± 5.7	.5	.25	.000019	.003952	.02
700	56.6	2.6	794.2 ± 4.2	.6	.16	.000022	.004059	.01
750	97.9	4.6	788.4 ± 3.4	.2	.05	.000008	.004113	0
800	162.4	7.7	795.2 ± 3.3	.1	.04	.000004	.004075	0
850	155.4	7.3	793.8 ± 3.3	0	.02	.000002	.004085	0
900	112.4	5.3	800.6 ± 3.3	0	.01	.000002	.004043	0
950	93.2	4.4	802.8 ± 3.5	0	.01	.000002	.004029	0
1000	105.4	5	807.5 ± 3.5	0	.01	.000001	.004001	0
1025	88.2	4.1	811.5 ± 3.5	0	.01	.000001	.003977	0
50	89.7	4.2	818.2 ± 3.6	.1	.01	.000003	.003933	0
1075	85.1	4	816.8 ± 3.7	.1	.01	.000005	.00394	0
1100	88.7	4.2	820.5 ± 3.5	.2	.01	.000007	.003915	0
1125	103.5	4.9	820.5 ± 3.6	.2	.02	.000007	.003916	0
1150	114.4	5.4	817.5 ± 3.5	.2	.01	.000007	.003934	0
1175	136.2	6.4	818.4 ± 3.4	.2	.02	.000008	.003927	0
1200	150.6	7.1	818.9 ± 3.4	.2	.01	.000007	.003925	0
1225	120.4	5.7	820.1 ± 3.5	.2	.01	.000009	.003915	0
1250	113	5.3	821.4 ± 3.6	.3	0	.000011	.003906	0
1350	132.3	6.2	827.6 ± 3.5	.8	.01	.000028	.003849	0
1450	26.1	1.2	828.4 ± 6.3	9.7	.03	.000328	.003501	0
1500	10.2	.4	866 ± 20	21.4	.09	.000726	.002879	0

TOTAL GAS AGE = 807.9 Ma

J = .002278

ERROR ESTIMATES AT ONE SIGMA LEVEL

31-LH K-FELDSPAR SUMMARY

	mV 39	% 39	AGE (Ma) 1σ	% ATM	37/39	36/40	39/40	% IIC
550	12	.7	1015.9 ± 14.6	3.4	.23	.000116	.002936	.02
600	21.3	1.2	954.9 ± 7.5	1.9	.12	.000065	.003231	.01
650	42.9	2.5	854.7 ± 5.2	.8	.11	.00003	.003759	.01
700	71.6	4.3	814 ± 3.9	.6	.15	.000022	.004005	.01
750	93.3	5.6	850.5 ± 21.5	.4	.12	.000014	.0038	.01
800	95.1	5.7	823.1 ± 3.5	.2	.28	.000007	.003967	.02
850	83.4	5	822.8 ± 3.9	.5	.23	.000019	.003955	.02
900	69.9	4.2	838.1 ± 3.9	.8	.17	.000027	.003856	.01
950	64.9	3.9	839.3 ± 3.9	.3	.13	.000011	.003868	.01
950	64.9	3.9	839.3 ± 3.9	.3	.13	.000011	.003868	.01
975	39.7	2.3	825.3 ± 4.9	1.5	.1	.000051	.003902	0
1000	43.8	2.6	850.3 ± 4.7	.2	.11	.000009	.003807	.01
1025	45.4	2.7	851.4 ± 4.3	.3	.12	.000012	.003797	.01
1050	43.9	2.6	866.2 ± 5	1.2	.14	.000041	.003684	.01
1075	85	5.1	878.5 ± 3.8	.7	.17	.000024	.003637	.01
1100	42.7	2.5	881 ± 5.1	2	.17	.000069	.003576	.01
1125	66.7	4	927.2 ± 4.5	.9	.21	.00003	.00339	.01
1150	80.2	4.8	933.6 ± 4.1	.9	.06	.000033	.003358	0
1175	95.6	5.7	934.7 ± 3.9	.7	.13	.000023	.003362	.01
1200	111.8	6.7	919.3 ± 3.8	.6	.16	.00002	.003438	.01
1225	136.1	8.1	895.6 ± 3.6	.5	.14	.000019	.003554	.01
1250	143.7	8.6	884.4 ± 3.8	.4	.13	.000016	.003615	.01
1350	103.7	6.2	954.9 ± 4	1	.37	.000035	.00326	.03
1450	1.4	0	2315.1 ± 134	15.8	2.48	.000535	.000742	.17
1550	2	.1	2744.9 ± 167.4	47.4	3.59	.001606	.000337	.25

TOTAL GAS AGE = 882 Ma

PLATEAU AGE (1100-1500)= 892.9 +/- 7.1 Ma J ERROR= .0000228 (1 %)

J = .00228

ERROR ESTIMATES AT ONE SIGMA LEVEL

37/39,36/40 AND 39/40 Ar RATIOS ARE CORRECTED FOR INTERFERING ISOTOPES

% IIC - INTERFERING ISOTOPES CORRECTION

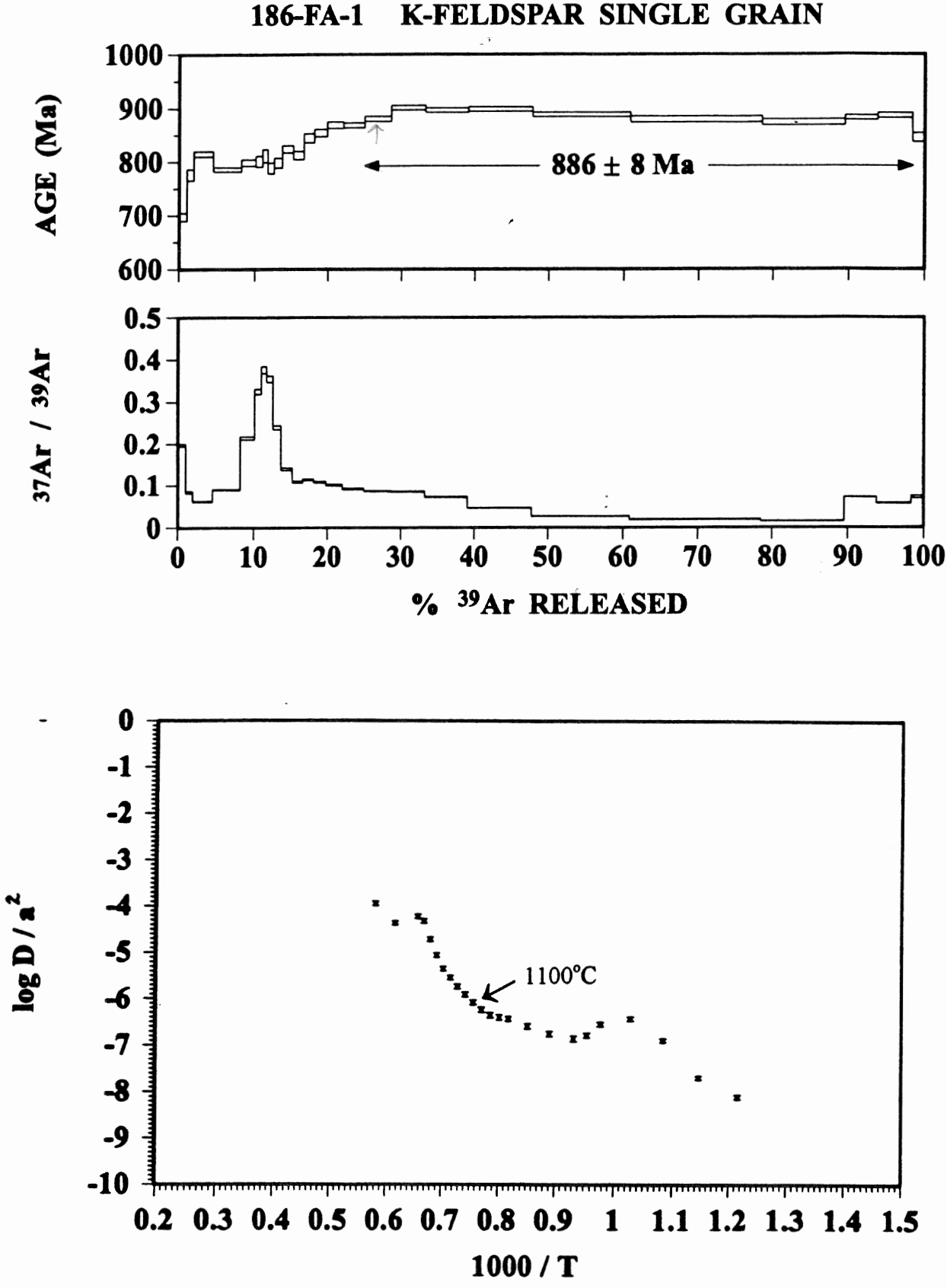

Fig. 10. Results from single grain K-feldspar sample 186-FA-1. Upper panel shows $^{40}Ar/^{39}Ar$ apparent age spectrum, middle panel shows $^{37}Ar/^{39}Ar$ spectrum (related to Ca/K), bottom panel shows Arrhenius plot. See text for further discussion.

186-FA-1 K-FELDSPAR SUMMARY

°C	mV 39	% 39	AGE (Ma) 1σ	% ATM	37/39	36/40	39/40	% IIC
550	25.5	1	696.4 ± 7.2	5.5	.19	.000188	.00461	.01
600	22.6	.8	775.5 ± 10.6	1.8	.08	.000063	.004201	0
650	65.7	2.5	815.4 ± 4.9	1.1	.06	.000039	.003977	0
700	95.1	3.7	785.3 ± 4.1	.8	.08	.000029	.00418	0
750	48.9	1.9	798.3 ± 5.7	.8	.21	.00003	.004094	.02
775	23.4	.9	800.7 ± 10	.7	.32	.000024	.004087	.03
800	17.9	.7	811.1 ± 12.1	1.1	.37	.000039	.004003	.03
850	21.5	.8	787.8 ± 10	2.2	.35	.000075	.004106	.03
900	28.7	1.1	797.7 ± 9.1	2.7	.23	.000092	.004022	.02
950	37.9	1.4	824.1 ± 6.9	1.2	.13	.000043	.00392	.01
975	36.5	1.4	812.3 ± 7.6	1	.1	.000034	.004002	.01
1000	36.6	1.4	844.4 ± 8	1	.11	.000034	.003813	.01
1025	43.8	1.7	854.1 ± 6.7	1.1	.1	.000039	.003754	.01
1050	56.4	2.2	869.2 ± 5.8	1	.1	.000035	.003676	0
1075	72.8	2.8	868.5 ± 4.8	.7	.09	.000026	.00369	0
1100	92	3.6	880.2 ± 4.6	.6	.08	.000022	.003632	0
1125	119.9	4.7	901.2 ± 4	.5	.08	.000018	.003529	0
1150	148.7	5.8	896.4 ± 4	.4	.07	.000014	.003557	0
1175	220.9	8.6	898.4 ± 4	0	.04	.000002	.00356	0
1200	333	13	887.8 ± 4	.2	.02	.000008	.003607	0
1225	449	17.6	879.5 ± 5.2	.2	.01	.000007	.003652	0
1250	279.9	11	874.1 ± 5.4	.5	.01	.000019	.003667	0
1350	106.2	4.1	882.8 ± 4.2	1.2	.07	.000043	.003596	0
1450	118.7	4.6	886.8 ± 4.3	2.3	.05	.000079	.003537	0
1700	41.9	1.6	845.3 ± 8	11.6	.07	.000392	.0034	0

TOTAL GAS AGE = 868.3 Ma

MEAN AGE(1100°C-1450°C)= 885.8 ± 6.1 Ma (2σ UNCERTAINTY,INCLUDING ERROR IN J)

= .002279 ± .000016 (.7 %)

ERROR ESTIMATES AT ONE SIGMA LEVEL

37/39,36/40 AND 39/40 Ar RATIOS ARE CORRECTED FOR INTERFERING ISOTOPES

% IIC - INTERFERING ISOTOPES CORRECTION

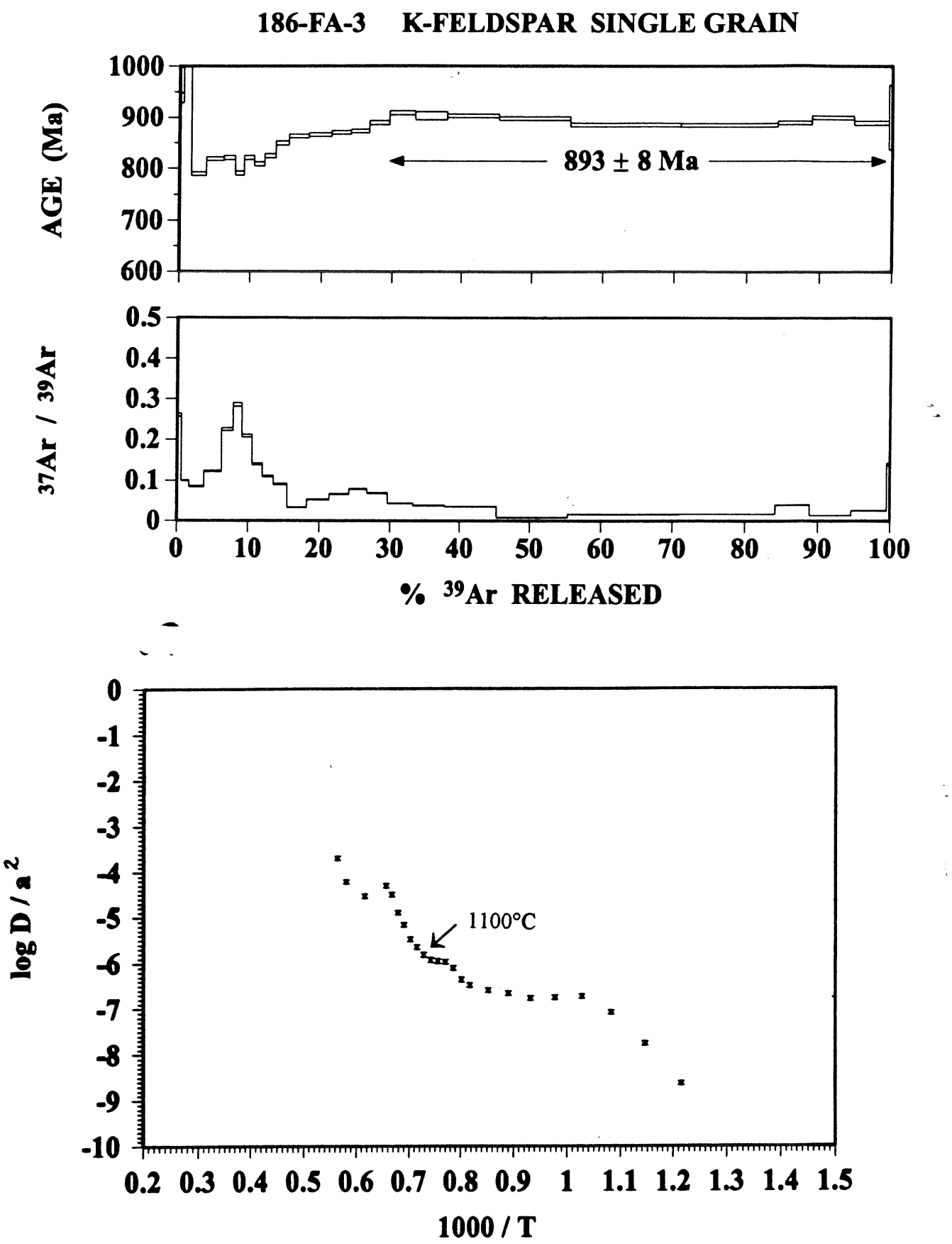

Fig. 11. Results from single grain K-feldspar sample 186-FA-3, a duplicate of 186-FA-1. Upper panel shows $^{40}Ar/^{39}Ar$ apparent age spectrum, middle panel shows $^{37}Ar/^{39}Ar$ spectrum (related to Ca/K), bottom panel shows Arrhenius plot. See text for further discussion.

186-FA-3 K-FELDSPAR SUMMARY

oC	mV 39	% 39	AGE (Ma)	% ATM	37/39	36/40	39/40	% IIC
550	11.7	.5	938.4 +/- 9.8	5.3	.25	.00018	.003191	.02
600	21.7	1	1067.9 +/- 5	2.1	.09	.000072	.002787	0
650	42.2	2	789.5 +/- 3.3	1.6	.08	.000055	.004122	0
700	50.8	2.4	819.2 +/- 3.4	1	.12	.000036	.00396	.01
750	33.2	1.6	821.2 +/- 4	1.4	.22	.000047	.003934	.02
800	26	1.2	790.9 +/- 3.8	1.6	.28	.000054	.004113	.02
850	29	1.4	821.2 +/- 4.1	1.4	.2	.00005	.003931	.01
900	29.3	1.4	808.5 +/- 3.7	1.6	.13	.000056	.004	.01
950	32.5	1.6	824.5 +/- 3.8	1.4	.11	.000048	.003914	.01
975	37.6	1.8	849.2 +/- 4	1.1	.09	.000039	.003782	0
1000	56.4	2.7	863.3 +/- 3.9	.9	.03	.000033	.003711	0
1025	64.7	3.1	865.7 +/- 3.5	.6	.05	.000021	.003712	0
1050	56.1	2.7	870.6 +/- 3.7	.8	.06	.000029	.003676	0
1075	51.6	2.5	873.1 +/- 3.6	.9	.07	.000032	.00366	0
1100	58.6	2.8	889.1 +/- 3.9	1	.06	.000034	.003575	0
1125	74.6	3.6	908.9 +/- 3.7	.7	.04	.000025	.003485	0
1150	93.9	4.6	903 +/- 7.9	.6	.03	.000023	.003517	0
1175	151.8	7.4	903 +/- 3.5	.3	.03	.000012	.003528	0
1200	203.4	9.9	898.2 +/- 3.6	.2	0	.000009	.003555	0
1225	317.4	15.5	885.3 +/- 3.5	.1	.01	.000006	.003624	0
1250	270.4	13.2	884.4 +/- 3.5	.2	.01	.000007	.003629	0
1350	95.1	4.6	889.3 +/- 3.6	.7	.03	.000024	.003584	0
1450	117.5	5.7	900 +/- 3.6	1.4	.01	.000049	.003504	0
00	100	4.9	889.6 +/- 3.7	2.7	.02	.000091	.003511	0
1550	9.7	.4	900.4 +/- 63.6	82.7	.13	.002801	.000611	.01

TOTAL GAS AGE = 885.5 Ma

MEAN AGE(1050°C-1250°C)= 903.9 ± 5.7 Ma (2σ UNCERTAINTY,INCLUDING ERROR IN J)

J = .002278 ± 1.5946E-05 (.7 %)

ERROR ESTIMATES AT ONE SIGMA LEVEL

37/39,36/40 AND 39/40 Ar RATIOS ARE CORRECTED FOR INTERFERING ISOTOPES

% IIC - INTERFERING ISOTOPES CORRECTION

Sample #: 132

Rock Type: non-migmatic granulite gneiss

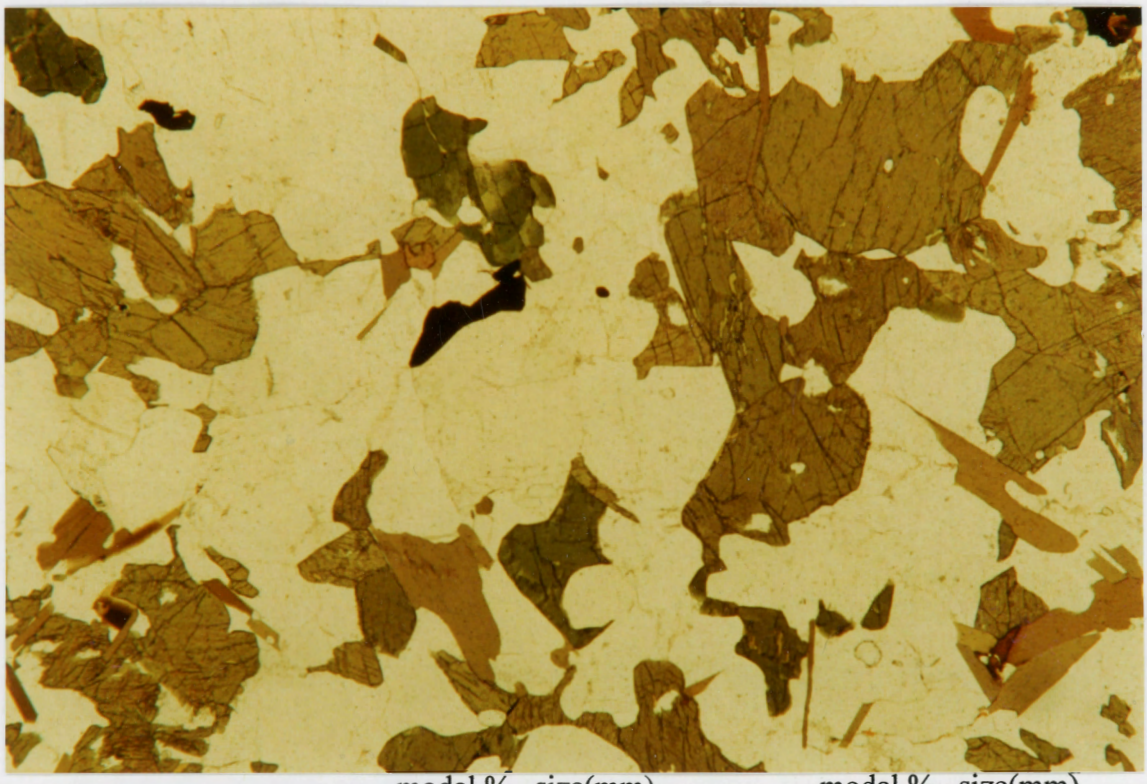

		modal %	size(mm)		modal %	size(mm)
Mineralogy:	K-feldspar:			A-feldspar:	35	0.5-1.5
	Hornblende:	20	0.3-2	Biotite:	15	0.3-2
	Quartz:	10	0.3-1	Opaque:	5	<0.5
	Others: clinopyroxene:	15	0.5-1			

texture: granoblastic, rare mymerkite, biotite defines weak foliation

sericite alteration along rare anastomizing fractures

mineral phase dated: hbl separate

grain shape: xenoblastic grains (rare sub-idioblastic); curved grain boundaries; rare sericite alteration along rare anastomizing fractures; hornblende replaces clinopyroxene; this hornblende more susceptible to chlorite alteration; rare biotite quartz inclusions

Sample #: 125

Rock Type: anorthosite

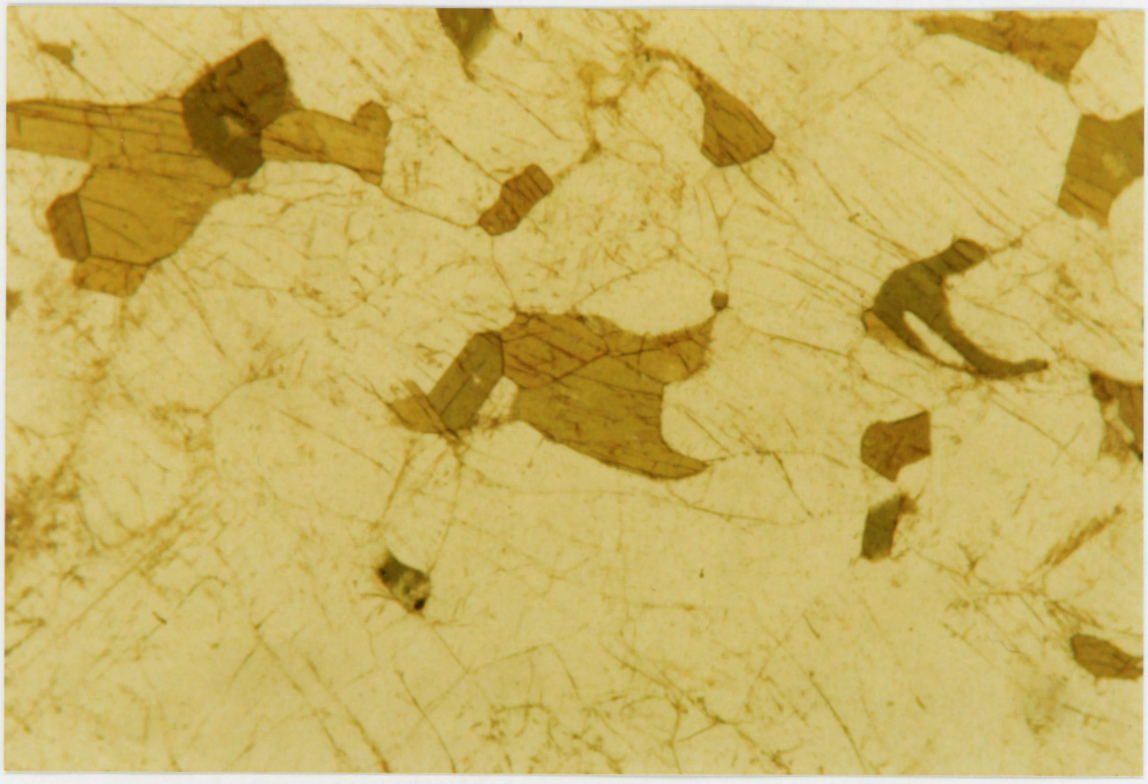

		modal %	size(mm)		modal %	size(mm)
Mineralogy:	K-feldspar:	-		A-feldspar:	60	
	Hornblende:	15	0.3-0.8	Biotite:	5	
	Quartz:	15	0.1-1.0	Apatite:	*	
	Opaque:	*				
	Other: clinopyroxene: 5%					

texture: granoblastic

mineral phase dated: hornblendebl grain seperate

grain shape: anhedral, curved grain boundaries; rare chlorite alteration

Sample #: 194 G1

Rock Type: quartzo-feldspathic amphibolite gneiss

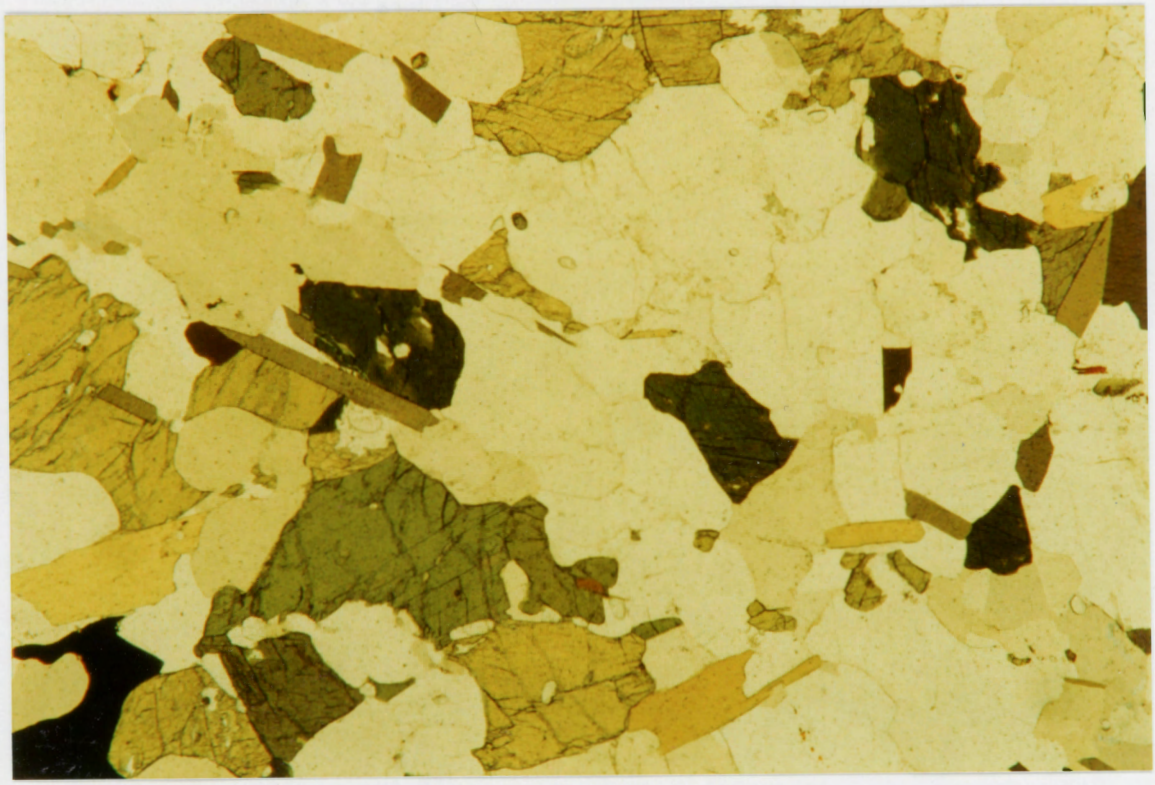

		modal %	size(mm)		modal %	size(mm)
Mineralogy:	A-feldspar:	25	0.3-1.5			
	Hornblende:	25	0.15-1.5	Biotite:	10	0.2-1
	Quartz:	35	0.1-2	Apatite:	*	
	Opaque:	<5	<0.5			

texture: xenoblastic, wide range of grain sizes; quartz subgrains

mineral phase dated: hornblende grain separate

notes: xenoblastic grains with curved > embayed margins; rare chlorite alteration along cleavage; rare biotite and apatite inclusions

Sample #: 47

Rock Type: amphibolite

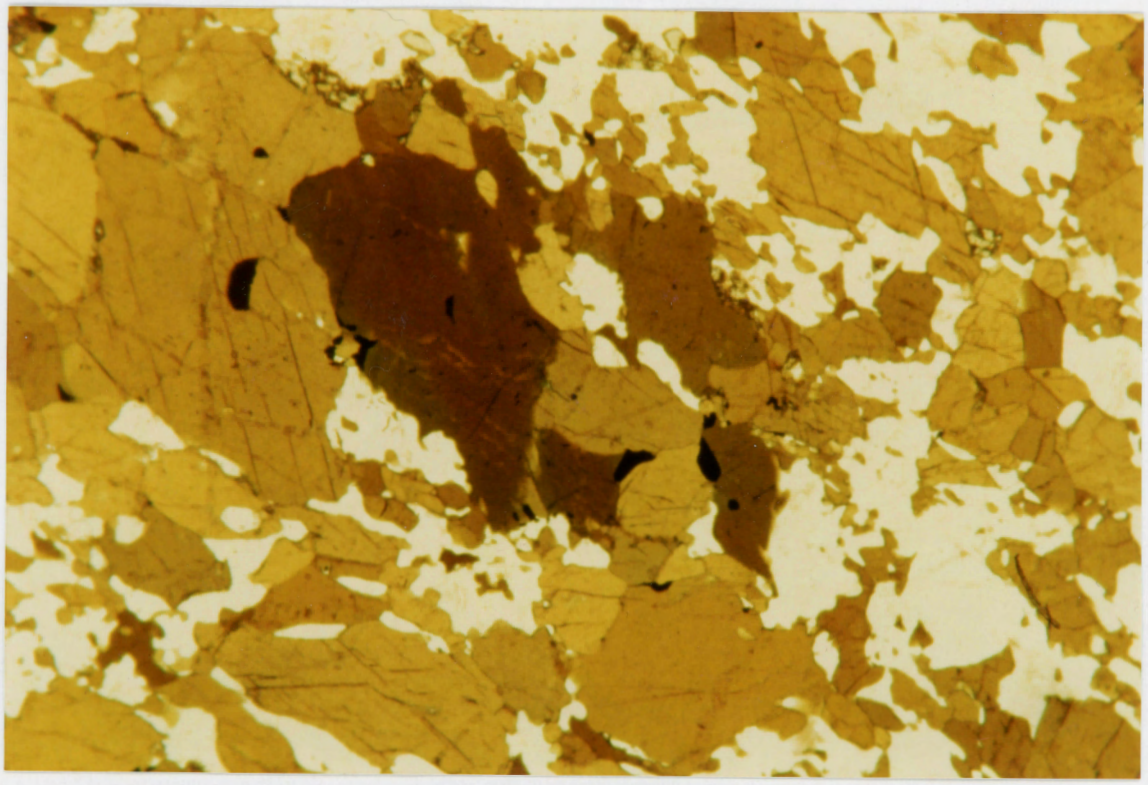

		modal %	size(mm)		modal %	size(mm)
Mineralogy:	Quartz:	15	0.1-0.5	A-feldspar:	25	0.1-0.5
	Hornblende:	45	0.05-1.2	Clinopyroxe:	10	<0.2
	Opaque:	5				
	Others: Apatite					

texture: granoblastic aggregates of hornblende, weakly foliated with embayed outer edges

mineral phase dated: hornblende separate

grain shape: idioblastic to subidioblastic; hbl - hbl contacts relatively straight, hbl-matrix contacts highly embayed, fine recrystallization: undergoing reaction or partial melting(?); hornblende replacing clinopyroxene; rare chlorite alteration

Sample #: 88

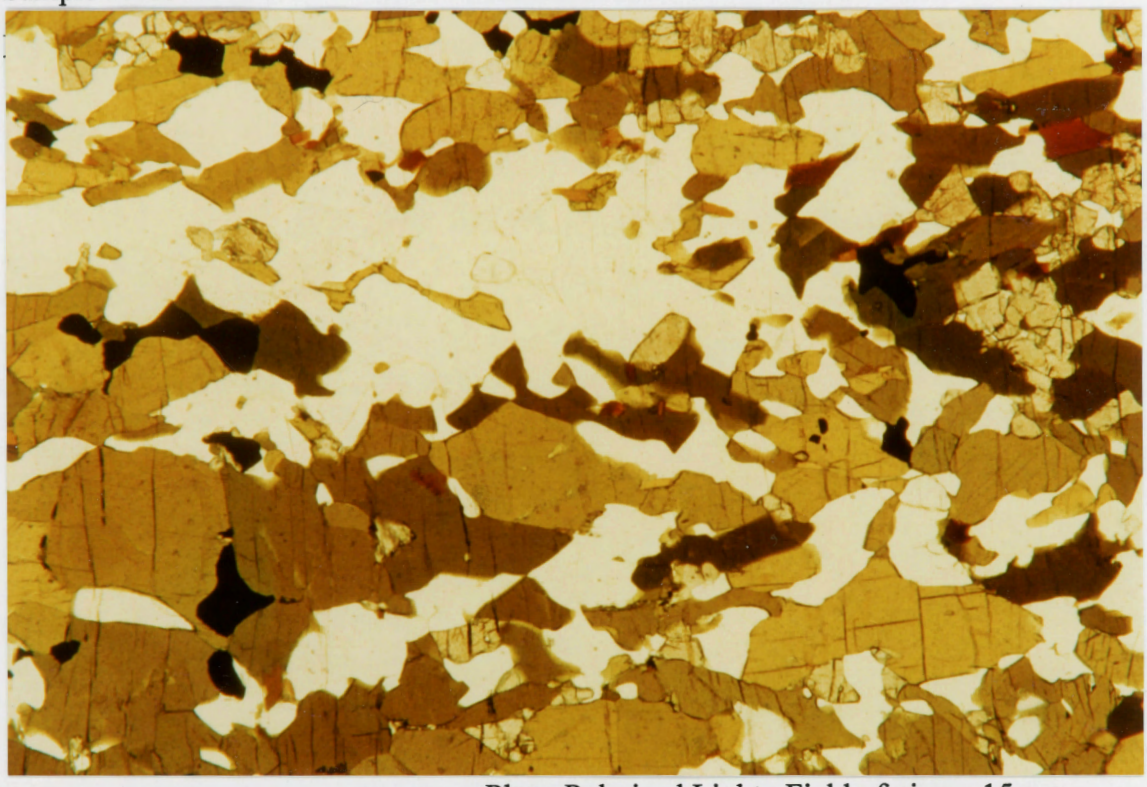

Plane Polarized Light, Field of view ~15mm

		modal %	size(mm)		modal %	size(mm)
Mineralogy:	A-feldspar:	25	0.3-1			
	Hornblende:	40	0.3-1.2	Biotite:	5	0.2-0.5
	Quartz:	20	0.3-1	Garnet:	10	0.2-0.7
	Opaque:	5				
	Others: cpx	5				

texture: foliated (defined by elongate grains)

mineral phase dated: hbl separate

notes: xenoblastic - subidioblastic grains; curved grain boundaries; very rare chlorite alteration; rare biotite intergrowth; some fracturing perpendicular to foliation

Sample #: 27

Rock Type: mafic lense cut by leucosome

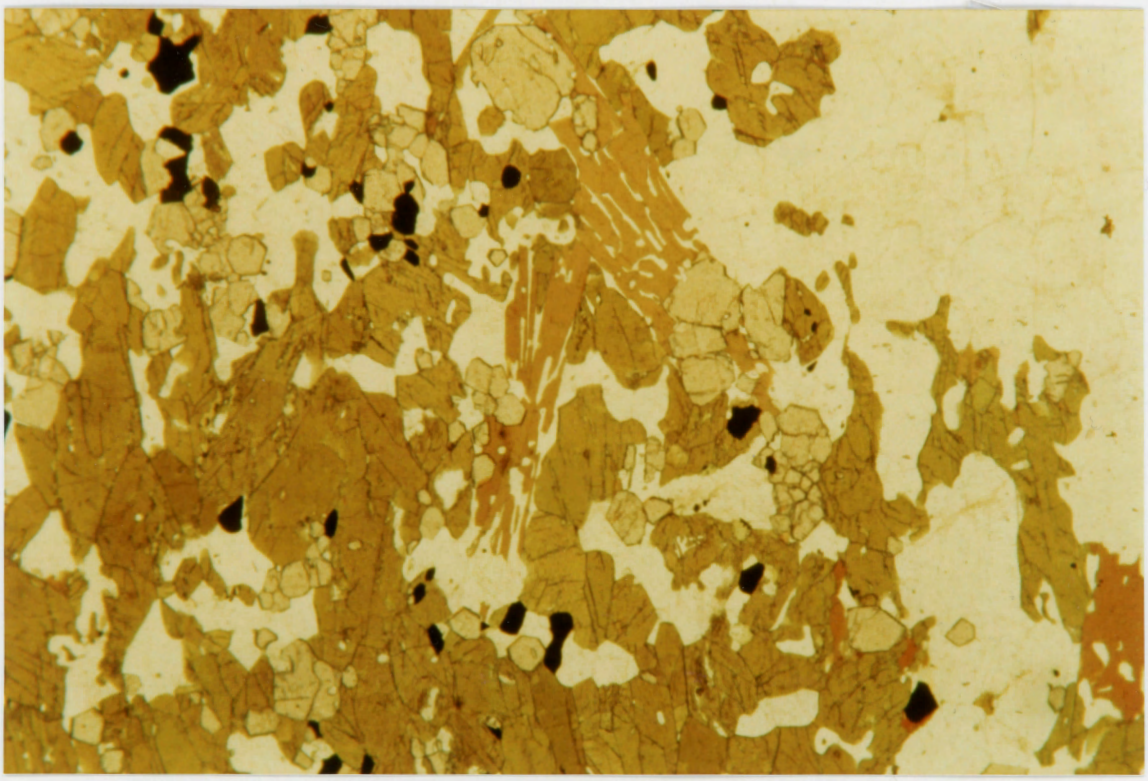

		modal %	size(mm)		modal %	size(mm)
Mineralogy:	A-feldspar:	20	0.3-1.5	Hornblende:	40	0.3-1.5
	Biotite:	10	0.2-1	Quartz:	20	
	Garnet:	10	<0.5			
	Apatite:	*		Opaque:	*	<0.5
	Others: Zircon					

texture: foliated; cut by quartz&plagioclase-rich leucosome

mineral phase dated: hornblende separate

notes: subidioblastic-idioblastic grains; rational > curved grain boundaries; patchy sericite alteration in leucosome; rare biotite quartz and plagioclase inclusions

Sample #: 60G2

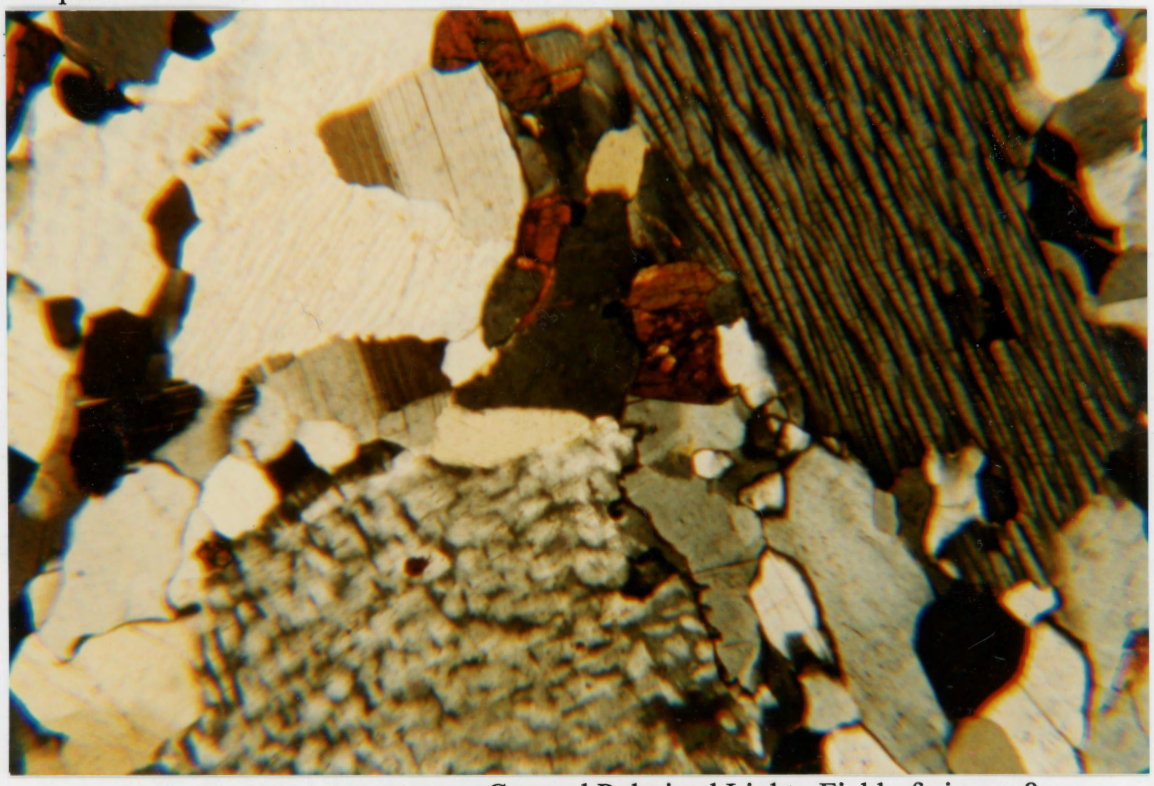

Crossed Polarized Light, Field of view ~ 8mm

		modal %	size(mm)		modal %	size(mm)
Mineralogy:	K-feldspar:	40	0.2-0.5,2-4	A-feldspar:	10	0.2-0.5
	Hornblende:	10	0.2-0.5	Biotite:	5	0.1-0.3
	Quartz:	35	0.2-0.5,2-4	Opaque:	*	
	Others: apatite, zircon					

texture: bimodal grain-size distribution; coarse K-feldspar/quartz leucosome in finer-grained matrix

mineral phase dated: microperthite grains from thick section

notes: 2-4 mm anhedral grains; embayed-curved grain boundaries; string perthite where Or:Ab ~ 60:40; rare fractures and very rare patchy sericite alteration, rare inclusions (quartz, zircon)

Sample #: 50

Rock Type: leucocratic granulite vein; cuts amphibolite facies migmatitic orthogneiss

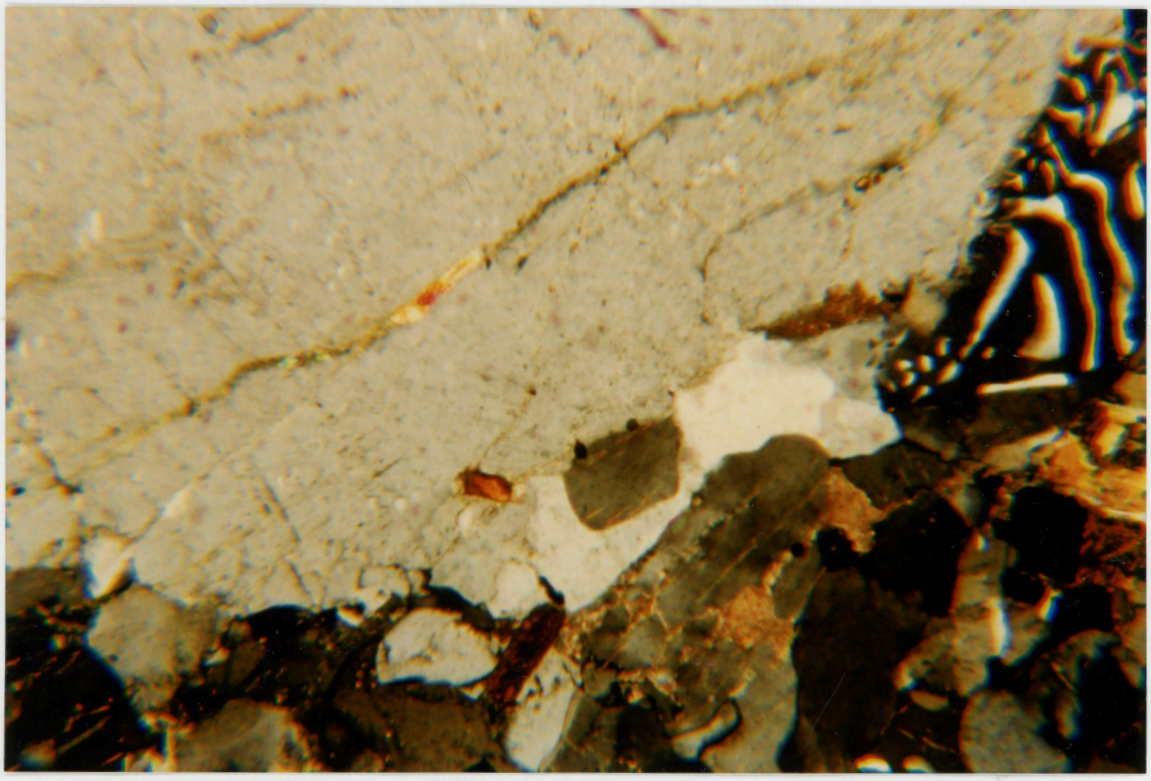

		modal %	size(mm)		modal %	size(mm)
Mineralogy:	K-feldspar:	20	0.3-2	A-feldspar:	10	0.2-1.5
	Hornblende:	15	0.5-2	Biotite:	10	0.2-1.5
	Quartz:	30		Opaque:	5	

Others: titanite 2%, apatite, chlorite 3%, clinopyroxene 5%

texture: granoblastic (recrystallized); hornblende pseudomorphed by chl + bi

mineral phase dated: K-feldspar seperate

notes: medium-grained anhedral orthoclase; embayed margins; untwinned; compositional zonation; narrow (~10 μm) perthite strings, and irregular blebs, Na-phase < than 10% of grains; inclusions of apatite, titanite; fractures up to 1mm wide, intersect grain boundaries, sericitization rare, concentrated along fractures.

Sample #: 31d

Rock Type: grey, foliated vein cuts leucosome of metapelitic host

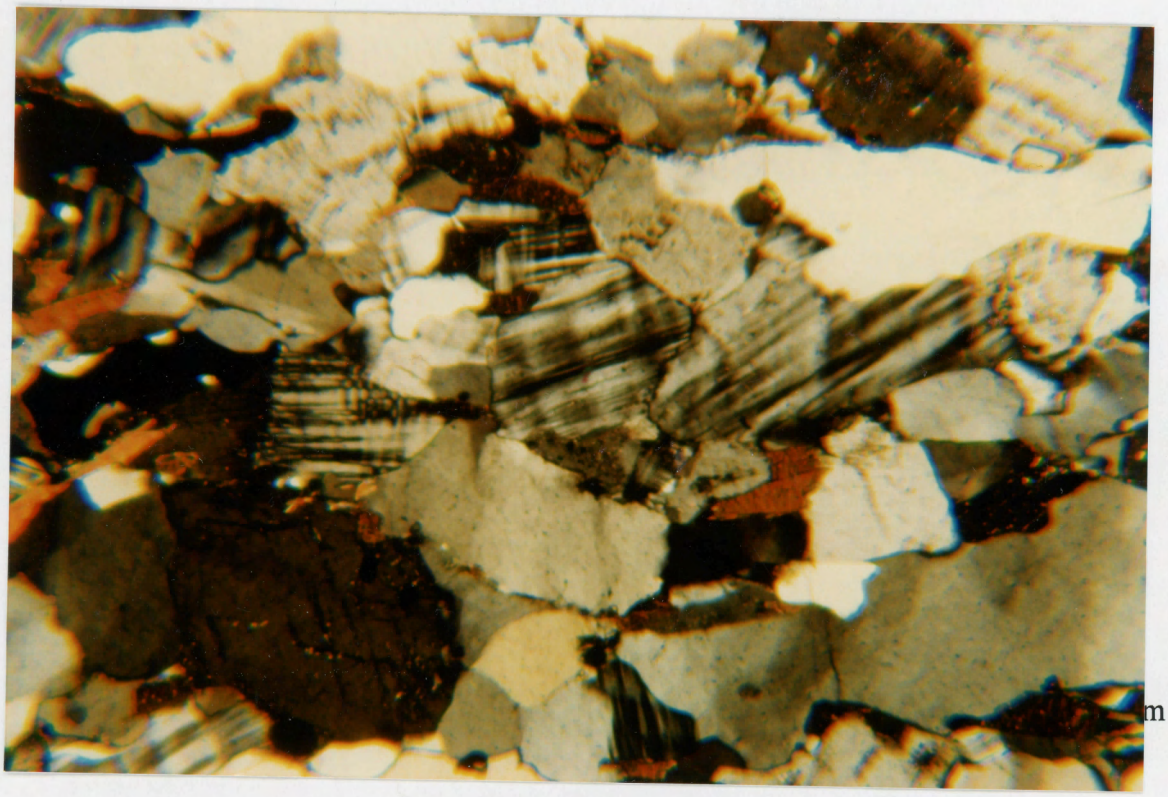

m

		modal %	size(mm)		modal %	size(mm)
Mineralogy:	K-feldspar:	20	0.2-0.5	A-feldspar:	10	0.2-0.5
	Quartz:	45	0.2-1.2	Biotite:	20	0.1-0.5
	Opaque:	5	<0.5			

texture: foliation defined by biotite & elongate grains; mymerkite

mineral phase dated: K-feldspar separate

notes: 0.2-0.5 mm anhedral microcline grains, grain boundaries curved > embayed, cross-hatch twinning throughout, pervasive sericite alteration; perthitization rare (needle-like strings <~5μm).

Sample #: 186G1

Rock Type: foliated megacrystic granitoid

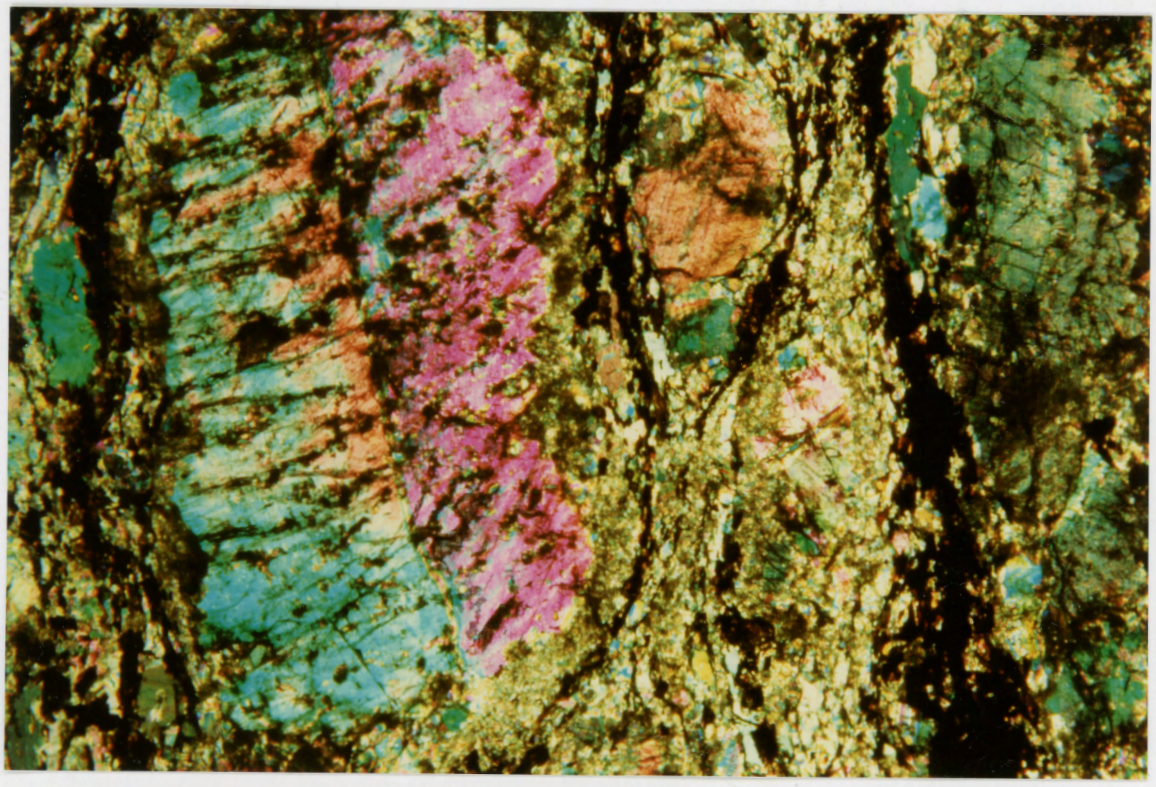

		modal %	size(mm)		modal %	size(mm)
Mineralogy:	K-feldspar:	15	1-10	A-feldspar:	35	0.1-10
	Quartz:	30	0.2-1.5	Biotite:	15	0.2-0.7
	Garnet:	5	0.3-0.5	Opaque:	*	
	Apatite:	*				

texture: K-feldspar porphyroclasts up to 0.5cm in fine foliated matrix (foliation defined by biotite grain shape preferred orientation)

mineral phase dated: grains from K-feldspar porphyroclast separated from thick section

notes: grain dated is a ~0.5 cm orthoclase, Carlsbad twin; exolution lamellae (~30 μm wide strings) parallel 001 cleavage plane, lamellae comprise ~30 % of grain; sericitization; inclusions of opaque minerals, quartz and apatite.